IN-SITU SPECTROSCOPIC INVESTIGATIONS OF MOLECULAR MECHANISMS ENABLING SORPTION OF DIOXINS AND PCBS BY SMECTITE CLAYS

by

Kiran Rana Bangari

A Dissertation

Submitted to the Faculty of Purdue University

In Partial Fulfillment of the Requirements for the degree of

Doctor of Philosophy

Department of Agronomy

West Lafayette, Indiana

May 2019

THE PURDUE UNIVERSITY GRADUATE SCHOOL
STATEMENT OF COMMITTEE APPROVAL

Dr. Cliff T. Johnston, Chair

    Agronomy, College of Agriculture

Dr. Linda S. Lee

    Agronomy, College of Agriculture

Dr. Paul Schwab

    Agronomy, College of Agriculture

Dr. Loring F. Nies

    School of Civil Engineering

Approved by:

    Dr. Ronal F. Turco

        Head of the Graduate Program

Dedicated to my brother late Captain Kailash Rana (1981-2009)

ACKNOWLEDGMENTS

I am very grateful to my Ph.D. advisor Dr. Cliff Johnston for providing me the great opportunity to work under his supervision and for his continued guidance and support during my graduate studies at Purdue. During this long journey I have learned a lot from his professional expertise and experience as well as passion, and enthusiasm for his work. It was his caring attitude that I am finally finishing this doctoral thesis after some unavoidable circumstances had led to interruption in my graduate program for an extended period. Thank you, Dr. Johnston, for taking time from your hectic schedule for reviewing and revising numerous drafts of our papers and thesis chapters, meeting regularly over the phone and helping me keep on track especially during last 10-12 months. I would also like to express my deepest gratitude to the members of my graduate committee- Drs. Linda Lee, Paul Schwab and Loring Nies, for their insightful guidance throughout this research and encouragement and support for the completion of this adjourned milestone of my graduate career.

Special thanks to Dr. Ganashri Premachandra and Dr. Darrell Schulze for all support in the lab, precious advice in life and for making graduate life at Purdue a memorable one. My deep appreciation goes out to Drs. Brian Teppen, Stephen Boyd and Hui Li, our collaborators from Michigan State University for their technical support for this study and generous sharing of knowledge.

A big shout out to my wonderful friends and colleagues at Purdue who helped me in my research work in numerous ways. So, Thank you Bushra Khan, Stephen Sassman, Kavitha Dasu, Nadia Carmosini, Laurel Royer, Eric Johnson, Shalamar Armstrong, Bibi Naz, Joyace Lok, Branley Eugene, and Pamela Obura. Special thanks to Bushra Khan for always being available to discuss research ideas and for her unconditional friendship. My sincere thanks to Karen Clymer, Patricia Oliver, Connie Foster and other administrative staff members in the Agronomy department. Without your help and guidance, this journey would not have been possible.

I would like to express my heartfelt thank you to my mom, dad, brothers, sister, and parent in-laws for all their love, encouragement and endless support in all my pursuits. Finally, to my husband Dinesh, who has always been by my side throughout this PhD, providing endless support, encouragement and understanding and without whom I would not have had courage to embark on

and revitalize this journey. Special hugs to our darling kids Ashwina and Abhijay for being good kids and helping me in their own little ways to complete what I had started a while back.

TABLE OF CONTENTS

LIST OF TABLES

LIST OF FIGURES

ABSTRACT

Author: Bangari, Kiran, Rana. PhD
Institution: Purdue University
Degree Received: May 2019
Title: *In-Situ* Spectroscopic Investigation of Molecular Mechanisms Enabling Sorption of Dioxins and PCBs on Smectite Clays
Committee Chair: Cliff Johnston

Dioxins and poly-chlorinated biphenyl (PCB) compounds are high priority organic pollutants which are similar in structure and well known for their toxicity, bioaccumulation and persistence in the environment. Dioxins and PCBs have a high affinity for certain types of clay minerals. However, the molecular mechanism for the observed high affinity of these compounds to clay minerals is not well understood and has been the main focus of this research work. The mechanisms that govern dioxin-clay and PCB-clay interactions were investigated from two perspectives. First, the influence of selected properties clay minerals on dioxin sorption was investigated via in-situ spectroscopic techniques (ATR-FTIRand Raman) structural (XRD) and macroscopic batch sorption methods using dibenzo-p-dioxin (DD) as a model solute. Second, the influence of solute properties, especially position and degree of chlorination and molecular planarity, on sorption was investigated.

Smectites, especially, Cs-saponite effectively adsorbs dibenzo-p-dioxin (DD) from water with values reaching 10,000 mg kg^{-1}, or one weight percent which greatly exceeds that by other naturally occurring sorbents such as soil organic matter. Adsorption was promoted by clay interlayer exchangeable cations with low hydration energies, and by smectites in which negative charge in the smectite originate from the tetrahedral siloxane sheets. IR-active bands of DD sorbed to saponite in the 1280 to 1500 cm^{-1} region were perturbed compared to the 'reference' IR spectra. Combined batch sorption, XRD and spectroscopic data confirm that the intercalation of DD occurred in the clay interlayer and site specific interactions occur between DD molecule and Cs^{+} cation.

Sorption of 1-chloro-dibenzo-p-dioxin (1-ClDD) and 2-chloro-dibenzo-p-dioxin (2-ClDD) on homoionic (Na^{+}, K^{+}, Rb^{+}, and Cs^{+}) smectites was evaluated to explore the effect of chlorine substitution position (and steric hindrance) of dioxin on sorption mechanisms. Similar to DD, adsorption was influenced by the hydration energy of exchangeable cations and the origin of

negative charge in the smectite. XRD measurements revealed that 1-ClDD molecules were oriented nearly parallel to the siloxane surface of the clay while 2-ClDD adopted a tilted orientation, similar to DD. The location of the chlorine constituent in 1-ClDD prevents the molecule from its apparent energetically more favorable orientation. In-situ ATR-FTIR spectra revealed that sorption of 1-ClDD to Cs-saponite resulted in the loss of interfacial H_2O and suggested that the sorption 1-ClDD displaces interlayer H_2O and 2-ClDD is less sterically restricted in the clay interlayer.

Sorption of three dioxins (DD, 1-ClDD and 2-ClDD) was compared to three PCBs (PCB-1, PCB-4, and PCB47) with similar octanol-partition coefficients (log K_{ow}) but varying molecular planarity and degree of chlorination onto Cs-saponite, which was shown to be representative of other smectites, revealed that despite having similar structure and hydrophobicity, dioxins have higher affinity for smectites than PCBs. Sorption studies also showed that sorption of PCBs is influenced by molecular planarity and hydrophobicity. Polarizability and dipole-moment were identified as important solute properties that affect the sorption behavior of dioxins and PCBSs. Linear relationships between these properties and log K_f'(subcooled liquid solubility normalized Freundlich sorption coefficient) values suggest that high sorption affinity of planar dioxins could be due to a combination of *Van der Waals* interactions with the siloxane surface, steric effects, and site-specific interactions between dioxin and exchangeable cations. In contrast, the sorption of PCBs was highly influenced by their molecular orientation.

CHAPTER 1.   INTRODUCTION

Polychlorinated–dibenzo-p-dioxins (PCDD or dioxins) and chlorinated biphenyl (PCBs) are priority and persistent organic pollutants known for carcinogenic and toxic effect (Borlak, 2001; Denison and Nagy, 2003; Goldstein, 1989; Mandal, 2005b; Swanson and Bradfield, 1993). Dioxins and PCBs are also known as aryl hydrocarbon receptor ligands (AhRLs) as the toxicity of these compounds is attributed to their ability to activate the aryl hydrocarbon receptor (AhR) at exceptionally low aqueous solution concentrations (Borlak, 2001; Denison and Nagy, 2003; Goldstein, 1989; Mandal, 2005a; Safe, 1990; Swanson and Bradfield, 1993). Among the AhRL compounds, 2,3,7,8 tetra-chloro-dibenzo-p-dioxin (TCDD) is considered to be the most toxic compound. It is classified as a carcinogen to humans by the International Agency for Research on Cancer and can cause many other potential health hazards (Lewis, 2000; Steenland et al., 2004; Pohl et al., 2002). The half-maximal effective concentration (EC50) of TCDD for induction of AhR-dependent gene expression in cellular system is 9 pM (Denison and Nagy, 2003). The action levels for dioxins and dioxin-like compounds in residential soils, as established by the U.S. Agency for Toxic Substances and Disease Registry (ATSDR), range from 90 ppt to 1 ppb toxic equivalents (TEQ; defines the toxicity-weighted mass of dioxins and dioxin-like compounds with respect to most toxic TCDD). This toxicity justifies the concern about the environmental fate of dioxins and dioxin-like halogenated aromatic compounds.

1.1   Sources and Environmental Fate of Dioxins and PCBs

The dibenzo-*p*-dioxin and biphenyl structures and substituent numbering schemes are shown in Figure 1.1. These structurally similar compounds are ubiquitous in the environment and are produced anthropogenically as a byproduct of many industrial processes such as waste

incineration, chemical and pesticide manufacturing, pulp and paper bleaching, as well as naturally from forest fire and volcanic eruption (Brzuzy and Hites, 1996; Hoekstra et al., 1999; Horii et al., 2008b; Kim et al., 2003; Rappe, 1996).

Dioxins/PCDDs   **PCBs**
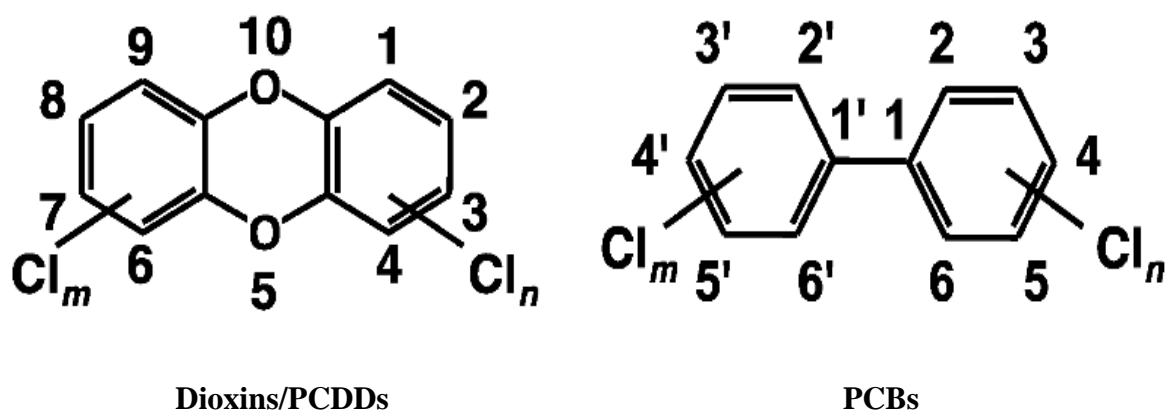
Figure 1.1. The structure and substituent position numbering of dibenzo -p-dioxin and biphenyl. Where m and n=0 to 5

Significant regulatory and academic efforts and industrial technology advancements in the last four decades have resulted in a significant reduction of the industrial emissions of dioxins and PCBs. However, human exposure to these compounds still pose a major risk as they are globally detected in food products, wildlife, humans, soils, sediments and natural clay deposits (Pius et al., 2019; van den Berg et al., 2017; Wong et al., 2013). Persistence of these compounds in the environment has been attributed to their physiochemical properties which include low water solubility, high lipophilicity, low vapor pressure, and slow degradation under ambient conditions (Shiu et al., 1988;Holmes et al., 1993;Shiu and Mackay, 1986; Kjeller et al., 1991; Furukawa et al., 2004)). Because of their low solubility, sorption to soil- and sediment-water systems is a key determinant that controls the environmental fate of these compounds. Detailed understanding of

molecular mechanisms controlling the sorption is important to predict their environmental fate and transportation (Figure 1.2).

In general, soil organic matter (SOM) and clay minerals are the main domains responsible for the sorption of environmental pollutants in soil, sediment- and water systems. For the dioxins and PCBs, which have low aqueous solubility, carbonaceous sorptive domains such as SOM were thought to be the dominant sorptive phase (Chiou, 1990; Frankki et al., 2006; Krauss and Wilcke, 2002; Larsen et al., 2004; Walters et al., 1989). As a result organic matter (or organic carbon) normalized partition coefficients (K_{OM} or K_{OC}) have traditionally been used to predict the soil-, sediment-water distribution of these hydrophobic compounds (Frankki et al., 2006; Jonker and Smedes, 2000;Choi and Al-Abed, 2009). In contrast, clay minerals were traditionally considered to be strongly hydrophilic in nature with low affinities for hydrophobic contaminants.

High levels of dioxins in chicken, baby food, farmed catfish and salmon in the USA and Europe was traced back to the use of a dioxin-contaminated clay mineral that had been used as an anti-caking additive in animal feed (Ferrario and Byrne, 2000; Hayward and Bolger, 2005; Hayward et al., 1999; Prange et al., 2002). Follow-up investigations found that high (up to 520,000 pg/g) amount of PCDD, PCB were present in prehistoric clay deposits (ball clays), kaolin, and smectites (montmorillonites /bentonites) and soils from different countries (Ferrario and Byrne, 2002; Ferrario et al., 2007; Ferrario et al., 2000; Gadomski et al., 2004; Green et al., 2004; Hoekstra et al., 1999; Holmstrand et al., 2006; Horii et al., 2008a; Rappe, 1996).
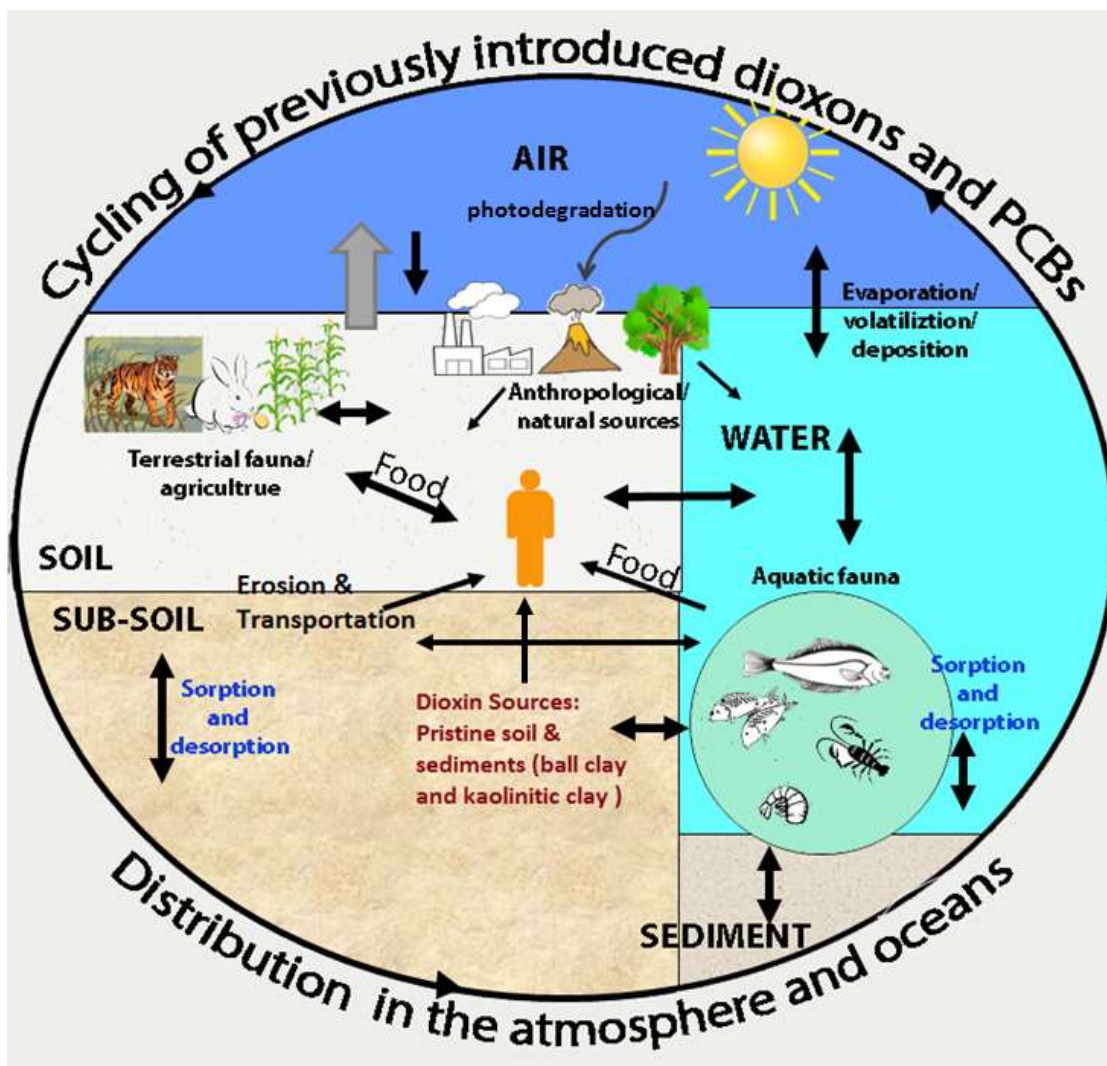
Figure 1.2. Environmental sources, fate and distribution dioxins and dioxin like compounds.

Similarly, many studies have established a previously unrecognized affinity between dioxins and other AhRL compounds and clay minerals (Ferrario and Byrne, 2002; Gadomski et al., 2004; Holmstrand et al., 2006; Prange et al., 2002; Rappe et al., 1998; Schmitz et al., 2011). Dioxin profiles in raw and processed kaolin/ball clays were different than that of anthropogenic sources and characterized by the domination of the congener octa-chloro-dibenzo-p-dioxin (OCDD), and the concentrations of other congeners decreased in the order of reduction in the

levels of chlorination (Horii et al., 2008a). These findings suggested that either clay minerals act as sink for dioxins and other AhRLs or they act as abiotic sources of formations for these compounds (Gu et al., 2011; Holt et al., 2008). In a case study of human exposure of dioxins in Michigan County, Michigan, Franzblau et al. (2008) reported that the congener pattern in the serum of individuals who used clay for pottery was strongly related to the dioxin contamination in clay minerals they used. The unfired ceramic clay samples from this and other studies had high amount of PCDD and PCBs. The estimated emission of PCDDs and PCD furans (PCDFs) from ceramic industries in China was estimated to be 7.94 kg/year. This corresponds to about 1.34% (I-TEQ basis) of the total emission of dioxins to the environment in China. These results suggest that the ceramic industry is a significant source of dioxins in the environment (Lu et al., 2012). Dioxin sorption studies on aluminum pillared smectite and smectites have shown that clay minerals can contribute two to three fold higher sorption than soil organic matter (Liu et al., 2008; Nolan et al., 1989). The affinity of hydrophobic compounds for smectite clays as evident by batch sorption studies and investigation results of kaolin/ ball clay-dioxin associations is surprising and the underlying mechanisms responsible for the high concentration of these AhRLs in clays is not clear.

On a surface area basis, clay minerals are often the most predominant constituents and can be potentially important environmental sinks for dioxins (McBride, 1994). In this context, the group of expandable clay minerals known as smectites are especially important due to their abundance in soils (specific surface area $\sim$800 m^2 g^{-1}) and medium to high cation exchange capacities (CEC: 80 to 120 $cmol_c$ kg^{-1}) (Guven, 1988).

1.2   Structure of Smectite

Smectites belong to the group of expansive 2:1 phyllosilicates, which are formed by the stacking of silicate layers. Each silicate layer consists of two tetrahedral sheets bound to an octahedral sheet (Figure 1.3).
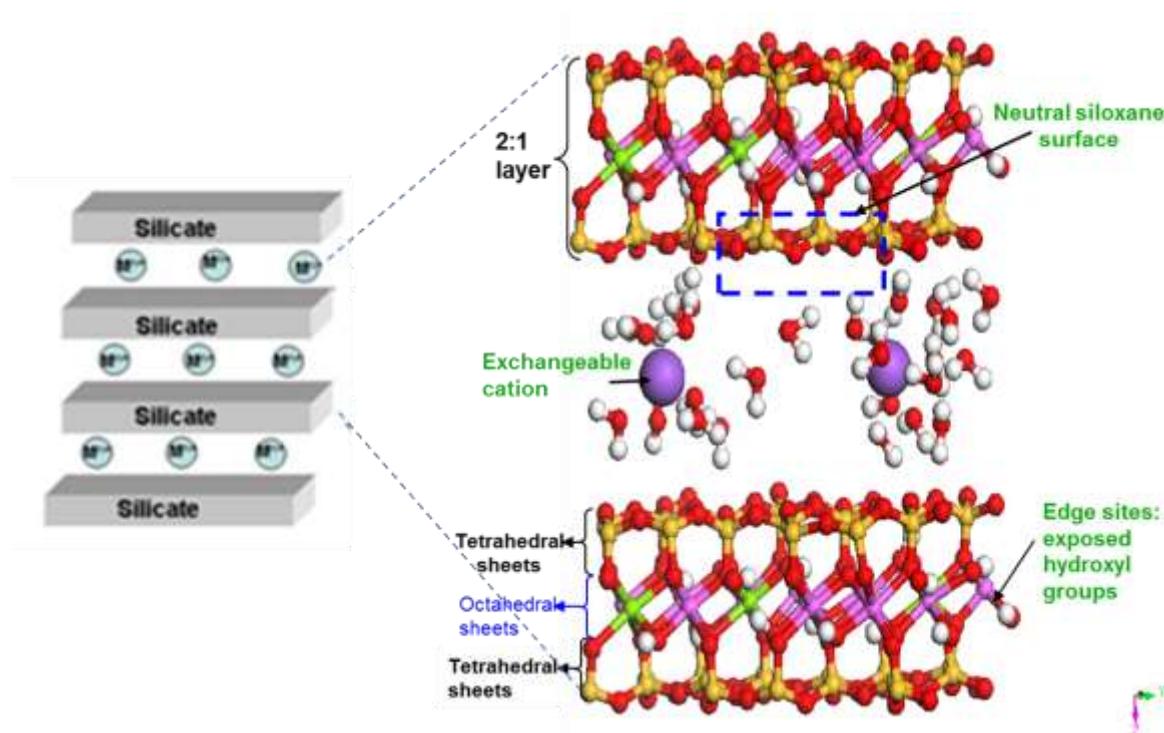
Figure 1.3. Diagram of smectite particle (left) and expanded side view (right) showing the structure and possible binding sites on smectite clay.

Due to isomorphic substitution in tetrahedral and/or octahedral layer, smectites carry permanent net negative charge and have charge densities of 0.5 - 1.2 sites nm^{-2}. The negative charge from these sites is neutralized by exchangeable cations. Hydration of these cations (hydration enthalpy range -4491 to -315 kJ mol^{-1}) creates a hydrophilic environment at the clay surface. The region between isomorphic substitution sites in clay interlayer are neutral and have been shown to stabilize the sorption of semi-polar and neutral organic compounds (NOCs) on smectites (Jaynes

and Boyd, 1991). The accessibility of organic solutes to these hydrophobic sites is inversely related to the charge density of clay (Figure 1.3 and Figure 1.4) and the enthalpy of hydration of the exchangeable cations.

1.3   Sorption of neutral and semi-polar aromatic compounds on smectites

Sorption studies of non-polar planar organic compounds (nitroaromatics, triazines and carbamates) on smectite have shown that the uptake of these compounds is highly influenced by the nature of exchangeable cations (Boyd et al., 2001a; Johnston et al., 2001a; Nolan et al., 1989; Sheng et al., 2001a). Sorption of these compounds on smectites from aqueous was influenced by three parameters: i) the favorable site-specific interaction between the compound and exchangeable cation (Johnston et al., 2001a; Johnston et al., 2002a; Liu et al., 2008; Sheng et al., 2001a); ii) the enthalpy of hydration of exchangeable cation (Sheng et al., 2001; Johnston.et al., 2001; Laird et al., 1996); and iii) steric constraints (planarity and molecular dimensions) (Sheng et al., 2001; and Laird et al., 1996).
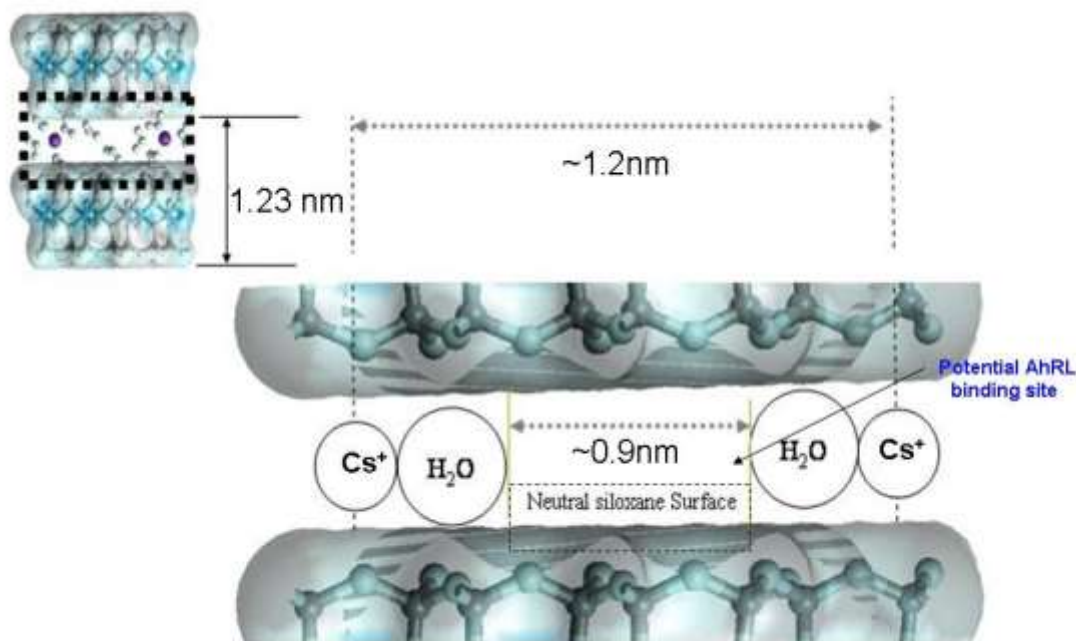
Figure 1.4. Expanded view of Cs-saponite interlayer showing the approximate neutral siloxane surface domain between two isomorphic substitution sites. Modified from Johnston et al. (2004b)

As the underlying mechanisms leading to the high affinity of dioxins for smectites are not well understood, there is a primary need for elucidating the mechanisms responsible for the interaction of dioxins and other PCB compounds to clay-water system. Previous studies on the sorption and distribution of PCBs on soil, sediments and geosorbents have shown that planar PCBs tend to sorb more than non-planar PCBs. (Jonker and Smedes, 2000; Bucheli and Gustafsson, 2003; Swackhamer and Skoglund, 1991). Furthermore, sorption of dioxins and PCBs generally increases with increasing chlorine content and is inversely related to the particle size of sediments (fine particles with particles size (ϕ) > 63 μm show higher sorption than coarse particles with ϕ < 63 μm) (Pierard et al., 1996; Schwarzenbach et al., 2003). Increase in degree of chlorination decreases the water solubility, resulting more chlorinated substances want to escape water more through

change in entropy. Therefore, the influence of the structure and degree of chlorination of dioxins and dioxin-like PCBs on sorption by smectites needs to be addressed.

Most of the reported sorption studies of dioxins and PCBs on different soil matrices (soil, OM, clay minerals etc.) have utilized the batch sorption techniques to elucidate sorption mechanisms. However, such macroscopic methods are incapable of providing concrete information about the molecular mechanisms underlying these interactions (Johnston and Sposito, 1987). Vibrational modes of solutes are sensitive to changes in their local environment and can be used as a molecular probe of interfacial reactions and sorption mechanisms (Davis and Hayes, 1986; Johnston and Sposito, 1987; Johnston et al., 1993). Therefore, in the current study, I took an integrated approach of macroscopic batch sorption and in-situ microscopic methods including infrared spectroscopy (IR), Raman spectroscopy and X-ray diffraction (XRD) techniques to investigate the extent and mechanisms of dioxin and PCB sorption on smectites.

A

4nm

Charge influence zone with isomorphic substitution in tectrahedral layer

1.2nm

1.2nm

0.2nm

0.8nm x 0.8nm =0.64 nm²

Top layer

Potential binding site for nonpolar organic compounds. This site has dimension similar to binding pockets of Aryl hydrocarbon recprtor (1.4 n m x 1.2 nm)

Neutral siloxane area

4nm

2.5"= 1nm

Smectite clay with isomorphic substitution in tetrahedral layer

B

4nm

Charge influence zone with isomorphic substitution in octahedral layer

0.8nm

0.8nm

0.8nm

Top layer

0.4nm

Potential binding site (0.16nmx0.16nm) for nonpolar organic compounds.

Neutral siloxane area

4nm

2.5"= 1nm

Smectite clay with isomorphic substitution in octahedral

Figure 1.5. Proposed molecular model (4 nm x 4 nm portion of the siloxane surface) for the estimation of the extent of non polar surface as a function of location of isomorphic substitution in smectite silicate layer: smectite clays with A) isomorphic substitution in tetrahedral layer (e.g. saponite); and B) isomorphic substitution in octahedral layer. Circles show the charge influence zones. Grey color and blue areas represent neutral siloxane area and the potential hydrophobic binding sites for AhRL compounds, respectively.

1.4   Research Goals and Objectives:

The overall goal of the research presented in this dissertation was to evaluate the role of clay minerals in the sorption of dioxin and structurally similar PCBs by investigating the molecular mechanisms of sorption of dioxin on smectite water interface and exploring quantitative structure activity relationships between sorption and the molecular properties of dioxins and PCBs. In order to accomplish this goal, experiments were conducted to address the following specific objectives and associated hypotheses:

Objective I: To investigate the factors affecting the adsorption of dioxins and determine the molecular mechanisms of dioxin sorption to smectite using dibenzo-p-dioxin (DD) as a model dioxin solute. **Hypothesis:** Sorption of DD from water on smectite is facilitated by direct interaction between interlayer exchangeable cations or neutral siloxane and π electrons of dioxin molecule. Clay properties such as hydration energy of clay interlayer exchange cations, charge density and distribution of clay layer charge (octahedral vs. tetrahedral) influence the intensity of such interactions.

Objective II: Analyze the influence of chlorine substitution and position of substitution on dioxin molecule on sorption. **Hypothesis:** Chlorine substitution increases the polarizability and hydrophobicity of dioxin molecule; therefore, sorption of chlorinated dioxin will be higher than non-chlorinated DD. If sorption is governed by direct interaction between exchangeable cations and oxygen atoms of dioxin, the steric hindrance posed by position of chlorine substitution (para vs meta) should interfere with the direct interaction between the exchangeable cations and oxygen atoms of dioxin, thus influence the extent of the dioxin sorption.

Objective III: Evaluate the influence of molecular planarity and degree and position of chlorine substitution of dioxin and structurally similar PCBs on adsorption by smectite using Cs-saponite as a model sorbent. **Hypothesis**: In aqueous suspensions, the distance between the opposing clay sheets is ~0.33 nm. This distance is similar to thickness of planar AhRL molecule (with ~0.3 nm thickness); therefore, the sorption of planar dioxin and PCBs is expected to be higher than that of non-planar compounds (with ~ 0.8 nm thicknesses).

1.5   Organization

This thesis is composed of five chapters including this introduction and the following four chapters:

CHAPTER II: The sorption of dibenzo-p-dioxin (DD) from aqueous suspension by smectite clays of different structures and saturated with different exchangeable cations was examined using integrated macroscopic batch sorption and *in-situ* spectroscopic methods. The mechanisms of DD sorption on smectites using integrated batch sorption, spectroscopic (IR, ATR-FTIR, and Raman) and XRD data is discussed. [Published: Kiran Rana, Stephen A. Boyd, Brian J. Teppen, Hui Li, Cun Liu and Cliff. T. Johnston. Probing the microscopic hydrophobicity of smectite surfaces. A vibrational spectroscopic study of dibenzo-p-dioxin sorption to smectite. *Phys. Chem. Chem. Phys.,* **2009**, 11, 2976–2985. Reproduced with the permission of The Royal Society of Chemistry (RSC), Copyright 2009].

CHAPTER III: To study the influence of chlorine substitution in the dibenzo-p-dioxin molecule on sorption mechanisms, the molecular interaction of two chlorinated dioxin congeners varied in position of chlorine substitution, with homoionic smectite clays was investigated. In situ spectroscopic (ATR-FTIR, XRD) and macroscopic batch sorption techniques were applied to

investigate the adsorption mechanism(s) of 1-chloro dibenzo-p-dioxin (1-ClDD) and 2-chloro dibenzo-p-dioxin (2-ClDD) at clays in aqueous systems. Manuscript in preparation: Kiran Rana Bangari, Bushra Khan, Cun Liu, Stephen A. Boyd, Brian J. Teppen, Hui Li, and Cliff. T. Johnston. Molecular mechanisms of chlorinated dibenzo-p-dioxins interactions with smectites, 2019]

CHAPTER IV: This chapter focuses on the influence of molecular planarity and degree and position of chlorination of dioxin and PCBs on sorption. The sorption of three planar dioxins and a coplanar PCB and two non planar PCBs, with similar K_{ow} values, on Cs-saponite was examined using batch sorption and XRD techniques. Measured log $K_{f'}$ (subcooled liquid solubility normalized Freundlich sorption model coefficients) values of dioxins and PCBs were compared and structure-specific sorption behavior of planar and non-planar solutes was explained based on the differences observed in these values. [Manuscript in preparation: Kiran Rana, Linda S. Lee, Stephen A. Boyd, Brian J. Teppen, Hui Li, and Cliff. T. Johnston Sorption of planar and nonplanar compounds to Cs exchanged smectite, 2019]

Chapter V: The major findings of the present study on sorption of dioxins and PCBs from aqueous suspension on smectites are summarized followed by highlighting future research needs.

CHAPTER 2. PROBING THE MICROSCOPIC HYDROPHOBICITY OF SMECTITE SURFACES. A VIBRATIONAL SPECTROSCOPIC STUDY OF DIBENZO-P-DIOXIN SORPTION TO SMECTITE

Kiran Rana, Stephen A. Boyd, Brian J. Teppen, Hui Li, Cun Liu and Cliff. T. Johnston. Probing the microscopic hydrophobicity of smectite surfaces. A vibrational spectroscopic study of dibenzo-p-dioxin sorption to smectite. Phys. Chem. Chem. Phys., 2009, 11, 2976–2985

2.1   Abstract

The interaction of dibenzo-p-dioxin (DD) from aqueous suspension to smectite was investigated using *in situ* vibrational spectroscopy (FTIR and Raman), structural and batch sorption techniques. Batch sorption isotherms were integrated with *in situ* attenuated total reflectance (ATR)-FTIR and Raman spectroscopy and X-ray diffraction. Sorption isotherms revealed that the affinity of DD for smectite in aqueous suspension was strongly influenced both by the type of smectite and by the nature of the exchangeable cation. Cs-saponite showed a much higher affinity over Rb-, K- and Na-exchange saponites. In addition, DD sorption was found to depend on clay type with DD showing a high affinity for the tetrahedral substituted trioctahedral saponite over SWy-2 and Upton montmorillonites and a structural model is introduced to account for the influence on clay type. Raman and FTIR data provided complementary molecular-level insight about the sorption mechanisms. In the case of Cs-saponite, the selection rules of DD based on D_{2h} symmetry were broken indicating a site-specific interaction between DD and intercalated Cs^+ ions in the interlayer of the clay. Polarized *in situ* ATR-FTIR spectra revealed that the molecular plane of sorbed DD was tilted with respect to the clay surface which was consistent with a d-spacing of 1.49 nm. Finally, cation-induced changes in both the skeletal ring vibrations and the asymmetric C-O-C stretching vibrations provided evidence for site specific interactions between the DD and

exchangeable cations in the clay interlayer. Together, the combined macroscopic and spectroscopic data presented here show a surprising link between a hydrophilic materials and a planar hydrophobic aromatic hydrocarbon.

2.2   Introduction

The planar tricyclic aromatic ether compounds known as dioxins are among the most harmful compounds known to man due to their toxicity and carcinogenicity (Steenland et al., 2004) . The chlorinated dioxins, toxic end-members of the group known as persistent organic pollutants, can activate the aryl hydrocarbon receptor (AhR) at exceptionally low aqueous solution concentrations (Denison and Nagy, 2003). In the case of 2,3,7,8-tetrachloro dibenzo-p-dioxin (TCDD), for example, the half-maximal effective concentration (EC50) concentration for induction of AhR-dependent gene expression is 9 pM (Denison and Nagy, 2003). This toxicity justifies concern about the fate of dioxins and related halogenated aromatic hydrocarbons (HAHs). The environmental fate of dioxins is considered to be mainly controlled by sorption processes as a consequence of their low aqueous solubilities (Liu et al., 2008). Traditionally the sorptive compartments thought to be responsible for dioxin sequestration were hydrophobic, organic phases and surfaces such as natural and anthropogenic organic matter and high surface area carbonaceous materials (Frankki et al., 2006;Pennell et al., 1995;Boyd and Sun, 1990). However, recent studies have established an previously unrecognized affinity between the dioxins and the group of expandable clay minerals known as smectites (Liu et al., 2008;Prange et al., 2002;Ferrario et al., 2000;Horii et al., 2008;Hoekstra et al., 1999). This surprising link is counterintuitive as the dioxins are strongly hydrophobic and the smectites are viewed as being strongly hydrophilic.

In a recent study, the affinity of dibenzo-p-dioxin (DD) for smectite was strongly influenced both by the nature of the exchangeable cation and by the type of smectite (Liu et al., 2008). Sorption of DD from aqueous suspension on Cs-exchanged saponite was greatest with values approaching 10,000 mg/kg^{-1}, or 1 weight percent, which greatly exceeds that by other naturally occurring sorbents such as soil organic matter. Smectites belong to the group of 2:1 phyllosilicates and are characterized by large specific surface areas of ~ 700 m^2 g^{-1} that carry a net negative charge due to isomorphous substitution in the clay lattice, and charge densities of ~ 0.6 sites/nm^2. These negatively charged sites are neutralized by the presence of exchangeable cations which are hydrophilic owing to their moderate to high enthalpies of hydration. The region of the siloxane surface between the hydrated exchangeable cations can act as a nanoscale adsorption domain for compounds such as nitroaromatics, triazines and trichloroethene (Aggarwal et al., 2006; Johnston et al., 2004; Boyd et al., 2001).

In prior sorption studies, the nature of the exchangeable cation was shown to significantly influence the uptake of aromatic hydrocarbons as well as semi-polar, planar aromatic compounds including nitroaromatics, triazines and carbamates (Boyd et al., 2001b; Chappell et al., 2005; De Oliveira et al., 2005; Johnston et al., 2004a; Johnston et al., 2001b; Johnston et al., 2002a; Laird et al., 1992; Laird et al., 1994; Lawrence, 1998; Li et al., 2003; Li et al., 2004a; Li et al., 2004b; Pereira et al., 2008; Sheng et al., 2002; Sheng et al., 2001b). Sorption of these compounds possessing moderately polar functional groups on smectites from aqueous was influenced by several key parameters. First, the interaction between the compound and exchangeable cation influences sorption (De Oliveira et al., 2005; Johnston et al., 2001b; Johnston et al., 2002a). Site-specific interactions between the organic solute and the clay surface and/or cations in the interlamellar region is one favorable force that allows the organic solute to enter into the

interlamellar region of the clay structure (Boyd et al., 2001b). Second, the enthalpy of hydration of the exchangeable cation has been shown to influence direct sorption processes (Boyd et al., 2001b; Johnston et al., 2004a; Sheng et al., 2002). The clay siloxane surfaces themselves are not strongly hydrophilic (Jaynes and Boyd, 1990, 1991). but the exchangeable cations satisfying the charge deficit of the clay have high affinities for water (Johnston and Tombacz, 2002) and impart a hydrophilic character to the smectite interlayer environment (Schoonheydt and Johnston, 2007). Hydration of these interlayer cations also controls smectite swelling, with a lower degree of swelling enhancing sorption of hydrophobic solutes by the smectite. In general, sorption of semi-polar organic solutes increases as the enthalpy of hydration of the exchangeable cation is decreased(Charles et al., 2006; Laird et al., 1992; Laird et al., 1994). For weakly hydrated exchangeable cations, organic solutes do not have to compete with as much water to interact with the siloxane surface or the cation itself. Finally, sorption depends on steric constraints. Generally, planar compounds show a higher affinity than non-planar or compounds that have bulky substituents (Boyd et al., 2001b; Sheng et al., 2002).

In the case of dioxins, polar functional groups are not present and site-specific interactions between dioxin and the siloxane surface or with the exchangeable cation would be expected, a priori, to be very small. So, the underlying forces and mechanisms leading to the affinity of DD for Cs-saponite from aqueous suspension are not well understood. The very high affinity of DD for Cs-saponite (sorbed up to 1% wt/wt) can be partially accounted for by presence of Cs^+. Cs^+ has the lowest enthalpy of hydration of the alkali metal or alkaline earth cations (-315 kJ mol^{-1}) (Friedman and Krishnan, 1973) allowing Cs+ to form inner sphere complexes (Sutton and Sposito, 2001) with the siloxane surface. One possibility is that such metal exchanged smectites can present microscopic hydrophobic sites with dimensions of nanometers. In prior work, sorption of semi-

polar organic solutes was correlated with the apparent amount of 'neutral siloxane surface' available which was inversely proportional to the hydrated radii of the exchangeable cations (Charles et al., 2006; Jaynes and Boyd, 1990; Jaynes, 1991; Lee et al., 1990; Roberts, 2006 ; Ruan, 2008; Sheng et al., 2002). Michot and co-workers (1994) presented evidence that the hydrophobic surface of talc, a 2:1 phyllosilicate without isomorphous substitution, had water molecules occupying siloxane ditrigonal cavities which they referred to as microscopic hydrophilic sites. The specific objectives of this study were to examine the molecular mechanisms of interaction between DD and smectite clays as influenced by clay type and by the nature of the exchangeable cation. From a broader perspective, DD can be considered as an interesting planar, O-heterocyclic, hydrophobic molecular probe to explore microscopic hydrophobic regions in the interlayers of smectites that may act as adsorption domains within an otherwise hydrophilic environment. There is a paucity of studies on the adsorption of such heterocyclic molecules by smectite clays.

2.3   Materials and Methods

2.3.1   Reference Clay

The clay minerals used in this study were SapCa-2 saponite, SWy-2 montmorillonite, and Upton montmorillonite. SapCa-2 and SWy-2 were obtained from the Source Clays Repository of the Clay Minerals Society at Purdue University, West Lafayette, IN. The Upton montmorillonite was from the American Petroleum Institute series collected from Upton, Wyoming (Mortland and Halloran, 1976). The structural formulae for the SapCa-2 saponite, Upton and SWy-2 montmorillonites are given in Table 2.1. Prior to size fractionation, each clay was exchanged with Na$^+$ by placing 40 g of the raw clay in 1 L of 0.5 M NaCl for 24 h. Resulting Na-smectite suspension was washed to remove excess salts by repeated centrifugation with Millipore® water. The < 2µm size fractions was collected by centrifugation. Homoionic K-, Rb-, or Cs- smectites

were prepared by shaking Na-exchanged clay with 0.1M solution of the respective metal chloride for 24 h. Fresh 0.1 M metal chloride solution was used to replace the original solutions after centrifugation. This process was repeated four times to ensure complete cation exchange. Excess salt was removed by repeatedly washing with Millipore® water, using Spectra/Por® dialysis tubing, until a negative for Cl^- test using $AgNO_3$ was obtained. The resulting clay suspension was subsequently quick-frozen, freeze-dried, and stored in a closed container for later use.

2.3.2   Solute:

Dibenzo-p-dioxin (DD) (99% pure) used in this study was obtained from Chem Service, West Chester, PA. Crystalline DD (Lot # 319-145 D) was used for taking reference Raman and IR spectra of DD. A 1000 mg/L stock solution of DD in methanol (anhydrous methyl alcohol obtained from Mallinckrodt Chemicals, Chrom AR^R (lot # C33 E24) was prepared to make aqueous solutions of DD. The amount of methanol in the aqueous solutions was kept < 0.1% to minimize the co-solvent effect. Diluted aqueous solutions of DD were sonicated for 60 min at room temperature in a water bath sonicator.

2.3.3   Batch Sorption Isotherms

All sorption isotherms were determined using the batch equilibrium method. Freeze dried clay (1-25 mg) was placed in 30 mL centrifuge tubes (Kimble HS-5600-30) with polytetrafluoroethylene (PTFE)-lined screw caps. Twenty mL (for Rb-saponite and Cs-saponite), 15 mL (for Cs-SWy-2), 10 mL (for Cs-Upton), 7mL (for K-saponite), and 4mL (for Na-saponite) of 0, 0.08, 0.1, 0.2, 0.4, 0.6 and 0.8 mg/L DD solutions in a methanol carrier (<1mL/L) were added to each test tube. Control samples containing 0.8 mg/L DD without clay were prepared for calibration to quantify losses of DD due to other processes. Experiments were conducted with two replicates. Cs-saponite and DD suspensions were vortexed for 30 sec and horizontally shaken at

the speed of 80 strokes min^{-1} in a horizontal shaker at room temperature for 24 h to achieve apparent sorption equilibrium (as indicated from preliminary experiments). The smectite- DD suspensions were centrifuged at 5920 g for 20 min to separate the liquid and solid phases and one mL aliquots of supernatant were transferred to HPLC vials. In order to prevent the sorption of DD on HPLC vials, 0.5 mL pure (99.9%) methanol was added to each vial prior to the addition of the supernatant. HPLC vials containing supernatant and methanol were vortexed for 30 sec and analyzed for DD concentrations by direct injection of 50 µl on a Shimadzu SLC-10 high-performance liquid chromatography (HPLC) system equipped with a UV detector and a 15 cm x 4.6 mm x 5 µm Supelcosil ABZ PLUS column. Isocratic elution was performed using a mobile phase of 80%methanol: 20% water (v/v) with a flow rate 1.0 mL min^{-1} and wavelength of 223 nm for detection. The amount of DD sorbed was calculated from the difference between the amount added and that remaining in the final solution. HPLC analysis of adsorption systems without clay (DD solution only) showed 99.5% recovery of dioxin in the supernatant and indicated minimal DD sorption on glass tubes, DD degradation or any other loss of DD.

Table 2.1 Characteristics of smectite clays used in this study

Clay type	Ideal formula	Octahedral sheet type	% tetrahedral charge [a]	Cation exchange Capacity (cmol/kg) [b]	Surface area (m^2/g)	Surface charge density (mmol/m^2)[f]
SapCa-2	$M^+_{0.33}(Si_{3.67}Al_{0.33})^{IV}(Mg_3)^{IV}O_{10}(OH)_2$	trioctahedral	100	94	750[d]	1.25
SWy-2	$M^+_{0.33}(Si_{4.})^{IV}(Al_{1.67}Mg_{0.33})^{IV}O_{10}(OH)_2$	dioctahedral	3.6	82	750[e]	1.07
Upton	$M^+_{0.33}(Si_{4.})^{IV}(Al_{1.67}Mg_{0.33})^{IV}O_{10}(OH)_2$	dioctahedral	1.6	95c	730[c]	1.30

[a] Source Clays repository of the Clay Mineral Society at Purdue University, West Lafayette, IN., [b] Measure by Cu-triethylene tetramine complex method, [f] from Laird et al. (1992),[d] Aggarwal et al. (2006),[e] Van Olphen and Fripiat (1979) Assuming CEC/surface area

2.3.4   FTIR Analysis

Infrared spectra were obtained on a Perkin-Elmer GX2000 Fourier Transform Infrared (FTIR) spectrometer equipped with deuterated triglycine (DTGS) and mercury-cadmium-telluride (MCT) detectors, an internal wire grid IR polarizer, a KBr beam splitter and a sample compartment purged with dry air. Grams /32 (Galactic software) program was used to analyze and plot spectra.

2.3.4.1   Self Supporting Clay Film Preparation

After sampling 1mL of supernatant for the HPLC analysis, the remaining Cs-saponite in the tubes was resuspended in the remaining supernatants and was used for the preparation of self-supporting clay films (SSCF). The clay suspension was passed through a membrane filter (0.45 µm Supor 450 hydrophilic polyethersulfone, 25 mm diameter) on a Millipore holder under vacuum. The resulting clay deposit on the membrane filter was allowed to air-dry for 2-3 h and was removed from the membrane filter by running the filter and clay deposit over a knife edge. FTIR spectra of SSCF films were obtained using a beam condenser. The unapodized resolution for the FTIR spectra was 2.0 cm^{-1}, and a total of 64 scans were collected for each spectrum.

2.3.4.2   ATR-FTIR measurements

A horizontal trough ATR cell (Pike Technologies, Madison, WI) was used in this study. The internal reflection element (IRE) used in the cell is a ZnSe crystal with dimensions of 73 mm x 7 mm and an angle of incidence of 45º. The total volume of the cell is 2 mL. Reference spectra of water and DD aqueous solutions were obtained by placing 1 mL of water or 0.8 mg/L DD solution in the horizontal trough cell. Ten mg of Cs-saponite was suspended in 5 mL of ultra-pure water and sonicated for 10 minutes in a water bath sonicator. One mL of this suspension containing 2 mg of Cs-saponite was placed in the ATR cell and allowed to air dry overnight. The Cs-saponite

deposit was washed multiple times using water (containing 0.1% methanol) and the intensity of the ν(Si-O) bands were monitored and the Cs-saponite deposit was found to be stable. After washing, the spectrum of the Cs-saponite deposit in water (containing 0.1% methanol) was obtained. Then, 1 mL aqueous solutions containing 0.8 mg/L of DD were added sequentially. After each addition, the ATR-FTIR spectrum was obtained, supernatant was decanted carefully and this procedure was repeated for a total of 21 additions. FTIR spectra were obtained using the MCT detector. The unapodized resolution for the FTIR spectra was 2.0 cm^{-1}, and a total of 64 scans were collected for each spectrum. Polarized ATR-FTIR spectra were obtained using a wire grid polarizer placed between the interferometer and the ATR cell. Spectra were obtained using perpendicular (S) and parallel (P) polarized light and are referenced as A_s and A_p (Johnston and Premachandra, 2001; Ras et al., 2003). Reference spectra of 9.2 mg DD dissolved in 50μl of CHCl$_3$ were obtained in a variable path length transmission cell fitted with ClearTran IR windows with an approximate pathlength of $\sim$ 20 μm (Perkin-Elmer). The FTIR spectra were collected with the unapodized resolution 2.0 cm^{-1}, and a total of 64 scans were collected.

2.3.5   Raman Spectroscopy

Raman spectra of crystalline DD, DD in CCl$_4$ and SSCF of clay-DD complex were obtained on an Acton Research Corporation SpectroPro500 spectrograph. A Melles-Griot helium–neon laser with 632.8 nm wavelength and a power output of 35 mW measured at the laser head was used as the excitation source. Raman-scattered radiation was collected in a 180-degree backscattering configuration. The entrance slits to the spectrograph were set to 50 μm. The spectrograph used a holographic super notch filter to eliminate Rayleigh scattering. The detector was a Princeton Instruments liquid N$_2$ cooled CCD detector. The spectrograph was calibrated daily

using a Ne-Ar calibration lamp based upon known spectral lines. The Grams/32 AI 6.00 program (Thermo Scientific, Waltham MA) was used to analyze and plot spectra.

2.3.5.1   Self-Supporting Clay Films of Cs-saponite DD Complex

The SSCFs of DD sorbed Cs- saponite used for FTIR analysis was also used for Raman analysis. The SSCF was mounted on a SpectRIMslide (Tienta Science, Inc. Indianapolis, In.). Raman spectra of the SSCF of Cs-saponite - DD complex were collected through an Olympus BX-60 microscope using a 50X objective and 180s of acquisition on the CCD array.

2.3.5.2   Solution Spectra of DD

Ten mg of DD was dissolved in 50 µl CCl_4. DD solution in CCl_4 was filled in a glass capillary tube and both ends were sealed. A Raman spectrum was collected through an Olympus BX-60 microscope using a 50X objective using 120s of acquisition on the CCD array.

2.3.6   X-ray Diffraction (XRD)

X-ray diffraction patterns of Cs-saponite-DD complexes were collected using a PANalytical B.V. (Model X'Pert PRO diffractometer; Almelo, Netherlands) using Co radiation. Dilute clay suspensions containing 10 mg of Cs-saponite in a volume of 900 mL, equilibrated with different DD concentrations, were passed through membrane filters (47 mm, 0.45 µm pore size, Millipore Co. Bedford, MA). The clay particles were then transferred into a vial and mixed with 200 µl of supernatant to form a slurry which was deposited on a glass slide and dried overnight at ambient conditions to obtain an oriented clay film. Data were collected from $2°$ to $60°$ 2θ, counting for 1 s every 0.02^0 2θ step. A 1^0 exit Soller slit was used between 2 to 12^0 2θ. Data analysis was done using X'Pert HighScore Plus software Version 2.2 (PANalytical B.V.).

2.3.7   Computational Analysis:

Molecular structures and crystal lattice structures of DD were generated using Material Studio Version 4.2 software (Accelrys, Inc., San Diego CA). The structure of DD was from Cordes and Fair (Cordes and Fair, 1974). The DFT method was utilized in geometry optimization, and subsequent IR and Raman harmonic vibration frequency calculations. The *ab initio* calculations were performed at the level of hybrid Becke-3Lee-Yang-parr parameters (B3LYP) density functional theory with the 6-31 G** basis set using the Gaussian 03W version (Scholtzova et al., 2003). The geometry optimization was done and the optimized geometry was characterized as a local minimum by harmonic vibration analysis. In order to compare the predicted vibration frequencies directly with experimental frequencies the predicted frequencies were scaled by a factor of 0.9628.

2.4   Results

Sorption isotherms of DD from aqueous suspension were strongly influenced by the nature of the exchangeable cation (Fig. 2.1A). Cs-saponite showed the highest affinity for DD and sorption decreased in the order ($Cs^+ \gg Rb^+ > K^+ > Na^+$). The amount of DD sorbed on Cs-saponite was ~ 300 times > than that on Na-exchanged saponite. In addition, sorption was dependent on clay type with Cs-saponite showing the highest affinity for DD followed by Cs-Upton montmorillonite and Cs-SWy2 montmorillonite (Fig. 2.1B). In the case of Cs-saponite, the highest amount of DD sorbed in our experiments was ~9000 mg kg-1, or 0.9 % (wt. /wt.).
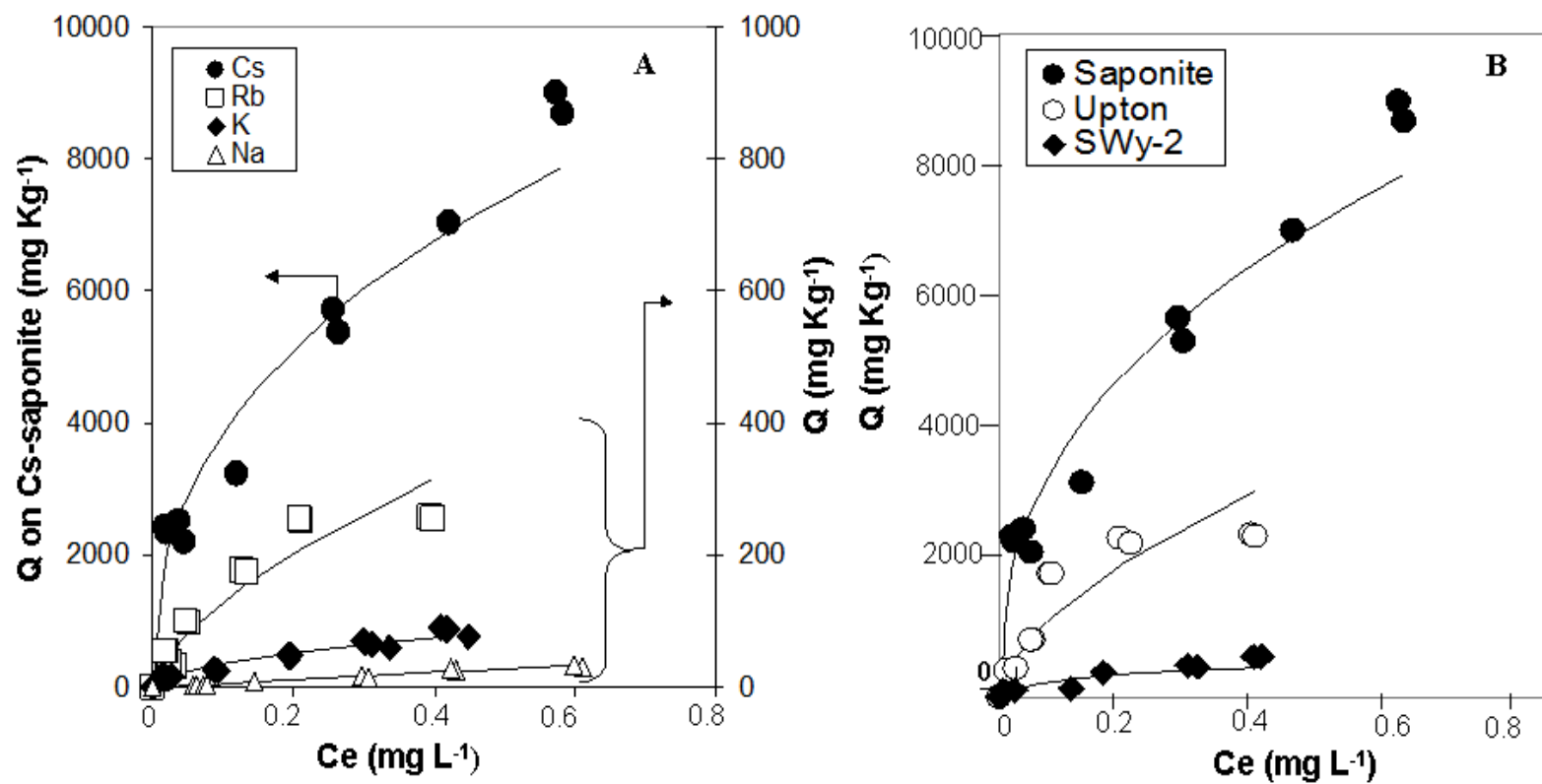
Figure 2.1 Aqueous HPLC derived sorption isotherm of DD on A) saponite saturated with different exchangeable cations, and B) Cs-saturated smectites (saponite, Upton and SWy-2).

The sorption isotherms were fitted using the Freundlich sorption model and the K_f and n values are summarized in Table 2.2.

These sorption results are in excellent agreement with a recent companion study of DD sorption to smectite (Liu et al., 2008).

Table 2.2 The value of Freundlich parameters for the dibenzo-p-dioxin sorption on smectites used in this study.

Clay	K_f (mg$^{(1-1/n)}$ kg^{-1}L$^{1/n}$)	1/n
Cs-SWy-2	691	0.40
Cs-Upton	5668	0.60
Cs-Saponite	98111	0.40
Rb Saponite	571	0.65
K-Saponite	119	0.52
Na-Saponite	58	1.03

The d-spacing of DD-Cs-saponite complexes increased from 1.23 to 1.49 nm with increasing DD surface loading (Figure 2.2). For Cs-saponite without DD, the X-ray diffraction pattern (Fig. 2.2A) revealed a d-spacing of 1.23 nm, which corresponds to the one layer hydrate Cs-saponite. The thickness of the clay is approximately 0.96 nm and that of a layer of water is ~0.27 nm. As the surface loading of DD increased, the d-spacing increased to a value of 1.49 nm (Figure 2.2). In a companion study of DD sorption on smectite clays, Liu et al. (2008) have demonstrated that the d-spacing of the Cs-saponite-DD complex increased from 1.23 to 1.52 nm with increasing concentration of DD in solution.

The macroscopic sorption and XRD data shown in Figure 2.2 provide the basis for the spectroscopic investigation in two ways. First, they confirm the sorption and intercalation of DD

by the smectite. Second, the spectroscopic measurements were integrated with the sorption data such that the DD-Cs-saponite complexes analyzed in the sorption study provided samples of known DD surface loading for the spectroscopic studies.

Figure 2.3 presents a summary of spectroscopic data from various experiments. The lower three spectra correspond to *in-situ* attenuated total reflectance (ATR)-FTIR spectra of water (Figure 2.3A), Cs-saponite (Figure 2.3B) and DD sorbed on Cs-saponite (Figure 2.3C). The most prominent bands are the OH stretching (~3500 cm^{-1}) and bending (1639 cm^{-1}) bands of water in Figure 2.3A-C. In addition, the ν(Si-O) bands of the Cs-saponite at 1016 and 974cm^{-1} are clearly evident in the spectra of Cs-saponite and of DD-Cs-saponite (Figure 2.3B and 2.3C, respectively).
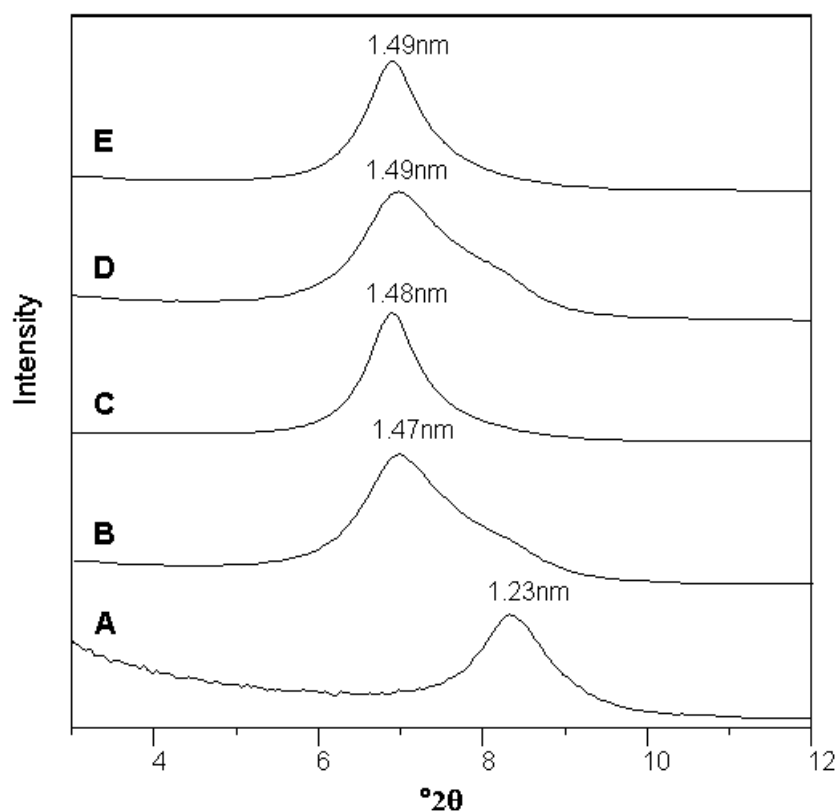
Figure 2.2 X-ray diffraction patterns of Cs-saponite clay films equilibrated with 0, 0.08, 0.2, 0.4, 0.6 mg/L concentrations of DD (A to E). Numbers on top of each XRD patterns correspond to basal d-spacings of Cs-saponite.

The ATR-FTIR spectrum of DD sorbed to Cs-saponite from aqueous suspension is shown in Figure 2.3C and the bands of sorbed dioxin are very weak (shown in the rubber-band box) and consist of three bands at 1493, 1285 and 1298 cm^{-1}. The region within this box is expanded by 50x along the y-axis and is shown in Figure 2.3D. For comparison, the DD bands in the ATR-FTIR spectrum of DD-Cs-saponite are similar to the ATR-FTIR spectrum of DD dissolved in CHCl$_3$ (shown in Figure 2.3E) and to the transmission FTIR spectrum of crystalline DD (Figure 2.3F). The Raman spectrum of DD sorbed to Cs-saponite is shown in Fig. 2.3G and is compared to the spectrum DD in CCl$_4$ and crystalline DD (Figure 2.3H and I, respectively). Band positions of DD and DD sorbed on Cs-saponite and their assignments are listed in the Table A.2 (appendix A).

In situ ATR-FTIR spectra of DD sorbed to Cs-saponite from aqueous suspension are shown in Figure 2.4A. Cs-saponite was deposited on the ZnSe internal reflection element from aqueous suspension (Spectrum B in Figure 2.3). The Cs-saponite deposit was stable to repeated washing as monitored by measuring the absorbance of the v(Si-O) bands at 1016 and 974 cm^{-1} in agreement with prior work (Johnston and Premachandra, 2001). The Cs-saponite deposit was dosed with different amounts of DD dissolved in water containing 0.1% methanol (solubility limit was ~0.9 mg L^{-1}).
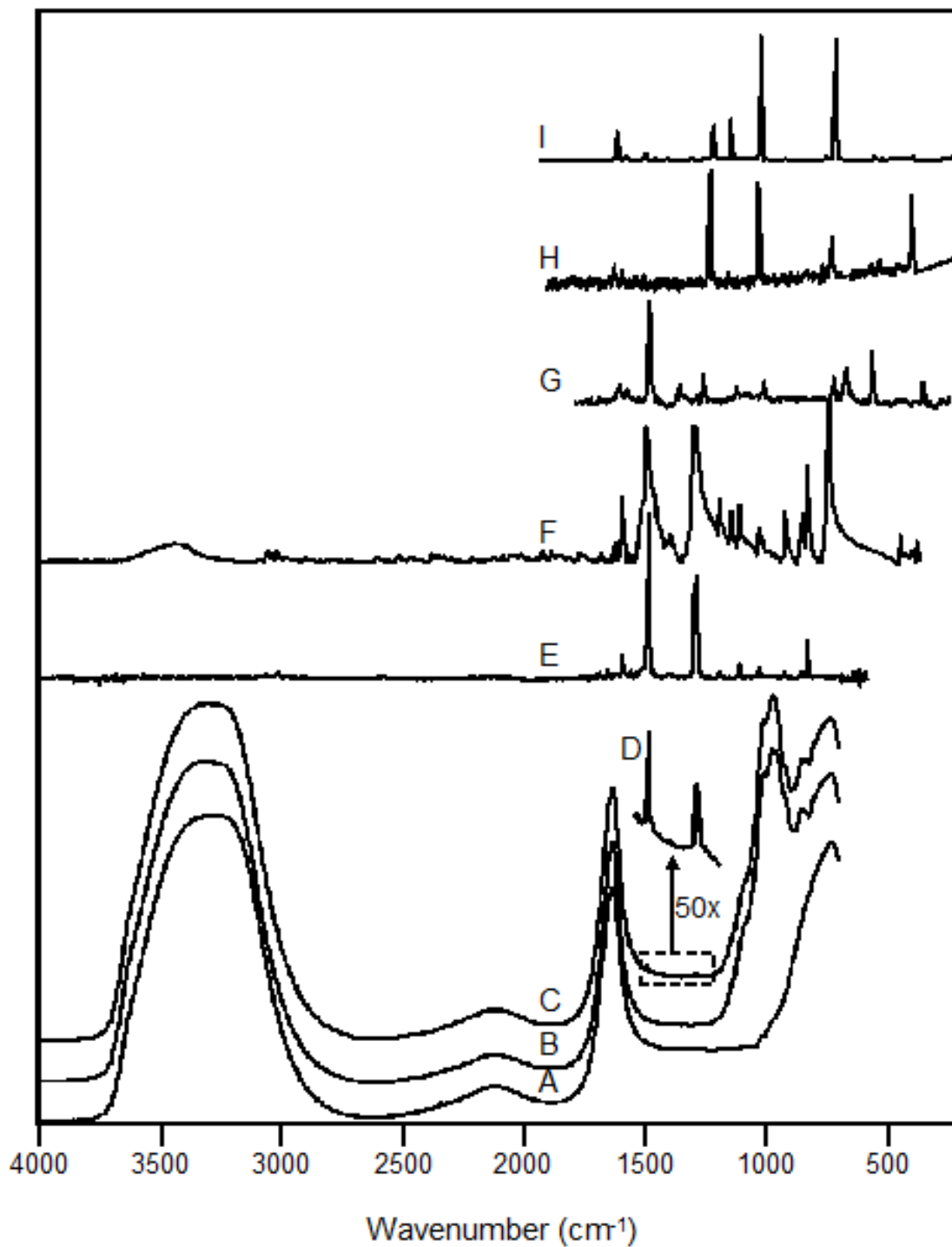
Figure 2.3. Survey ATR-FTIR spectra of (A) H_2O, (B) Cs-saponite in water, (C) Cs-saponite and aqueous suspension of DD, (D) the extended view of spectrum C showing the diagnostic vibration bands of DD sorbed in clay, (E) transmission IR spectra of crystalline DD in KBr pellet,(F) transmission IR spectra DD in $CHCl_3$,(G)Raman spectra of DD- Cs-saponite complex, (H) Raman spectra of DD in CCl_4, and (I) Raman spectra of crystalline DD.
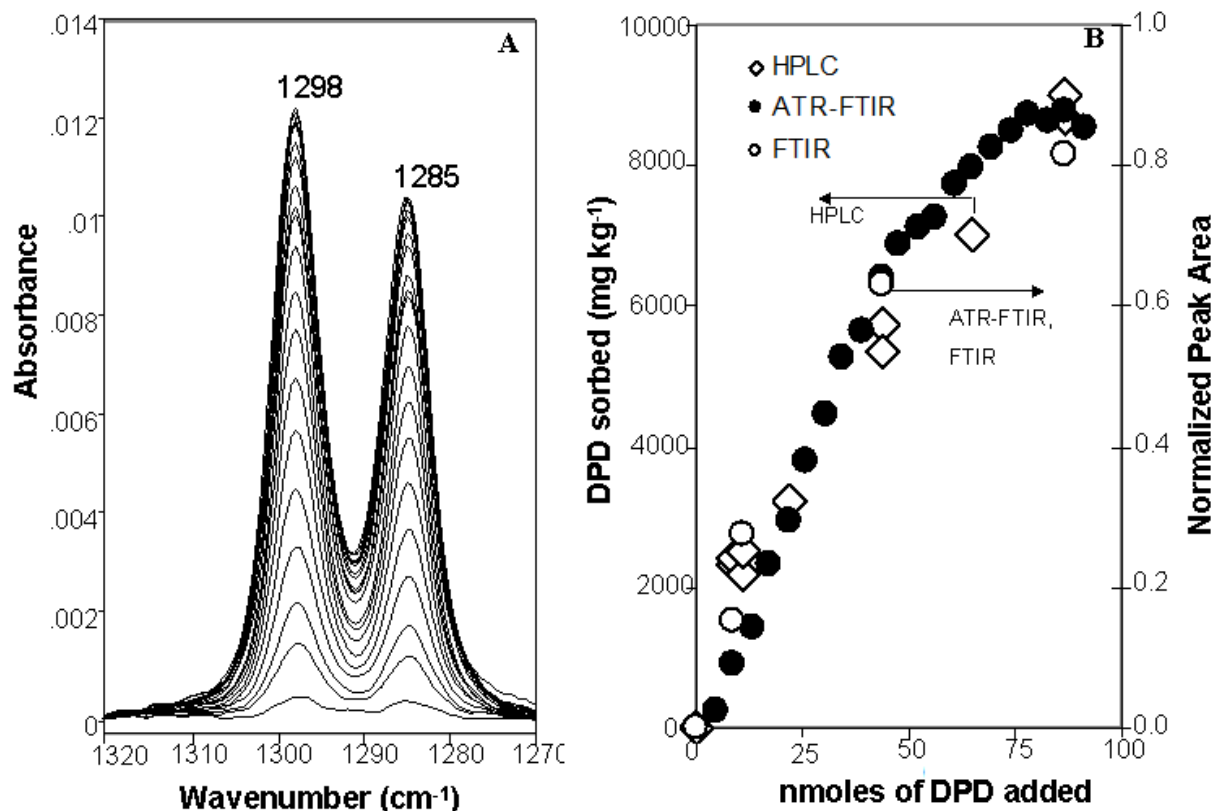
Figure 2.4. ATR-FTIR sorption isotherm of DD was generated using the peak area of coupled 1285 and 1298 cm^{-1} band (A) and plotted them against the amount of dioxin added through 21 sequential 1 mL additions of 0.8 mg L^{-1} DD (B). Spectroscopic sorption data were compared to the HPLC derived batch sorption data. In addition to ATR-FTIR sorption data, FTIR spectra of self-supporting clay films of DD-Cs-saponite complex were also collected and peak area plotted against initial dioxin concentrations are shown on the right side (B).

The intensity of the DD bands at 1298 and 1285 cm^{-1} increased as the amount of DD added increased from 0 to ~ 90 nanomoles of DD. The increase in intensity of the DD bands as a function of the amount of DD added is shown in Figure 2.4B. For comparison, the sorption isotherm of DD to Cs-saponite measured using HPLC is included in Figure 2.4B. The spectra shown in Figure 2.4A correspond to *in situ* ATR-FTIR spectra. Spectra were also obtained from self-supporting clay films (e.g., Figure 2.5C) and these data are represented by the open circles in Figure 2.4B.

The spectral data from ATR-FTIR and self-supporting clay films provide direct evidence that DD is sorbed and that there is good agreement between the macroscopic sorption and spectroscopic results.
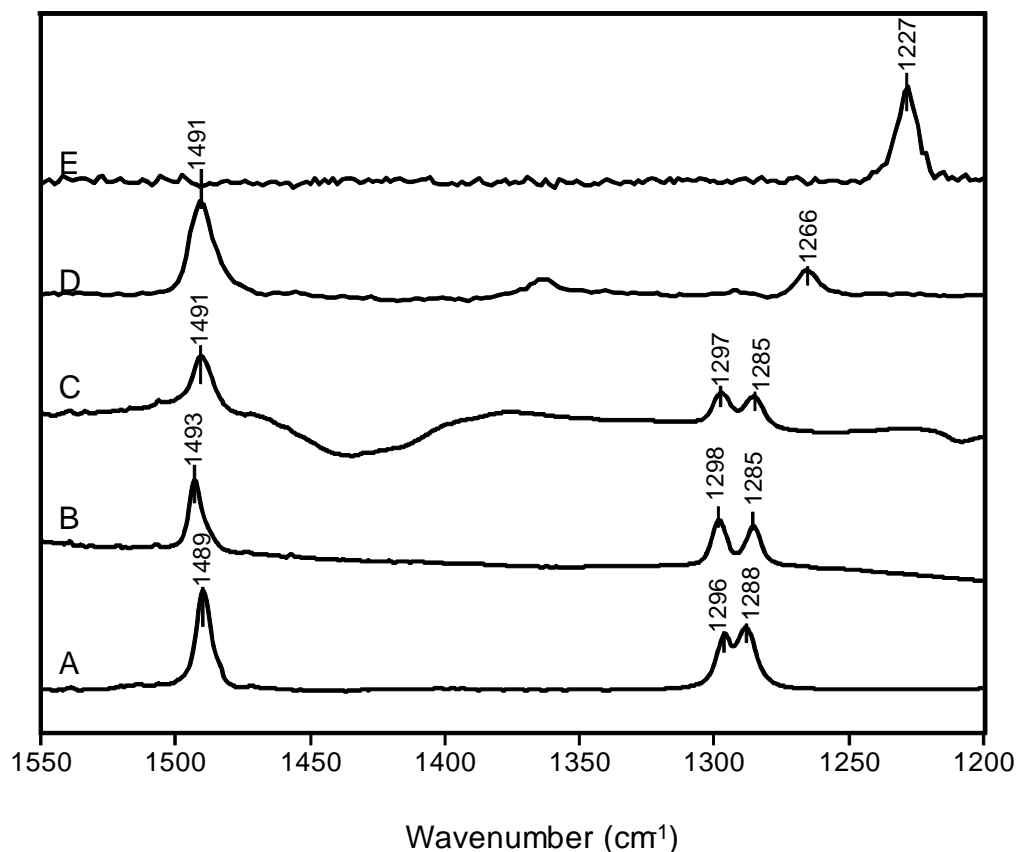
Figure 2.5. Comparison of FTIR spectra of A) DD in CHCl$_3$, B) DD sorbed from water to Cs-saponite film on ZnSe ATR cell, C) self-supporting clay film (SSCF) of DD-Cs-saponite complex, D) Raman spectra of SSCF of DD- Cs-saponite complex, and E) Raman spectra of DD in a CCl$_4$ in the region of 1500-1200 cm^{-1}.

Expanded views of FTIR, ATR-FTIR and Raman spectra of DD sorbed on Cs-saponite in the 1550 to 1200 cm^{-1} region are shown in Figure 2.5. The bottom three spectra (Figure 2.5A-C) correspond to DD in CHCl$_3$, ATR-FTIR, and transmission FTIR spectra of DD-Cs-saponite complexes, respectively. As shown in Figure 2.3 and Figure 2.5, the dominant DD bands appear

at approximately 1490, 1296 and 1288 cm^{-1} in the FTIR spectra and at 1491, 1363, 1293 and 1266 cm^{-1} in the Raman spectra (Figure 2.5D).

For comparison, the solution Raman spectrum of DD in CCl$_4$ is shown in Figure 2.5E and is characterized by a band at 1227 cm^{-1}. The band positions of DD in solution and solid DD are listed in the Table A.1 (Appendix A) along with their vibrational assignments. It is interesting to note that the Raman-active DD features of the DD-Cs-saponite complex show bands that are similar to IR-active modes; however, these features are absent in the Raman spectrum of DD in solution.

Table 2.3 Band positions of vibrations bands of dibenzo-p-dioxin sorbed in saponite exchanged with alkali metal cations.

Clay /solvent	Band position	Band Area	Intensity ratio ($I_{\nu 49}/I_{\nu 50+\nu 51}$)
Cs-saponite	1493.0	0.1547	0.89
	1297.9	0.0923	
	1285.1	0.0821	
Rb-saponite	1490.9	0.0310	0.90
	1285.2	0.0223	
	1297.8	0.0121	
K-saponite	1488.5	0.0119	0.94
	1285.9	0.0079	
	1296.3	0.0047	
Na-saponite	1487.7	0.0134	1.07
	1296.8	0.0032	
	1286.8	0.0092	
CHCl$_3$	1489.0	0.9001	0.78
	1296.5	0.4609	
	1288.0	0.6953	

To examine the influence of the exchangeable cation on the sorption of DD, in situ ATR-FTIR spectra of DD sorbed to M-saponite (M = Cs^+, Rb^+, K^+ and Na^+) were obtained. The three principal DD bands of interest at 1288, 1296 and 1490 cm^{-1} were fitted to mixed Gaussian-Lorentzian line shapes in the Figure 2.6 and the results are shown in Table 2.3. The 1288 and 1296 cm-1 bands are assigned to asymmetric C-O-C stretching bands (νCOC (asymm)) and the 1491 cm^{-1} band to a combined aromatic ring skeleton vibration and C-H in plane bend (Eriksen et al., 2008; Gastilovich et al., 2000; Grainger et al., 1988, 1989). The observed band positions and intensities are given in Table 2.3 Band positions of vibrations bands of dibenzo-p-dioxin sorbed in saponite exchanged with alkali metal cations.
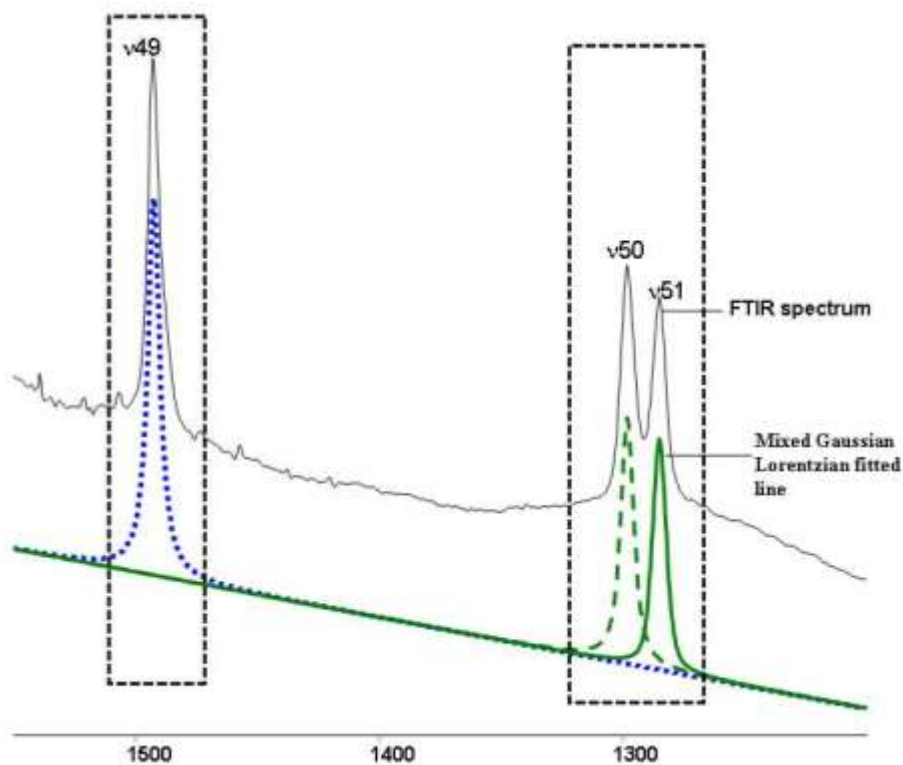
Figure 2.6. Peak-fitted spectra of DD –Cs-saponite complex in the region of 1520 - 1270 cm^{-1}. Peak fitting was done using mixed Gaussian-Lorentzian function. Peak intensity and Peak area of fitted spectra were used for quantitative and qualitative analysis of DD sorbed to smectite clay with different exchangeable cations.

As shown in Figure 2.7 both the position and intensity of the DD bands were influenced by the nature of the exchangeable cation. The position of the C-O-C stretching band (~1288 cm^{-1}) increased as the enthalpy of hydration increased. In contrast, the position of the aromatic skeleton *in plane* ring stretching band at 1491 cm^{-1} decreased. As shown in Figure 2.7, both the position and intensity of the DD bands were influenced by the nature of the exchangeable cation. The position of the C-O-C stretching band (~1288 cm^{-1}) increased as the enthalpy of hydration increased. In contrast, the position of the aromatic skeleton *in plane* ring stretching band at 1491 cm^{-1} decreased.
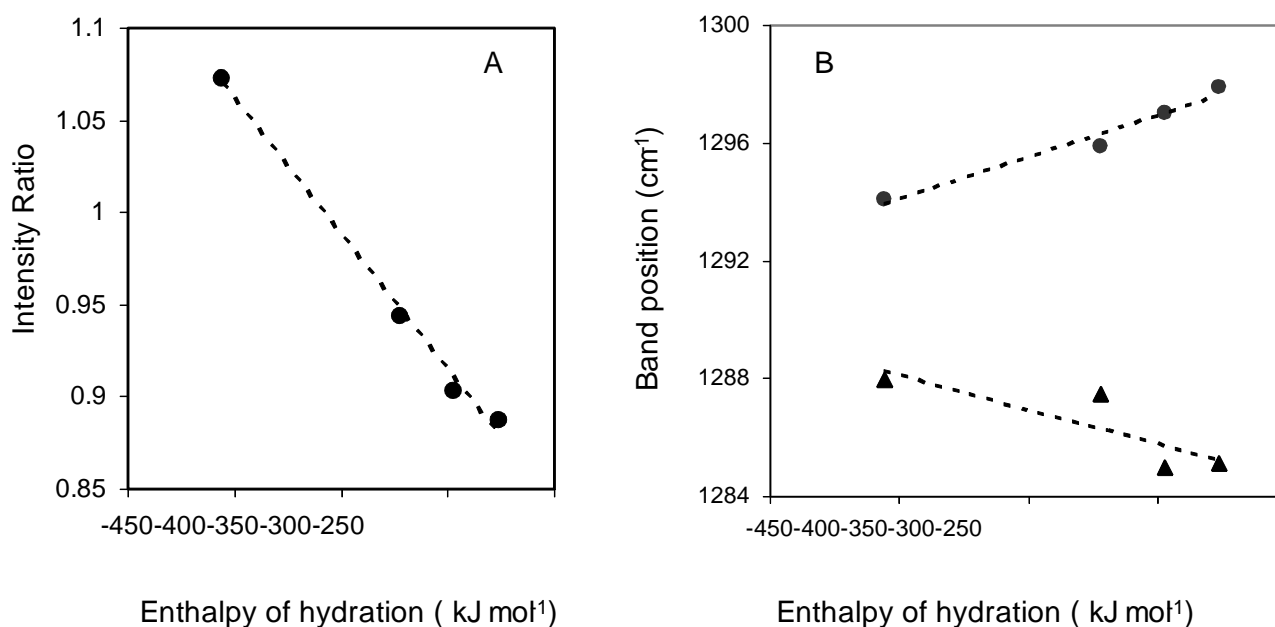
Figure 2.7 Intensity ratio of the 1491 cm-1 /(1295 + 1288 cm-1) bands (left side), and the positions of 1295 and 1288 cm-1 bands as a function of the enthalpy of hydration of the exchangeable cations.

Polarized ATR-FTIR spectra were obtained to determine the molecular orientation of DD sorbed on Cs-saponite with respect to the plane of the siloxane surface (Johnston and

Premachandra, 2001; Ras et al., 2003; Ras et al., 2007). A schematic representation of the ATR cell, with the conventional axis system defined is shown in Figure 2.8 and follows prior work (Ahn and Franses, 1992; Ras et al., 2007). The refractive indices are defined as that of the IRE (n_1), clay (n_2) and water (n_3). Parallel (P) polarization is contained within the x-z plane and results in an evanescent wave polarized in both the x and z axis, E_x, and E_z. Perpendicular (S) polarization produces an evanescent wave with an electric field amplitude solely in the y axis, E_y. The differential response between spectra recorded with S and P polarization can be used to determine the molecular orientation of solutes at the IRE interface. We will refer to ATR-FTIR spectra recorded with S and P polarization as A_s and A_p.
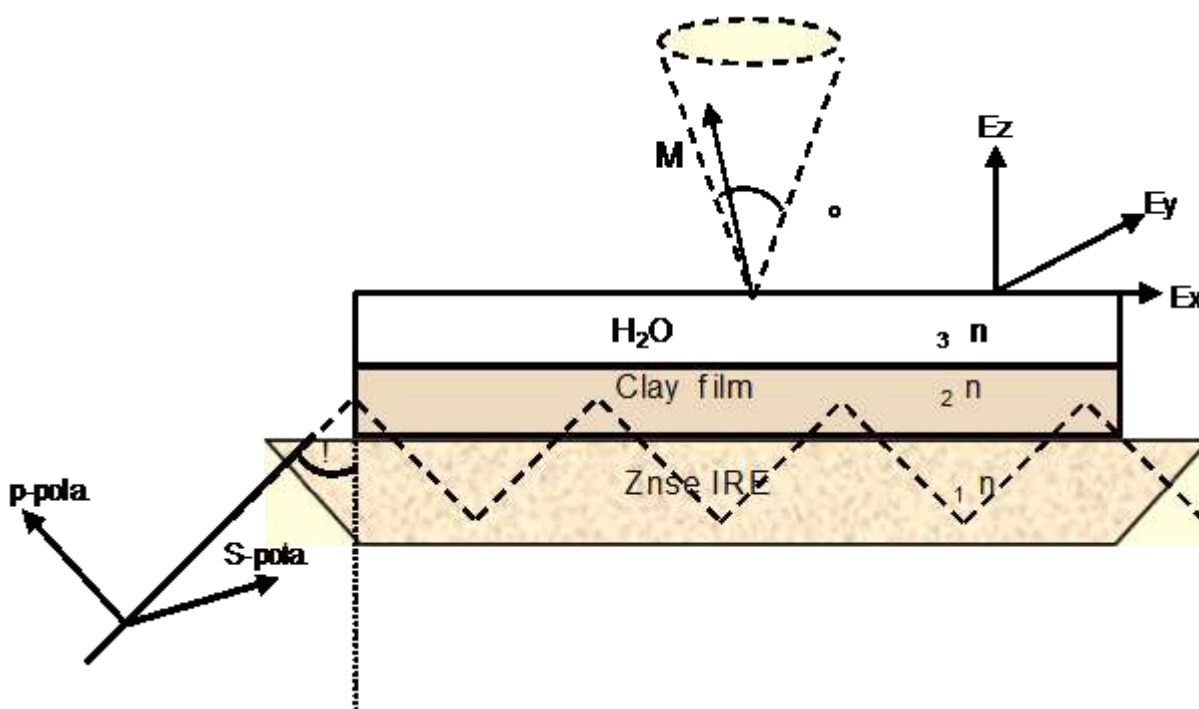
Figure 2.8 Schematic presentation of polarized ATR-FTIR study for the orientation of DD sorbed on thin clay film of refractive index n_2 on the ZnSe internal reflection element of refractive index n_1 in contact with water medium of refractive index n_3. In uniaxially oriented films, the transition dipole moments (M) have a preferred tilt angle (γo). In this configuration s-polarized light probes the y component of the film and p-polarized probes the x- as well as the z-components of the film.

In prior work, we have demonstrated that the [001] plane of individual clay layers are oriented parallel to the surface of IRE (contained in the x-y) plane (Johnston and Premachandra, 2001;Ras et al., 2007;Ras et al., 2003). We used the thin film model (also called three phase approximation) in this study to estimate the tilt angle of the transition moments of the three DD vibrational bands relative to the surface of the IRE (Koppaka and Axelsen, 2001). The development of the model and underlying assumptions for polarized ATR-FTIR studies of ultra-thin clay-containing Langmuir-Blodgett (LB) films has recently been reported (Ras et al., 2007; Koppaka and Axelsen, 2001). The model is applied here to provide some estimate of the molecular orientation of sorbed DD to Cs-saponite. In the three phase approximation (Ras et al., 2007), the electric field amplitudes can be expressed as:

$$E_x := \frac{2\cos(\beta)\left(\sin(\beta)^2 - n_{31}^2\right)^{0.5}}{\left(1 - n_{31}^2\right)^{0.5}\left(\left(1 + n_{31}^2\right)\sin(\beta)^2 - n_{31}^2\right)^{0.5}} \quad (1)$$

$$E_y := \frac{2\cos(\beta)}{\left(1 - n_{31}^2\right)^{0.5}} \quad (2)$$

$$E_z := \frac{2\sin(\beta)\cos(\beta)\, n_{32}^2}{\left(1 - n_{31}^2\right)^{0.5}\left(\left(1 + n_{31}^2\right)\sin(\beta)^2 - n_{31}^2\right)^{0.5}} \quad (3)$$

The dichroic ratio is defined as:

$$D = \frac{A_s}{A_p} \quad (4)$$

For a uniaxially oriented thin film, the dichroic ratio, D, can also be calculated based on E_x, E_y and E_z and the tilt angle of the transition moment according to Eq. (5) (Grahn et al., 2008).

$$D = \frac{E_y^2 \sin^2 \gamma}{E_x^2 \sin^2 \gamma + 2E_z^2 \cos^2 \gamma} \quad (5)$$

Where γ is the angle between the surface normal and the transition moment of the molecule. The dichroic ratios (D values) of the DD bands are given in Table 2.4 and range from 0.98 to 1.14.

Table 2.4 Band position, band intensities, dichroic ratios (D) and tilt angle (γ) of observed dibenzo-p-dioxin (DD) bands in the polarized ATR-FTIR spectra obtained using ZnSe IRE with 45° angle of incidence.

Band	Band intensity		$D(A_s/A_p)$	γ [a]
	A_p	A_s		
1493	0.0188	0.0199	1.0615	65
1298	0.0116	0.0118	1.0115	64
1854	0.0115	0.0113	0.9819	63
980	1.1100	1.2700	1.1441	67

[a] Average tilt angle (γ) of the IR transition dipole moment was calculated using the refractive index of ZnSe (2.406), Clay: saponite (1.504) and water (1.333)

The calculated tilt angles are listed in Table 2.4 and indicate, on average, that the molecular plane of DD is tilted on the clay surface making an angle of approximately 25° with respect to the clay surface. The observed D values are included in the Figure 2.9 and absorbance values, dichroic ratios and calculated tilt angles from Eq. (5) given in Table 2.4.
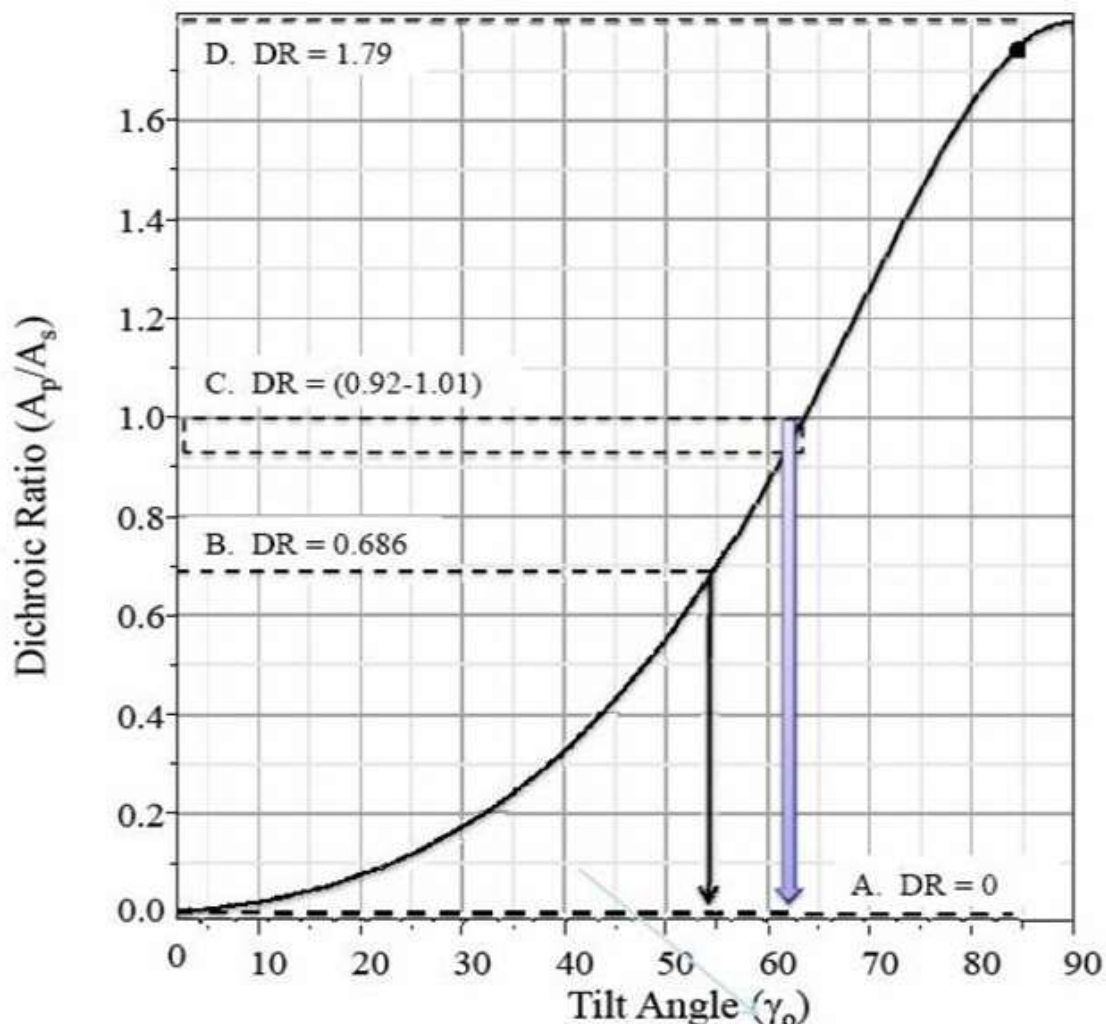
Figure 2.9. Relationship between ATR dichroic ratios (D) and tilt angle (γ) of solute with respect to the surface of IRE. A, B, and D indicate the solute is oriented perpendicular, parallel, and isotropically to the IRE surface, respectively. The relationship between the dichroic ratio and tilt angle of DD sorbed on Cs-saponite are shown in C. Average tilt angle (γ) of the IR transition dipole moment was calculated using the refractive index of ZnSe (2.406), Clay: Saponite (1.504) and water (1.333) and angle of incidence 45°.

2.5   Discussion

The sorption and X-ray diffraction results shown in Figs. 2.1-2.2 are in good agreement with a recent study of DD sorption to smectites from aqueous suspension confirming the high affinity of DD for Cs-saponite (Liu et al., 2008). The nature of the exchangeable cation was the

strongest determinant that governed DD sorption consistent with (Liu et al., 2008). This can be explained, in part, by the fact that Cs^+ has the lowest enthalpy of hydration (-315 kJ mol^{-1}) of the other cations studied (i.e., Rb^+, K^+, Na^+, and Ca^{2+}) (Aggarwal et al., 2006; Johnston and Tombacz, 2002). In addition, Cs^+ can form an inner sphere complex with the siloxane ditrigonal cavity so that part of the cation is sequestered in the clay structure further lowering its affinity for water (Labouriau et al., 2003; Sutton and Sposito, 2001). The net result is that the interlamellar region of Cs-smectite is less-hydrated; creating a less hydrophilic interlayer environment that is more favorable for sorption of DD.

The structural formulae for the SapCa-2 saponite, Upton and SWy-2 montmorillonites are given in Figure 2.10 Saponite is a trioctahedral 2:1 phyllosilicate with isomorphous substitution exclusively located in the tetrahedral layer (Figure 2.10). In contrast, both Upton and SWy-2 montmorillonites are dioctahedral smectites with > 95 % of their charge originating from isomorphous substitution in the octahedral layer (Figure 2.10). In the case of saponite, the charge deficit is manifest only on one side of the siloxane surface and the charge is distributed over a comparatively small number of siloxane oxygen atoms. This is represented schematically by the small circles in Figure 2.11A.

Based on this simple mode, only ~ 9% of the siloxane surface would be directly impacted by isomorphous substitution. In contrast, the charge in dioctahedral montmorillonites is more delocalized over the siloxane oxygen atoms and, unlike saponite, this occurs on both sides (and Figure 2.10 and Figure 2.11B). The net result is most of the siloxane surface of Upton and SWy-2 montmorillonite would have been impacted by these types of structural charge imbalances (Fig. 2.8B). Thus, the reactive siloxane surfaces of saponite, and SWy-2 and Upton montmorillonites are distinct.

Isomorphous Substitution of Mg → Al in the octahedral layer (montmorillonite)

0.7 nm
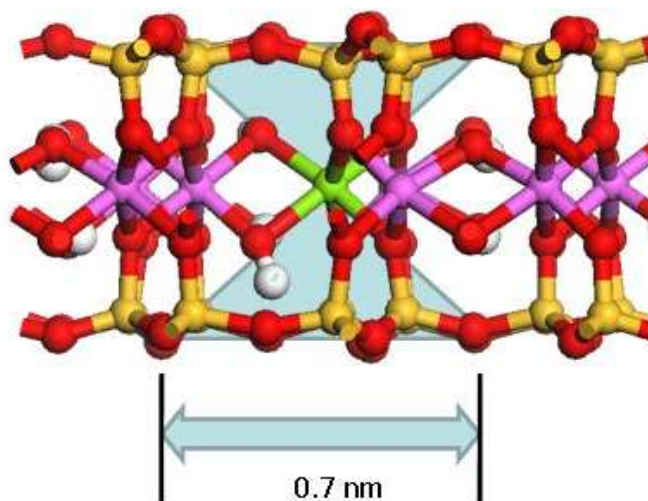
Isomorphous Substitution of Al → Si in the tetrahedral layer (saponite)

0.3 nm
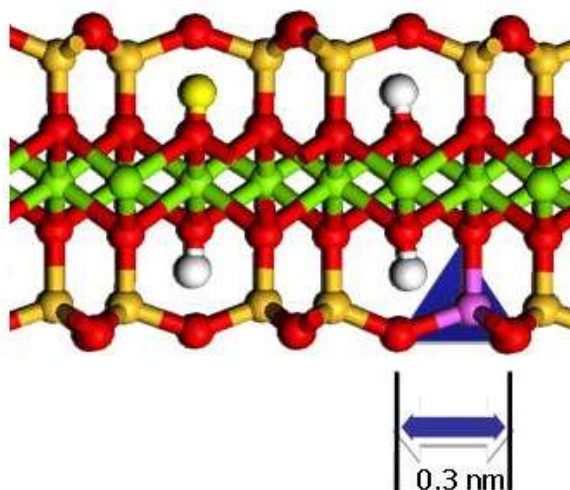
Figure 2.10. Ball and stick representation of charge distribution on smectite clay with isomorphic substitution in octahedral sheet (top) and tetrahedral sheet (bottom) representing the approximate charge distribution for montmorillonite and saponite, respectively.
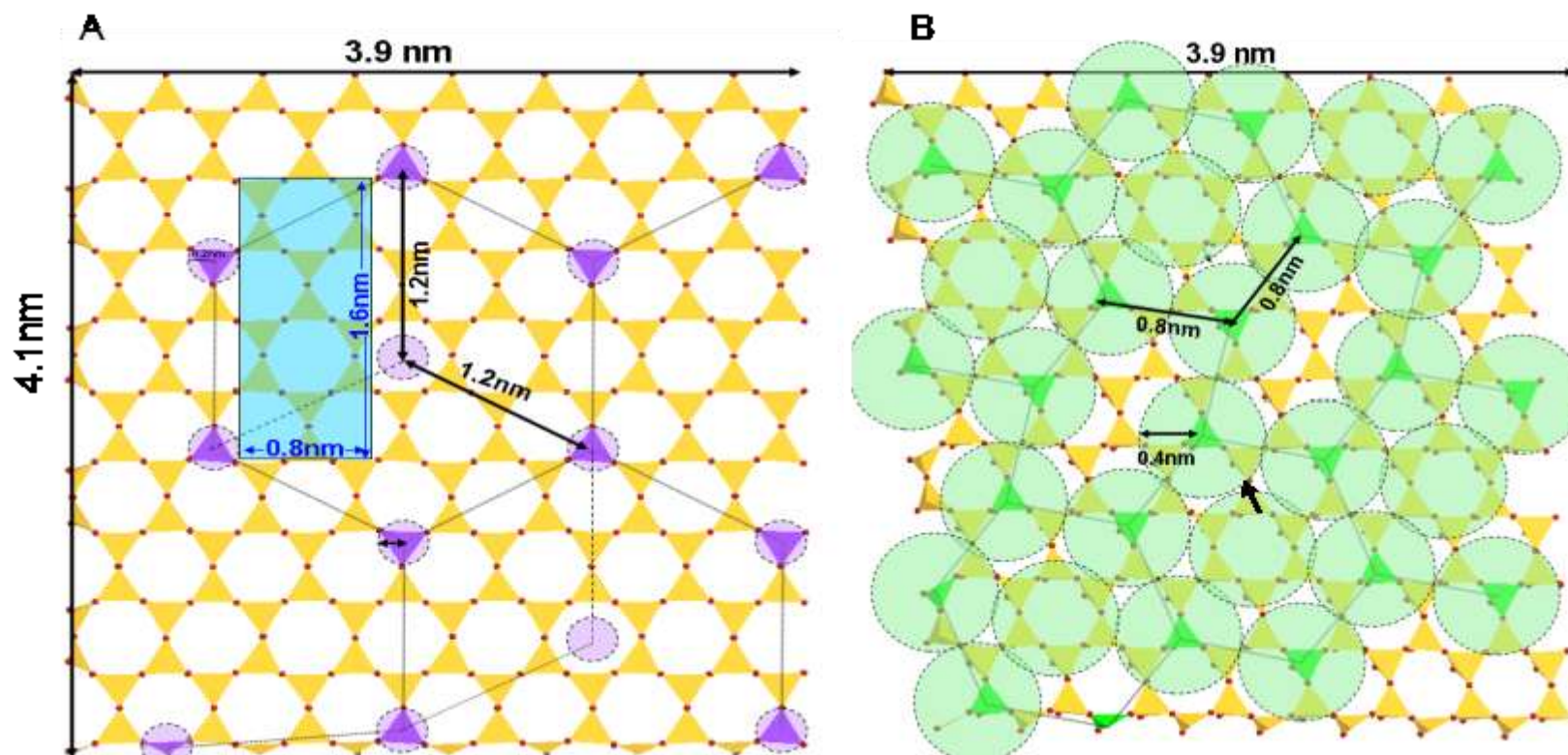
Figure 2.11 Schematic diagram of charge distribution on smectite clay with isomorphic substitution in tetrahedral layer (A) and octahedral layer (B) on the hydrophobic DD adsorption domain in the smectite. Charge distribution on clay surface was calculated using total surface area of 750 m^2 g^{-1} and cation exchange capacity 94 cmol$_c$ kg^{-1}.

The preference of DD for saponite over montmorillonite may be due to the fact that Cs^+ ions have a greater tendency to form inner-sphere surface complexes with the more localized tetrahedral substitution sites of saponite (Sutton and Sposito, 2001). As discussed earlier, we hypothesize that a portion of the Cs^+ ion is keyed into the siloxane surface, lowering the effective enthalpy of hydration of these ions.

A second possibility is that more 'charge neutral' siloxane surface (siloxane surface not influenced by isomorphous substitution) is available on saponite and this neutral surface may, in turn, be able to interact favorably with the planar hydrophobic DD through *Van der Waals* interactions. A third possibility is that because tetrahedrally charged smectites tend to swell less than those with similar octahedral charge, the saponite may be less swollen in water, providing a less hydrated environment for the hydrophobic DD. It is interesting to observe the clay-dependent affinity of DD for smectite, which is similar to the clay-dependent sorption observed for triazines (Laird et al., 1992) and nitroaromatics.(Johnston et al., 2001; Johnston et al., 2002; Sheng et al., 2002). In the case of DD sorption, however, DD shows a much stronger affinity for Cs^+ versus K^+-smectite relative to prior work.

The d-spacing of the DD-Cs-saponite complex is 1.49 nm suggesting that DD is tilted with respect to the surface of the clay. Based on the observed dichroic ratios and application of the uniaxially oriented thin film model, the molecular plane of DD has an average tilt angle of ~ 25 ° with respect to the clay surface (assuming that the clay particles are contained within the x-y plane of the IRE). One possible representation of the DD-Cs-saponite complex is shown in Figure 2.12 where the short axis of DD (in plane) is tilted on a Cs^+ion in clay interlayer. In prior work, we have shown that nitroaromatic compounds are preferentially oriented with their molecular plane

parallel to the siloxane surface of smectites exchanged with K^+ resulting in a d-spacing value of 1.25 nm (Sheng et al., 2002) in contrast to the tilted configuration observed here.

The quantitative ATR-FTIR results (Figure 2.4) demonstrate that ATR-FTIR methods can be used to observe DD on smectites even at very low concentrations. Furthermore, these results provide a link between the macroscopic sorption behavior and the molecular mechanisms of interaction such that the molecular level scale information provided by our spectral data is relevant to DD sorption observed in batch studies of sorption in clay suspension. In general, the band positions and intensities of DD observed using ATR-FTIR and transmission spectra were in agreement with each other and showed modest shifts relative to each other and to reference spectra. In contrast, the Raman spectrum of DD sorbed to Cs-saponite (Figure 2.3G and Figure 2.5D) is very different compared to Raman spectra of DD in organic solutes (Figure 2.3H and Figure 2.5E) or crystalline DD (Figure 2.3I). In fact, the Raman spectrum of DD sorbed to Cs-saponite is characterized by a relatively strong band at 1491 cm^{-1} which is not observed in the spectrum of DD dissolved in CCl_4 and this band has only weak Raman intensity in the spectrum of crystalline DD (Figure 2.3I). The molecular symmetry of DD is D_{2h} meaning that DD is centrosymmetric. Certain vibrational bands of DD are Raman-active but not IR-active and vice versa (Cordes and Fair, 1974;Gastilovich et al., 2002). For DD in the crystalline state or in solution, the aromatic stretching band at 1491 cm^{-1} is not Raman active but has strong activity in the IR. The appearance of this band in the Raman spectrum for sorbed DD on Cs-saponite indicates that the selection rules are relaxed resulting from a loss of symmetry. One possible explanation consistent with the spectroscopic and XRD data is that one of the oxygen atoms of a sorbed DD molecule in the clay interlayer is tilted on a Cs^+ ion resulting in a loss of D_{2h} symmetry.
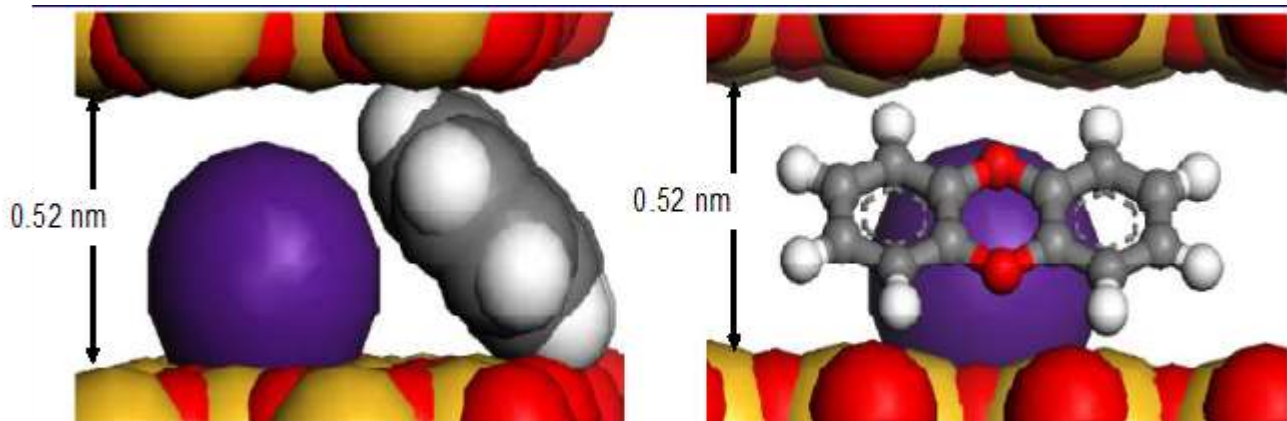
Figure 2.12 Proposed molecular model of DD -smectite complex showing the arrangement of DD in the interlayer space of the smectite clay.

The influence of the exchangeable cations on the vibrational spectra of sorbed DD indicate that the nature of the exchangeable cations exert some influence on the molecular properties of sorbed DD or in the DD-clay interaction. From the macroscopic sorption data, the cation effect is dramatic with Cs-saponite showing a much higher affinity for DD than Na-saponite. One possible explanation is the different cations and their associated waters of hydration function as molecular props with different dimensions. The modest changes that occur in position and relative intensity may be attributed to a siloxane 'slot' with varying dimensions. In our opinion, the data presented here for DD sorbed on Cs-saponite are more consistent with a more direct site-specific interaction. Recent theoretical calculations of DD sorbed to Cs-saponite considered several different modes of interaction between DD and Cs^+ ions in the interlamellar region. Based on theoretical calculations, DD sitting on top of a interlayer Cs^+ ion (Complex II) was the most favored complex on the basis of energetics (Liu et al., 2008). There are two supporting lines of evidence for site specific interactions between DD and Cs-saponite in this study. First, the Raman results clearly show that the selection rules of DD are broken when sorbed on Cs-saponite. The 1491 cm^{-1} and 1266 cm^{-1} bands become prominent in the Raman spectra of the DD-Cs-saponite complex while in solution,

these bands have no Raman activity. These data would suggest that the Raman-active DD bands are locally enhanced. Second, these observations are supported by the cation-induced perturbations. The intensity ratio of ring skeletal vibration band at 1491 cm^{-1} band relative to the asymmetric C-O-C stretching band is linearly correlated to the enthalpy of hydration of interlayer cations (Figure 2.7) and could suggest that DD is sitting on top of or propped up against the interlayer cation (Phillips and Kirkpatrick, 1994) .

The combined application of *in situ* ATR-FTIR and Raman spectroscopy integrated with structural and sorption data reveal that DD shows a surprising dependence on the nature of the exchangeable cation and clay type. Although smectite surfaces are generally viewed as being hydrophilic, the partial hydrophobic character of these clays becomes manifest when weakly hydrated cations, such as Cs$^+$ are present. The unexpected association with of DD on Cs-saponite further reveals an interesting dependence on clay type. Cs-saponite, dominated exclusively by isomorphous substitution in the tetrahedral layer shows a much greater affinity for DD than Cs-exchanged montmorillonites with octahedral substitution. For Cs-saponite, the more localized charge substitution in the siloxane surface may favor the formation of an inner surface complexed Cs ion whose ability to attract water molecules is partially compromised by its proximity to the clay surface, creating a weakly hydrated site with some polar character than can interact favorably with one or both of the dioxin ether linkages.

2.6   Acknowledgement

CHAPTER 3.   MOLECULAR MECHANISMS OF CHLORINATED DIBENZO-P-DIOXINS INTERACTIONS WITH SMECTITES

3.1   Abstract

The molecular interaction of two chlorinated dioxin congeners with a group of expandable 2:1 clay minerals known as smectites was investigated. Prior work found that the non-chlorinated dibenzo-p-dioxin (DD) congener had a surprisingly high affinity for Cs-exchanged smectites. Mechanistic knowledge regarding the sorption of chlorinated dioxin congeners to clay minerals is lacking and is the focus of this study. In order to explore structure-activity relationships, two chlorinated dioxin congeners were selected with the chlorine positions, 1-chloro-dibenzo-p-dioxin (1-ClDD) and 2-chloro-dibenzo-p-dioxin (2-ClDD), which effect steric hindrances and solubility. Homoionic smectites were prepared using three different types of smectites (SWy-2 montmorillonite, Upton montmorillonite, and SapCa-2 saponite) that differed in CEC and the origin of negative charge. The most significant determinant of ClDD sorption was the nature of the interlayer cation with Cs-exchanged smectites showing the highest affinity which is attributed to presence of more hydrophobic surface area. To a lesser extent, 1-ClDD showed a sorption preference for saponite > Upton > SWy-2 which can be explained based on where isomorphic substitution occurs in the clay lattice in each of the three clays. XRD measurements revealed that 1-ClDD molecules were oriented nearly parallel to the siloxane surface of the clay while 2-ClDD adopted a titled orientation, similar to DD. The location of the chlorine constituent in 1-ClDD prevents the molecule from its apparent energetically more favorable orientation. In addition, to the XRD results, in-situ ATR-FTIR spectra revealed that sorption of 1-ClDD to Cs-saponite resulted in the loss of interfacial H_2O. These data suggest the sorption 1-ClDD displaces interlayer H_2O. 2-ClDD is less sterically restricted in the clay interlayer. The sorption free energies were

calculated for 1-ClDD and DD molecules using the adaptive biasing force (ABF) method with an extended interlayer–micropore two-phase model consisting of cleaved clay hydrates and "bulk water". Results indicate that the higher sorption of 1-ClDD is due to the hydrophobic interactions and partial dehydrations.

3.2   Introduction

Chlorinated dibenzo-p-dioxins (PCDDs; also referred to hereafter as dioxins) are a group of exceptionally toxic compounds whose fate and transport in soil and subsurface environments is of continued concern (Denison and Nagy, 2003). Interestingly, dioxins can originate from both anthropogenic and natural sources. Anthropogenic sources of dioxins include uncontrolled solution chemistry of organochlorine products (e.g., by-product of herbicides manufactured from chlorophenols such as 2,4-D), chlorine bleaching of lignin from paper, the chloralkali industry, as well as a waste incineration and, in general, incomplete combustion and pyrolysis including forest fires (Schecter, 1994). In contrast, relatively little is known about dioxins that occur naturally and are associated with clay minerals (Abad et al., 2002; Ferrario and Byrne, 2002; Ferrario et al., 2007; Ferrario et al., 2000; Rappe, 2000; Rappe et al., 1998). 'Prehistoric' clay-dioxin deposits have been found in diverse geologic settings in North America (Ferrario and Byrne, 2002; Ferrario et al., 2007; Gadomski et al., 2004; Holmstrand et al., 2006), Germany (Schmitz et al., 2011), and Australia(Gaus et al., 2002; Gaus et al., 2001; Prange et al., 2002). Regardless of their source, PCDD/Fs represent an important class of highly toxic contaminants and smectite clay minerals are ubiquitous in soils and sediments. It follows that understanding smectite-dioxin interactions will improve our understanding of the fate and transport of PCDD/Fs in the environment.

Mechanisms of non-chlorinated dioxin congener dibenzo-p-dioxin (DD)-smectite interactions are known (Boyd et al., 2011; Liu et al., 2012; Rana et al., 2009). The nature of the exchangeable cation is the primary determinants of DD sorption to smectite with weakly hydrated alkali metal cations showing the highest affinity (i.e., Cs^+). Sorption affinity was attributed a direct cation-DD interlayer interaction that was facilitated by the low enthalpy of hydration of Cs^+ that allowed DD-Cs^+ interactions to occur with minimal competition from H_2O. These interactions were evidenced by spectral changes in the FTIR and Raman spectra, a change in molecular symmetry and changes in the interlayer space where DD adopted a titled configuration "resting" on the interlayer Cs^+ ion. Among different types of smectites, sorption preference was in the order of saponite > Upton > SWy-2. This is attributed to where isomorphic substitution occurs in each of the clays. Saponite has a relatively low cation exchange capacity (CEC) and charge density (1.21 μmole/m^2) with isomorphous substitution occurring mainly in the tetrahedral layer resulting in a more localized charge. For this particular clay and exchangeable cation, the extent of hydrophobic surface area is large (Rana et al., 2009). In addition, this combination of cation and clay type was found to control other types of organic contaminants including nitroaromatics and herbicides (Aggarwal et al., 2006; Boyd et al., 2001a; C.T. et al., 2004; Li et al., 2004a; Weissmahr et al., 1998). Although some details about how the non-chlorinated DD interacts with clay surfaces are known, a current gap in our understanding is related to how the presence of chlorine substituents influences the sorption. To the best of our knowledge, no mechanistic information regarding the interaction of chlorinated dioxins with clay minerals has been reported and is the focus of the present study.

As a group, hydrophobic dioxin molecules have intrinsically low aqueous solubilities and correspondingly high affinities for hydrophobic surfaces. Both their toxicity and solubility are

largely defined by the number and distribution of chlorine substituents with the most toxic congener being 2,3,7,8-tetrachloro dibenzo-p-dioxin (2,3,7,8-TCDD) with a toxic equivalency factor (TEF) of 1.0, (Mckinney, 1985; Steenland et al., 2004) and the least soluble congener being the fully chlorinated octachloro dibenzo-p-dioxin (OCDD) with a solubility value 0.4 ng/l (Shiu, 1988). Our approach has been to merge aqueous sorption studies with spectroscopic and structural analysis (Johnston et al., 2001c; Johnston et al., 2002b; Rana et al., 2009). Dixons are experimental challenging due to their low solubility and being able to detect the sorbed species corresponding to a few nanomoles of solute/mg of material. The non-chlorinated DD congener has the highest aqueous solubility of 0.9 mg/L. The aqueous solubilities of 1-ClDD and 2-ClDD selected for this study are high enough (400 μg L^{-1}, and 250ug L^{-1} respectively) to permit detection in the solution using traditional liquid chromatographic techniques as well as spectroscopically for mechanistic analysis. The specific objective of this study was to how the position of the chlorine substituent influenced sorption behavior compared to the non-chlorinated DD molecule.

3.3 Materials and Methods

3.3.1 Solutes

Structure and physio-chemical properties of 1-chloro-dibenzo-p-dioxin (1-ClDD) and 2-chloro-dibenzo-p-dioxin (2-ClDD) used in this study are summarized in Figure 3.1. Both solutes 1-ClDD and 2-ClDD were obtained from Chem Service, West Chester, PA. Stock solutions of 1-ClDD (400 mg/L), and 2-ClDD (250 mg/L) were prepared in anhydrous methanol. These solutions were then used to prepare aqueous solutions of 1-ClDD and 2-ClDD, respectively. Methanol content was maintained at < 0.1 volume % to minimize cosolvent effects.

M.W. (g/mol)	218.6
Aq. Solubility (mg L^{-1})	0.422
Subcooled liquid solubility(S_{sc}) (mg L^{-1})	2.65
Log K_{ow}	4.90
M.P.(^{O}C)	105.5
Vapor pressure @ 25°C(Pa)	1.2 X10^{-2}

M.W. (g/mol)	218.6
Aq. Solubility (mg L^{-1})	0.278
Subcooled liquid solubility(S_{sc}) (mg L^{-1})	1.197
Log K_{ow}	5.45
M.P.(^{O}C)	88
Vapor pressure @ 25°C(Pa)	1.7 X10^{-2}
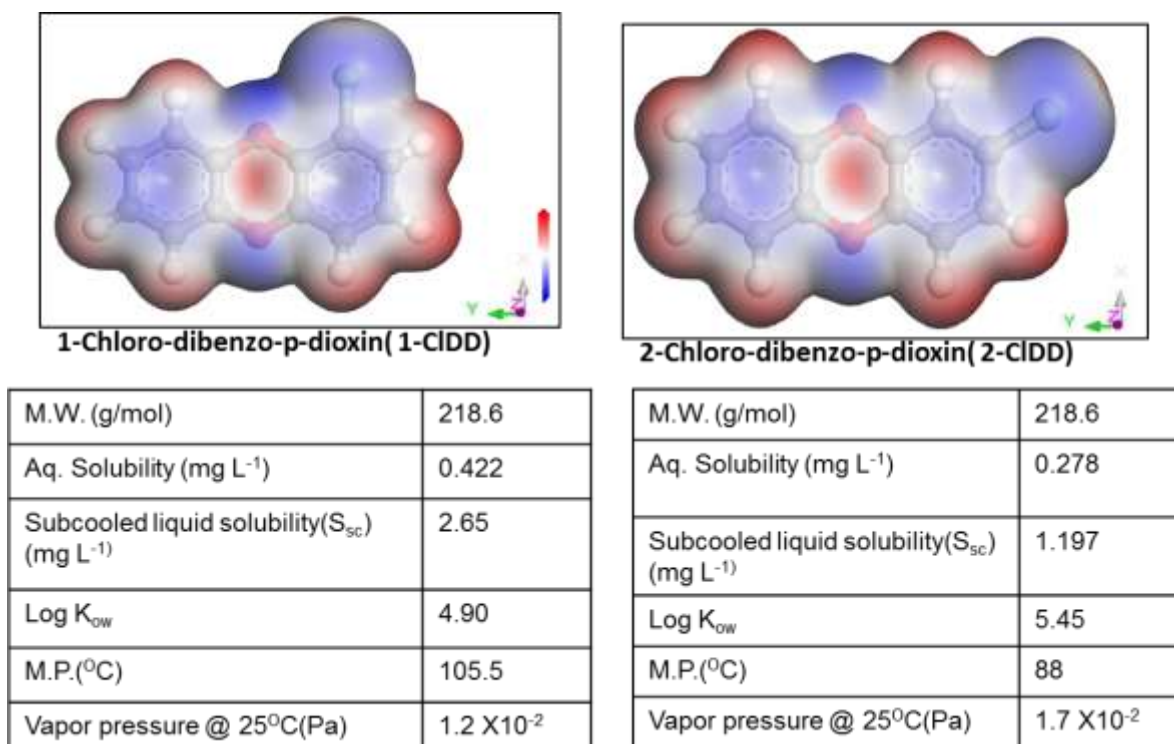
Figure 3.1 Molecular structures and selected physiochemical properties of 1-chloro-dibenzo-p-dioxin (1-ClDD), dibenzo-p-dioxin (DD) and 2-chlorol- dibenzo-p-dioxin (2-ClDD).

3.3.2   Reference Clay

The reference clay minerals used in this study were SapCa-2 saponite from California, SWy-2 montmorillonite (SWy-2) from Wyoming and Upton montmorillonite from Upton, Wyoming (Upton). Saponite and SWy-2 were obtained from the Source Clays Repository of the Clay Minerals Society at Purdue University, West Lafayette, IN. The Upton montmorillonite was from the American Petroleum Institute series collected from Upton, Wyoming (API 25). Major physio-chemical characteristics of smectites used in this study are summarized in Table 2.1

3.3.3   Batch sorption

All sorption isotherms were determined using a batch equilibrium method. Freeze-dried clay (1-25 mg) was placed in 30-mL COREX ® centrifuge tubes (Kimble HS-5600-30) with

polytetrafluoroethylene (PTFE)-lined screw caps. The amount of clay varied for a constant solution volume depending on the magnitude of sorption expected so that both solution and sorbed concentrations could be quantified. Solutions containing between 0-0.4 mg L^{-1} of 1-ClDD and 0-0.25 mg L^{-1} 2-ClDD were added to each test tube. Control samples containing 0.4 mg L^{-1} of 1-ClDD and 0.255 mg L^{-1} 2-ClDD without clay were used to quantify losses of solute. Experiments were conducted with two replicates. Clay-solute mixtures were vortexed for 30 sec and shaken at 80 strokes min^{-1} in a horizontal shaker at room temperature for 24 h to achieve apparent sorption equilibrium as indicated from preliminary experiments. After 24 h, the clay suspensions were centrifuged at 5920 g for 20 min to separate the liquid and solid phases and 1-mL aliquots of supernatant were transferred to glass high pressure liquid chromatography (HPLC) vials. In order to minimize sorption of 1-ClDD and 2-ClDD onto the vials, 0.5 mL pure (99.9%) methanol was added to each vial prior to the addition of the supernatant. Vials containing supernatant and methanol were vortexed for 30 sec and analyzed for 1-ClDD and 2-ClDD concentrations by direct injection of 50 μL on a Shimadzu SLC-10 high-performance liquid chromatography (HPLC) system equipped with a UV detector and a Supelcosil ABZ PLUS column (15 cm x 4.6 mm x 5 μm). Isocratic elution was performed using a mobile phase of 80/20 v/v acetonitrile/water with a flow rate 1.0 mL min-1 and wavelength of 227 nm for 1-ClDD and 228 nm for 2-ClDD detection, respectively. The amount of 1-ClDD and 2-ClDD sorbed was calculated from the difference between the mass added and that remaining in the final solution.

3.3.4 FTIR Analysis of Self Supporting Clay Films

Infrared spectra were obtained on a Perkin-Elmer GX2000 or on a Thermo Scientific Nicolet Model 6700 FTIR spectrometer. Both were equipped with a mercury-cadmium-telluride (MCT) detector, wire grid IR polarizer and KBr beam splitter. Spectra were collected using a

unapodized resolution of 2.0 cm^{-1} and a minimum of 64 scans were collected for each spectrum. FTIR spectra were post processed using the Grams/32 AO (6.00) software from Galactic Industries (Thermo Electron Corporation, Madison, Wisconsin) and with the Thermo Fisher Scientific Omnic (Version 8) software. Self-supporting clay films were prepared for analysis by FTIR from the first duplicate sample at each 1-ClDD and DD concentration in the smectite sorption isotherm experiments. After sampling 1 mL of supernatant for the HPLC analysis, the remaining smectite clay in the tubes was resuspended in the remaining supernatants and was used for self-supporting clay films (SSCF) preparation. The clay suspension was passed through a membrane filter (0.45 μm Supor 450 hydrophilic polyethersulfone, 25 mm diameter) on a Millipore filtration system under vacuum. The resulting clay deposit on the membrane filter was allowed to air-dry for 2-3 h and was removed from the membrane filter by running the filter and clay deposit over a knife-edge. FTIR spectra of SSCF films were obtained using a beam condenser.

3.3.5   In-situ ATR-FTIR measurements

A horizontal trough ATR cell (Pike Technologies, Madison, WI) was used in this study. Reference spectra of bulk water and aqueous solutions of 1-ClDD and 2-ClDD were obtained by placing 1 mL of water or 0.25 mg/L 1-ClDD or 2-ClDD aqueous solution with 0.1% methanol in the horizontal trough cell. One mL of a suspension containing 2 mg of Cs-Saponite was placed in the ATR cell and allowed to air dry overnight. The Cs-saponite deposit was washed multiple times using water (containing 0.1% methanol) and the intensity of the ν(Si-O) bands was monitored until a stable deposit was obtained as confirmed by no additional loss of intensity in the ν(Si-O) region. After the Cs-saponite deposit was stable, 1-mL aliquots of 0.25 mg L^{-1} 1-ClDD or 0.25 mg L^{-1} 2-ClDD aqueous solution were added sequentially. After each addition (31 additions of 1-ClDD and

10 additions of 2-ClDD), the ATR-FTIR spectrum was obtained, supernatant was decanted carefully and this procedure was repeated till dioxin band height was saturated.

3.3.6 Raman spectroscopy

Raman spectra of crystalline 1-ClDD, 1-ClDD in CCl_4 and SSCF of clay-1-ClDD complex were obtained on an Acton Research Corporation SpectroPro500 spectrograph. A Melles-Griot helium–neon laser with 632.8 nm wavelength and a power output of 35 mW measured at the laser head was used as the excitation source. The same self-supporting films of 1-ClDD sorbed Cs-saponite used for FTIR analysis was also used for Raman analysis.

3.3.7 Solution Spectra of 1-ClDD

1-ClDD (8.8 mg) was dissolved in 200 μL CCl_4. 1-ClDD solution in CCl_4, placed filled in a glass capillary tube and both ends were sealed. A Raman spectrum was collected through an Olympus BX-60 microscope using a 50X objective using a 120-s acquisition time on the CCD array.

3.3.8 X-ray diffraction (XRD)

Oriented clay films of smectite- 1-ClDD or 2-ClDD complex were prepared for X-ray diffraction analysis from the duplicate sample at each 1-ClDD or 2-ClDD concentrations in the smectite sorption isotherm experiments. X-ray diffraction patterns of smectite and 1-ClDD or 2-ClDD complexes were collected using a PANalytical B.V. (Model X'Pert PRO diffractometer; Almelo, Netherlands) using Co radiation. Dilute clay suspensions containing 10 mg of Cs-saponite in a volume of 900 mL; equilibrated with different concentrations of 1-ClDD and 2-ClDD, were passed through membrane filters (47 mm, 0.45 mm pore size, Millipore Co. Bedford, MA). The clay particles were then transferred into a vial and mixed with 200 mL of supernatant to form a

slurry, which was deposited on a glass slide and dried overnight at ambient conditions to obtain an oriented clay film. Data were collected from 2° to 60° 2θ at 0.02° 2θ steps per second. A 1° exit Soller slit was used between 2° to 12° 2θ. Data were analyzed using X'Pert HighScore Plus software Version 2.2 (PANalytical B.V.).

3.3.9   Computational Analysis

3.3.9.1   Geometry Optimization by The Density Functional Theory (DFT)

Molecular structure of 1-ClDD was generated using Material Studio Version 4.2 software (Accelrys, Inc., San Diego CA). The density functional theory (DFT) method was utilized in geometry optimization, and subsequent IR and Raman harmonic vibration frequency calculations. The *ab initio* calculations for 1-ClDD in gas phase were performed at the level of hybrid Becke-3Lee-Yang-parr parameters (B3LYP) DFT with the 6-31 G** basis set using the Gaussian 09W version (Mckinney and Singh, 1981). The geometry optimization was done and the optimized geometry was characterized as a local minimum by harmonic vibration analysis. In order to compare the predicted vibration frequencies directly with experimental frequencies of 1-ClDD the predicted frequencies were scaled by a factor of 0.9628.

3.4   Results

Sorption isotherms of 1-ClDD from water by three Cs-exchanged smectites (saponite, Upton and SWy-2) are shown in Figure 3.2A. Among the three Cs-exchanged smectites, 1-ClDD showed the highest affinity for saponite: CS-saponite > Cs-Upton montmorillonite > Cs-SWy2 montmorillonite. The maximum amount of 1-ClDD sorbed was 4000 mg/kg. The amount of 1-ClDD sorbed from water by Cs-saponite was significantly higher ($P < 0.05$) than Cs-Upton-montmorillonite and Cs-SWy2-montmorillonite. At an equilibrium concentration of

0.03 mg L^{-1}, Cs-Upton-montmorillonite and Cs-SWy2-montmorillonite sorbed 39% and 16% less 1-ClDD, respectively, than sorbed by Cs-saponite. The influence of the exchangeable cation on 1-ClDD sorption is shown in Figure 3.2B. The data for Cs-saponite is plotted using the primary y-axis (left) in Figure 3.2B. The amount of 1-ClDD sorbed on Na$^+$, K$^+$, and Rb$^+$-exchanged saponites was much lower, thus plotted using the secondary y-axis (right) in Figure 3.2B with maximum sorption values of ~200 mg/kg, or ~ 20 times less than that on Cs-saponite. Among the four homoionic smectites shown in Figure 1B, the sorption affinity for 1-ClDD was Cs$^+$ >>> Rb$^+$ > K$^+$ >> Na$^+$.
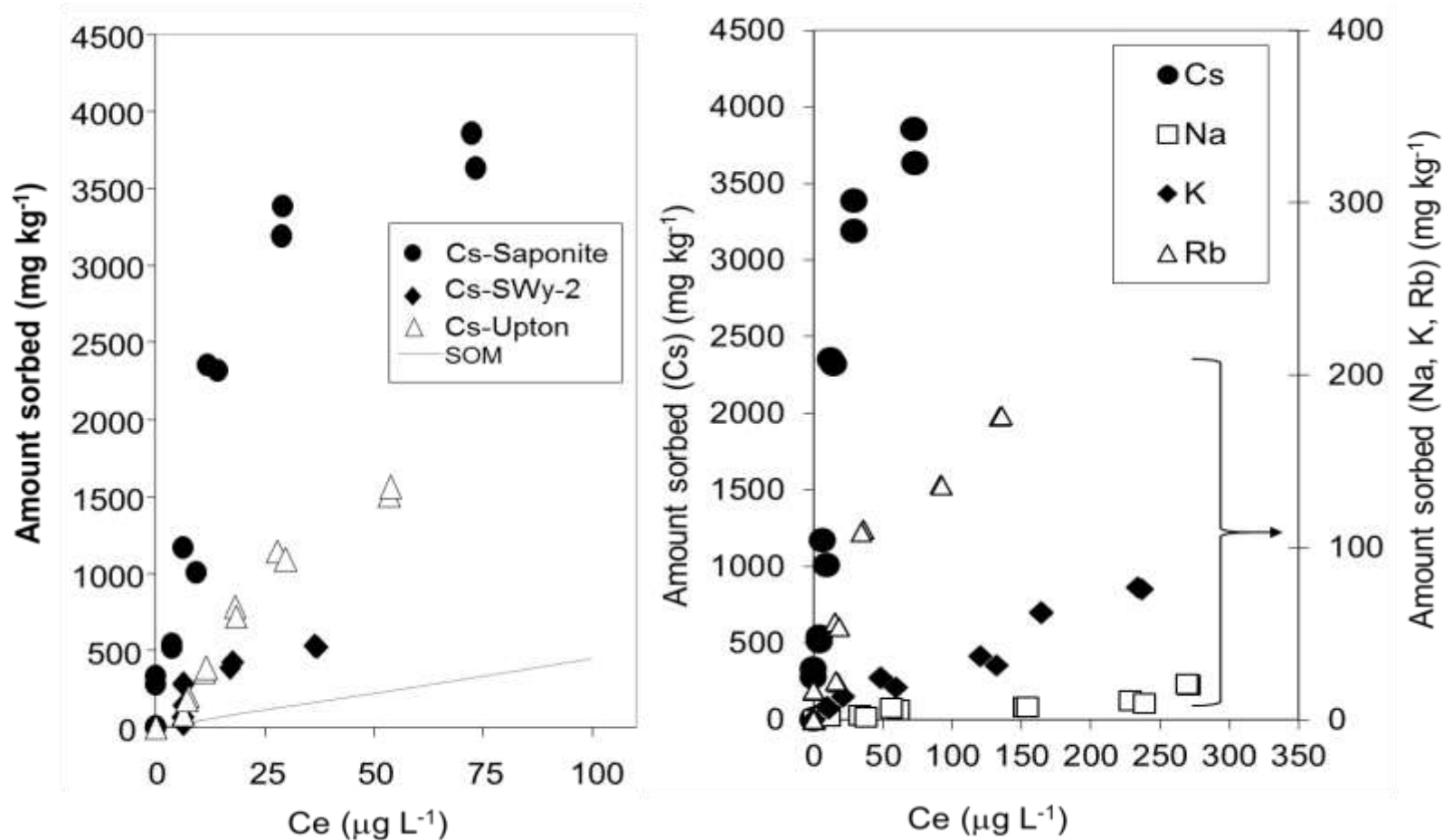
Figure 3.2 Batch sorption isotherm representing the sorption of 1-chloro-dibenzo-p-dioxin (1-ClDD) from water by (A) homoionic Cs^{+} -smectites (Cs-saponite, Cs-Upton montmorillonite; Cs-Upton, Cs-SWy-2 montmorillonite; Cs-SWy-2) and by (B) homoionic saponite saturated with Cs^{+}, Rb^{+}, K^{+} and Na^{+} metal cations. The data Cs-saponite is the same as in Figure 1A. The dotted line is for 1-ClDD sorption by soil organic matter (SOM) using the equation: $\log K_{OM} = 0.904\log - 0.779 \, K_{OW}$.
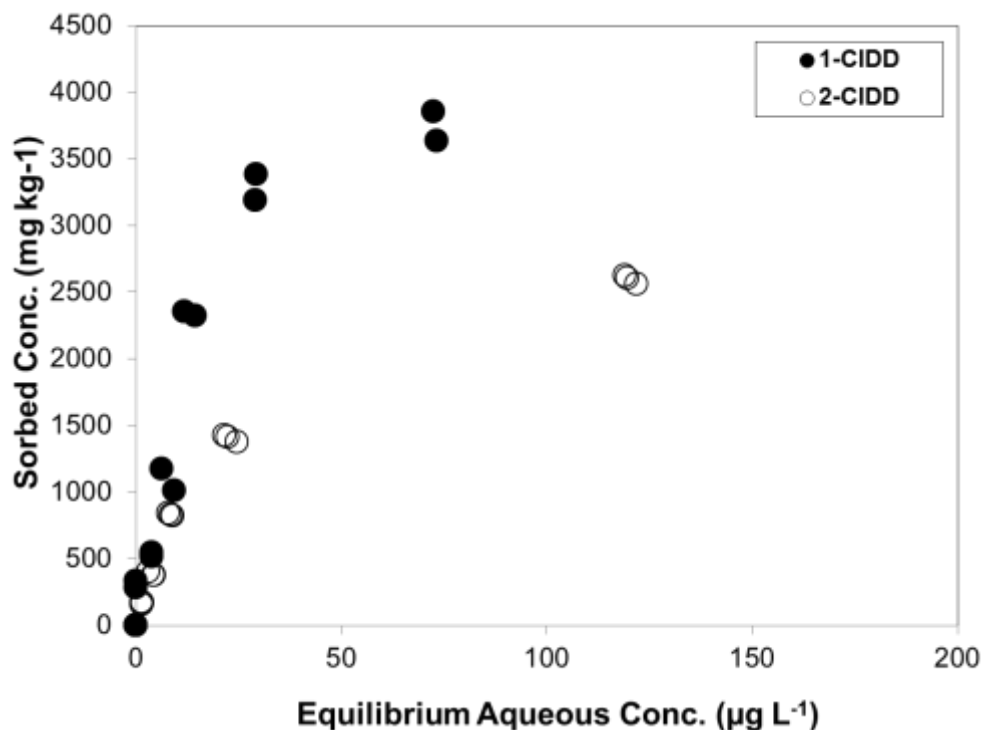
Figure 3.3 Sorption isotherm representing the sorption of 1-chloro-dibenzo-p-dioxin (1-ClDD) and 2-chloro-dibenzo-p-dioxin (2-ClDD) by Cs-saponite

Sorption isotherms of 1-ClDD and 2-ClDD from water by Cs-saponite are compared in Figure 3.3.

The sorption data were fit to the Freundlich equation: $C_s = K_f C_e^{1/n}$ ……………..(1) where C_s is the concentration of solute sorbed ($\mu g\ g^{-1}$), C_e is the equilibrium aqueous concentration ($\mu g\ mL^{-1}$), K_f is the Freundlich adsorption coefficient ($\mu g^{\ 1-1/n}\ g^{-1}\ mL^{1/n}$) and n is the coefficient of sorption nonlinearity. The resulting K_f values for 1-ClDD, DD and 2-ClDD are listed in Table 3.1. The $\log_{10} K_f$ values for 1-ClDD, 2-ClDD and DD sorption to saponite saturated with homoionic exchangeable cations (Cs^+, Rb^+, K^+ and Na^+) are plotted in Figure 3.4 as a function of the exchangeable cation hydration energies. The inverse relationship between the $\log_{10} K_f$ values and the enthalpy of hydration indicates that maximum sorption for all three dioxins occurs when weakly hydrated cations are on the clay interlayer exchange sites (Rana et al., 2009).

Table 3.1 Comparison of Freundlich isotherm parameters for the dibenzo-p-dioxin (DD), 1-chloro-dibenzo-p-dioxin (1-ClDD) and 2-dibenzo-p-dioxin (2-ClDD) sorption on smectites saturated with homoionic cations

Clay	DD*		1-ClDD		2-ClDD	
	K_f $(mg^{(1-1/n)} kg^{-1} L^{1/n})$	$1/n$	K_f $(mg^{(1-1/n)} kg^{-1} L^{1/n})$	$1/n$	$K_f (mg^{(1-1/n)} kg^{-1} L^{1/n})$	$1/n$
Cs-Saponite	9811	0.40	29228	0.68	12103	0.62
Rb Saponite	571.1	0.65	897.6	0.76		
K-Saponite	119.1	0.52	146.9	0.57		
Na-Saponite	58.43	1.03	28.07	0.57		
Cs-swy-2	690.7	0.40	735.7	0.42		
Cs-Upton	5668	0.60	5713	0.59		

*K_f and $1/n$: Freundlich isotherm parameters from chapter 2
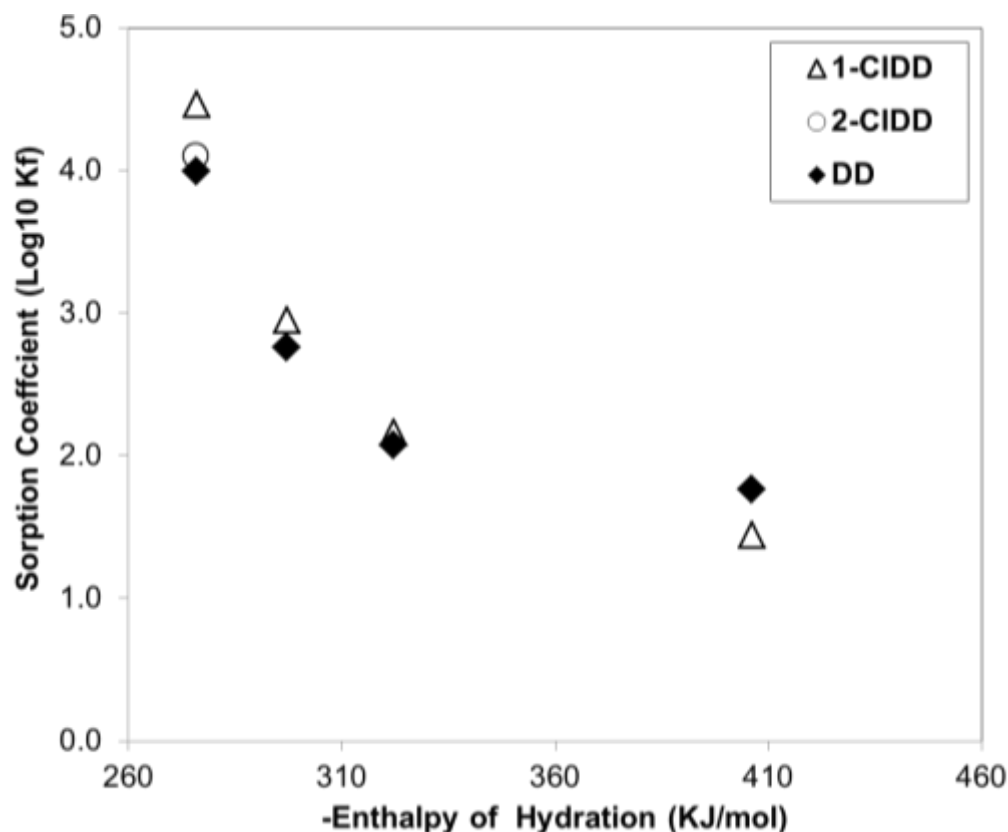
Figure 3.4 Freundlich isotherm coefficient (K_f) for the 1-chloro-dibenzo-p-dioxin (1-ClDD), 2-chloro-dibenzo-p-dioxin (2-ClDD) and dibenzo-p-dioxin (DD) sorption on saponite saturated with homoionic exchangeable cations from aqueous suspensions as a function of the enthalpy of hydration of exchangeable cations.

XRD patterns of oriented deposits of Cs-saponite with different loadings of 1-ClDD and 2-ClDD are shown in Figure 3.5. The d_{001} spacing of air-dried Cs-saponite without 1-ClDD or 2-ClDD is 12.3 Å and corresponds to about one molecular layer of water in the interlayer (Liu et al., 2009). For 1-ClDD, a modest increase in the d_{001} spacing from 12.3 to 12.7 Å occurs with increasing surface loading to ~ 4000 mg kg^{-1} (Figure 3.5A). The gradual increase in basal spacing confirms intercalation of 1-ClDD in Cs-saponite and that the intercalated 1-ClDD molecules are oriented parallel with the clay surface. In contrast, increasing surface loading of 2-ClDD resulted in a significant increase in the d_{001} spacing from 12.3 to 14.65 Å. This increase in d_{001} is similar to

what we observed for DD (Liu et al., 2009; Rana et al., 2009) indicating that molecular plane of the intercalated 2-ClDD molecules adopt a tilted orientation in the clay interlayer.
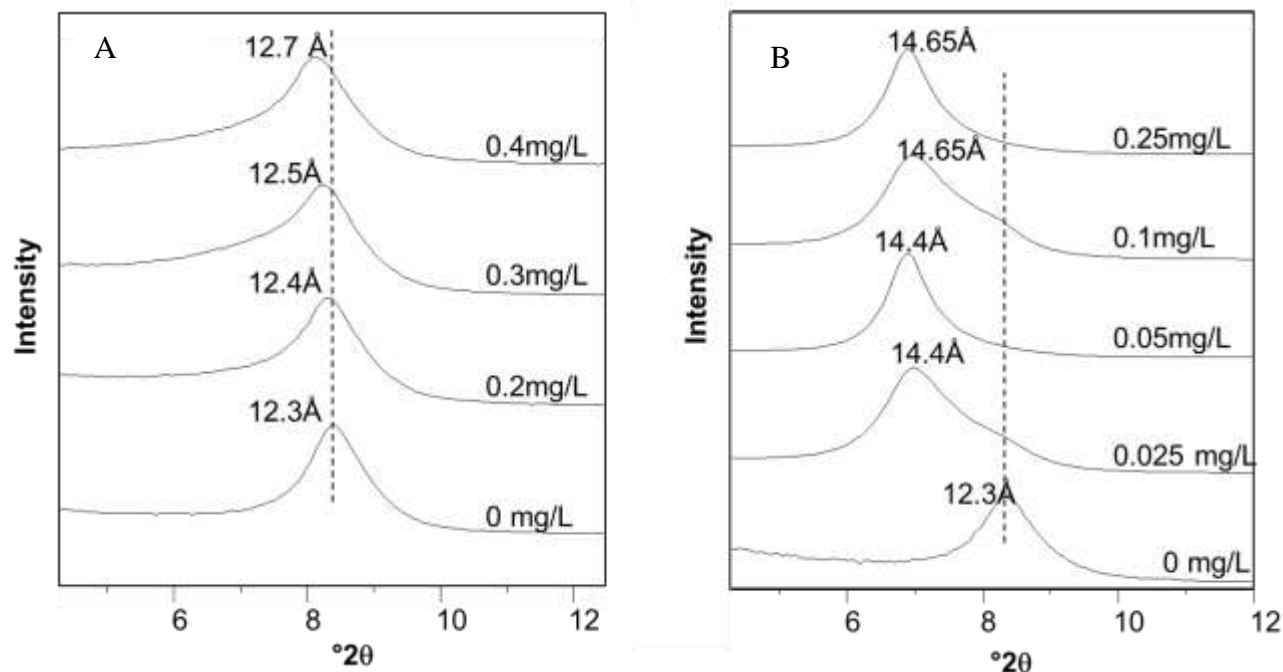
Figure 3.5 X-ray diffraction patterns of Cs-saponite clay films equilibrated with increasing concentrations of (A) 1-chloro-dibenzo-p-dioxin (1-ClDD) and (B) 2-chloro-dibenzo-p-dioxin (2-ClDD) solution.

FTIR spectra of self-supporting clay films of 1-ClDD sorbed to Na$^+$-, K$^+$-, Rb$^+$-, and Cs$^+$-exchanged smectites are shown in Figure 3.6 For vibrational band identification solution, reference FTIR/Raman spectra of crystalline 1-ClDD and 1-ClDD dissolved in CCl$_4$ were collected (shown Figure 3.7).   The FTIR features of 1-ClDD are most evident in spectrum of 1-ClDD sorbed to Cs-saponite (Figure 3.6D and Figure 3.7D) with bands at 1495, 1480, 1470, and 1295 cm^{-1}. The 1495, 1480, and 1470 cm^{-1} bands correspond to C-C aromatic ring skeletal motions (ν_{C-C}) and the 1295 cm^{-1} band is assigned to the asymmetric C-O-C stretching motion ($\nu_{asym\ COC}$). Additional details about the FTIR and Raman band assignments are given in Appendix B Table B1 and B2. The positions of the 1-ClDD 1295 ($\nu_{asym\ COC}$) and 1495 (ν_{C-C}) bands were not significantly influenced by the exchangeable cation. However, a significant reduction in the

intensity of the 1295 cm^{-1} ($\nu_{asym\ COC}$) and 1495cm^{-1} (ν_{C-C}) bands was observed for more strongly

hydrated cations (Table 3.2).
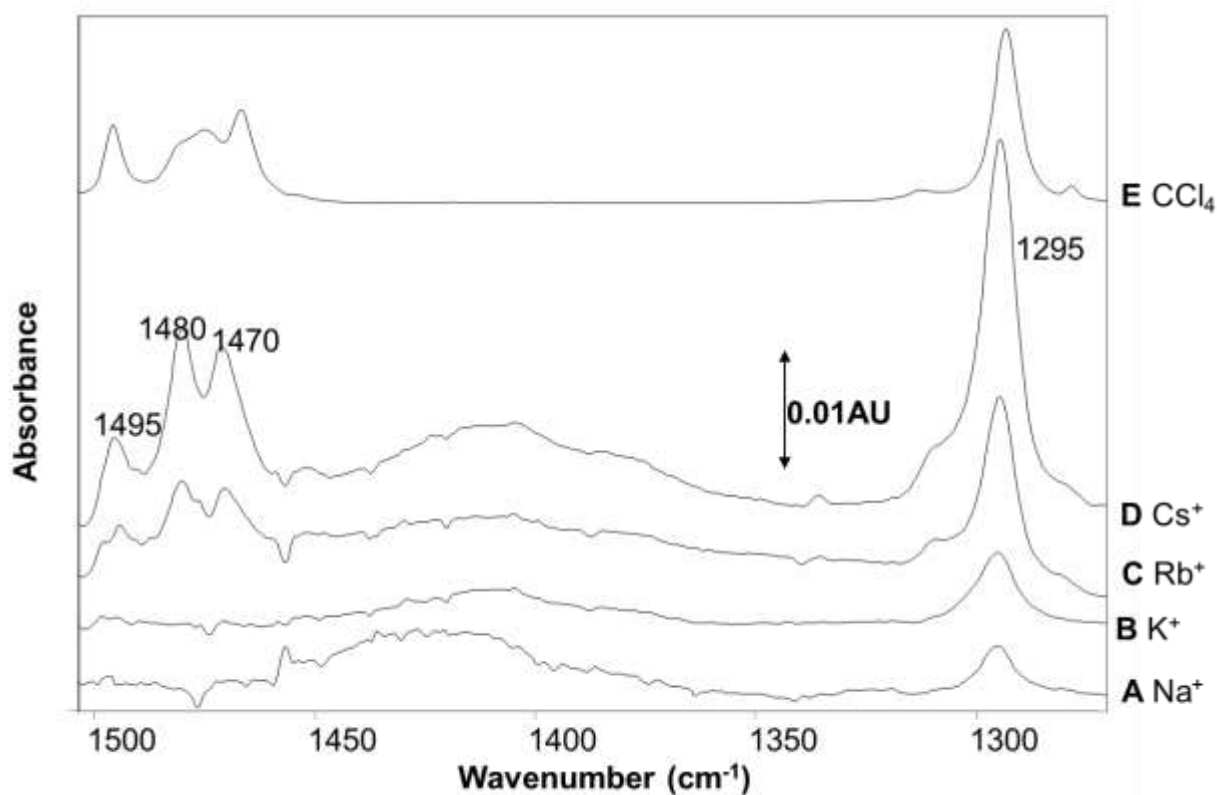
Figure 3.6 FTIR spectra of self supporting clay films of 1-chloro-dibenzo-p-dioxin (1-ClDD) sorbed to saponite saturated with different alkali cations in the 1500-1270 cm^{-1} region. For comparison a reference solution spectra of 1-ClDD dissolved in CCl$_4$ is overlaid. All spectra , except E, are in same scale.
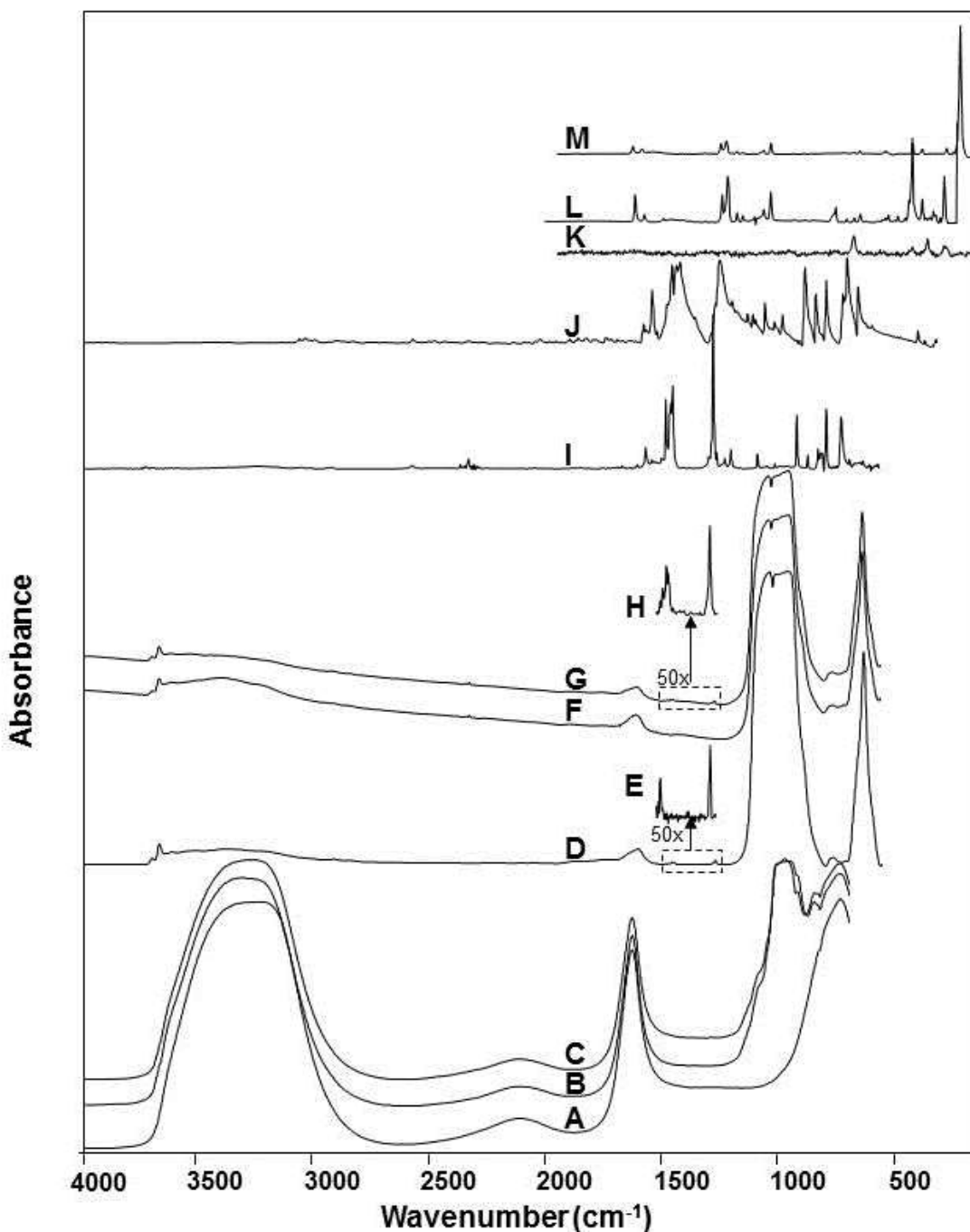
Figure 3.7 Survey ATR-FTIR spectra of A) H$_2$O, B) Cs-saponite in water C) Cs-saponite and aqueous suspension of 1-chloro-dibenzo-p-dioxin (1-ClDD), D) ratio of spectra A and C, E) the extended spectrum of D showing diagnostic vibration bands of 1-ClDD sorbed on clay, F) transmission IR spectra of SSCF of Cs-saponite, G) transmission IR spectra of SSCF of Cs-saponite-1-ClDD complex, H) the extended spectrum of B showing diagnostic vibration bands of 1-ClDD sorbed on clay, I) transmission IR spectra of 1-ClDD in CCl$_4$, J) transmission IR spectra of 1-ClDD in KBr, K) Raman spectra of 1-ClDD-Cs-saponite complex ,L) Raman spectra of crystalline 1-ClDD, and M) Raman spectra of 1-ClDD in CCl$_4$.

Table 3.2 Band positions of vibrations bands of 1-chloro-dibenzo-p-dioxin (1-ClDD)sorbed in saponite exchanged with alkali metal cations.

Clay/ solvent	ν C-C	$I_{\nu C\text{-}C}$	νC-O-C	$I_{\nu C\text{-}O\text{-}C}$	Intensity ratio* $(I_{\nu\ C\text{-}C\ (1495cm^{-1})} / I_{\nu C\text{-}O\text{-}C})$
Cs-Saponite	1495	0.0059	1295	0.0321	0.1823
	1480	0.0119			
	1470	0.0110			
Rb-Saponite	1495	0.0060	1295	0.0164	0.3671
	1480	0.0066			
	1470	0.0067			
K-Saponite	1495	nd**	1295	0.0064	nd
	1480	nd			
	1470	nd			
Na-Saponite	1495	nd	1295	0.0040	
	1481	nd			
	1470	nd			
CCl$_4$	1496	0.1032	1293	0.0116	nd
	1481	0.0356			
	1472	0.0875			

*Intensity ratio calculated using 1495 cm^{-1}/ 1295 cm^{-1} bands; **not detected

In the case of Na-and K-saponite, the $\nu_{C\text{-}C}$ band 1495 cm^{-1} was below detection limit. Although the specific mechanisms responsible for these band intensity changes are not known, they do indicate that site-specific interactions occur between the intercalated 1-ClDD molecules and the weakly hydrated Cs$^+$ (and Rb$^+$ to a lesser extent).

In-situ ATR-FTIR spectra of 1-ClDD sorption to Cs-saponite are shown in Figure 3.8 in two expanded regions corresponding to the strongest 1-ClDD band at 1295 cm^{-1} and the H-O-H bending band at 1632 cm^{-1}. After a stable deposit of Cs-saponite was obtained on the ZnSe internal reflection element of the ATR cell, sequential additions of solutions containing 0.25 mg/L of 1-

ClDD or 2-ClDD were added to the ATR cell, the samples were allowed to equilibrate and the ATR-FTIR spectrum was recorded. For 1-ClDD and 2ClDD total 31 and 10 additions were performed, respectively.
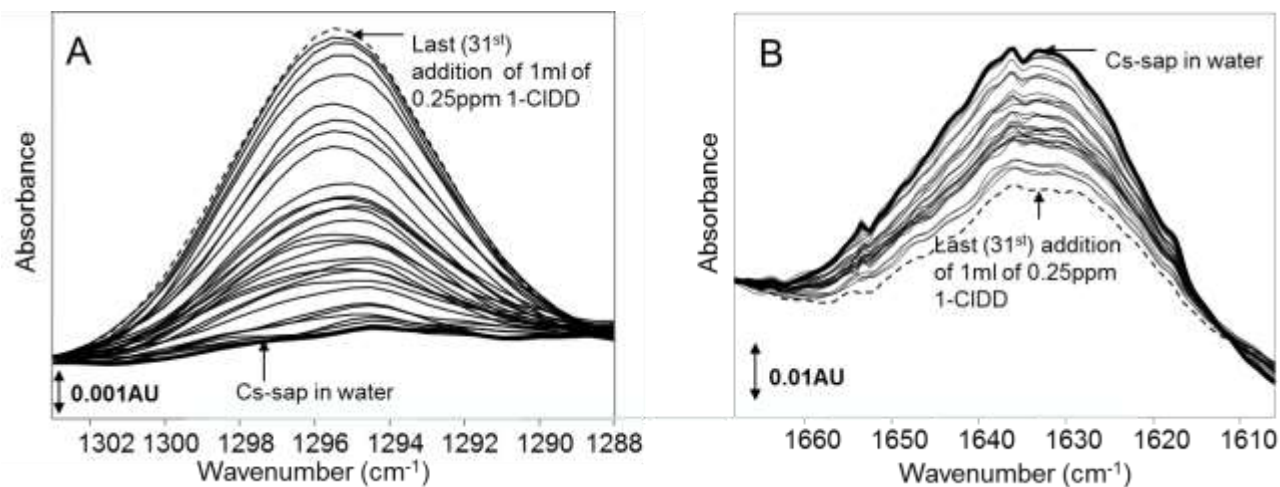
Figure 3.8 Changes in ATR-FTIR intensities on Cs-saponite deposit with sequentil additions of 1-chloro-dibenzo-p-dioxin (1-ClDD) for (A) the sorbed water at 1632 cm^{-1} and (B) 1-ClDD) at 1295 cm^{-1}). In total, 31 additions sequentially of 1 mL 0.25 ppm 1-Cl DD on Cs-saponite deposit.

Figure 3.8A shows the increase in intensity of the 1295 cm^{-1} band with increasing additions of 1-ClDD. Also shown in Figure 3.8B is the H-O-H bending band of water at ~1632 cm^{-1}. In the case of 1-ClDD, the intensity of the H-O-H bending bands decreases with increasing sorption of 1-ClDD (Figure 3.8 and Figure 3.9). These data provide direct evidence that sorption of 1-ClDD results in a partial "dewatering" of the clay interlayer. *In-situ* ATR-FTIR spectra of bulk water, Cs-saponite in contact with water, and Cs-saponite in contact with an aqueous solution of dioxin (1-ClDD) are show in the Figure 3.7.
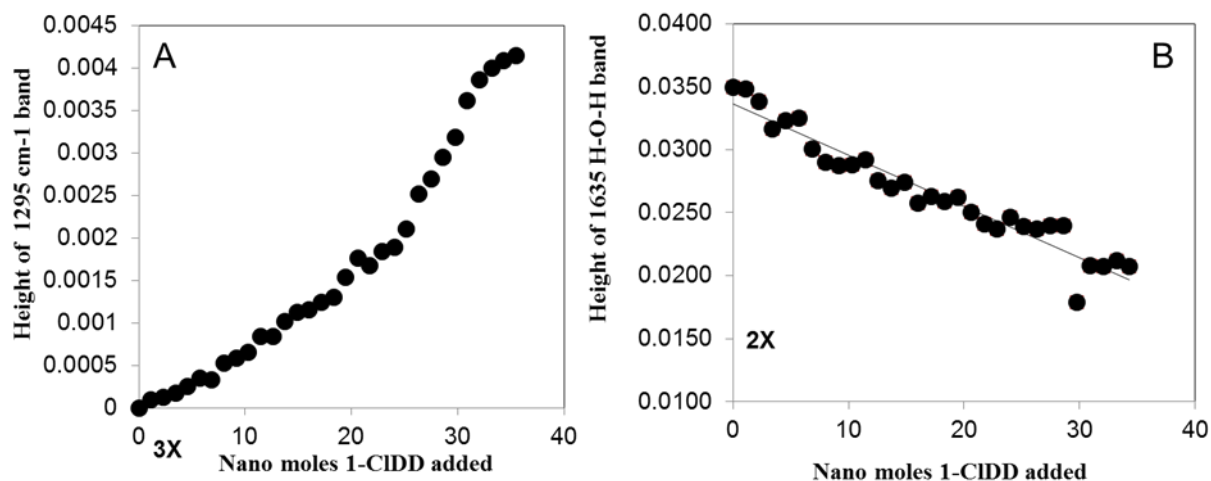
Figure 3.9 ATR-FTIR analysis of change in 1-chloro-dibenzo-p-dioxin (1-ClDD) (1295 cm^{-1}) band (A) and sorbed water (1632 cm^{-1}) (B) after sequential 31 additions of 1 mL 0.25 ppm 1-Cl DD on Cs-saponite deposit.
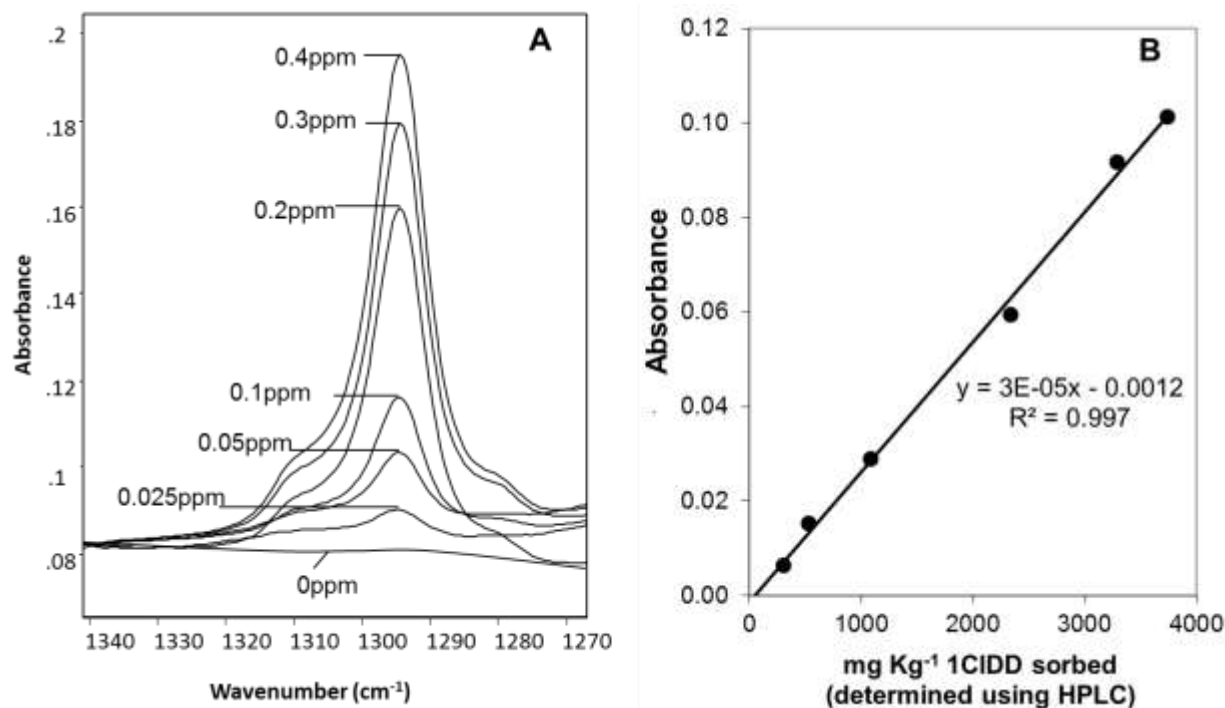
Figure 3.10 Combination of HPLC and FTIR derived sorption isotherms of 1-ClDD on Cs-saponite (A) and relation between HPLC derived sorption isotherm and ν(C-O-C) absorbance band of 1-1-ClDD on Cs-saponite surfaces (B).

The spectroscopic sorption isotherm based on the intensity of the 1295 cm^{-1} ($\nu_{asym\ C-O-C}$) band are strongly correlated with the traditional batch sorption HPLC-derived isotherm (Figure 3.10). The strong correlation of HPLC and *in-situ* ATR-FTIR derived isotherm establishes a direct relationship between the macroscopic sorption results and the molecular insights from the spectroscopic results.

3.5   Discussion

Similar to earlier work on non-chlorinated DD, the sorption affinities of 1-ClDD and 2-ClDD were inversely proportional to the enthalpy of hydration of the exchangeable cation. The high sorption affinity of 1-ClDD and 2-ClDD molecules for Cs-exchanged smectites is twofold. First, the interlayers of these clays are weakly hydrated which allows these molecules to interact favorably with the hydrophobic siloxane surface. Second, the FTIR data reveal that site-specific interactions between the Cs^{+} interlayer cation and the sorbed dioxin molecules occur. The bridging oxygen atoms of the 1-ClDD would be possible interaction sites. Among the three smectites studied, sorption affinity of 1-ClDD followed Cs-saponite > Cs-Upton montmorillonite > Cs-SWy-2 montmorillonite. Saponite is a trioctahedral 2:1 phyllosilicate with isomorphic substitution mainly in the tetrahedral sheet. Thus, the layer charge in saponite is localized and distributed over a relatively small number of siloxane oxygen atoms that leaves much of the internal siloxane surface as "charge neutral" and hydrophobic. For this molecule, sorption affinity likely involves contributions from both (1) ion-dipole interactions and (2) London forces (Rana et al., 2009). These data indicate that site-specific interactions occur between Cs^{+} and 1-ClDD and that competition with excess H$_2$O will limit sorption.

The overall sorption behavior for both 1-ClDD and 2-ClDD agree with prior studies on the non-chlorinated DD congener. However, several interesting observations for the chlorinated congeners stand out. The first is the parallel orientation of the 1-ClDD congener with respect to the clay surface. XRD and polarized ATR-FTIR measurements of DD sorbed to Cs-saponite confirmed that the molecule was tilted in the clay interlayer. Raman measurements showed that the molecular symmetry of DD was "broken" that was assigned to DD "resting" on the Cs^+ ion in the clay interlayer. This is assumed to be the energetically favorable structure/orientation. In the case of 1-ClDD, however, the position of the Cl substituent in the 1 position sterically hinders the molecule from taking on a tilted orientation (Figure 3.1). Possible representations of the DD-, 2-ClDD-, and 1-ClDD-Cs-saponite complex are shown in Figure 3.11 where the short axis of DD and 2-ClDD (in plane) is tilted on a Cs^+ ion in clay interlayer while 1-ClDD molecule are oriented parallel to the siloxane surface.

DD
(dibenzo-p-dioxin)
$d_{001} = 1.49$ nm

2-ClDD
(2-chloro-dibenzo-p-dioxin)
$d_{001} = 1.47$ nm

1-ClDD
(1-chloro-dibenzo-p-dioxin)
$d_{001} = 1.27$ nm
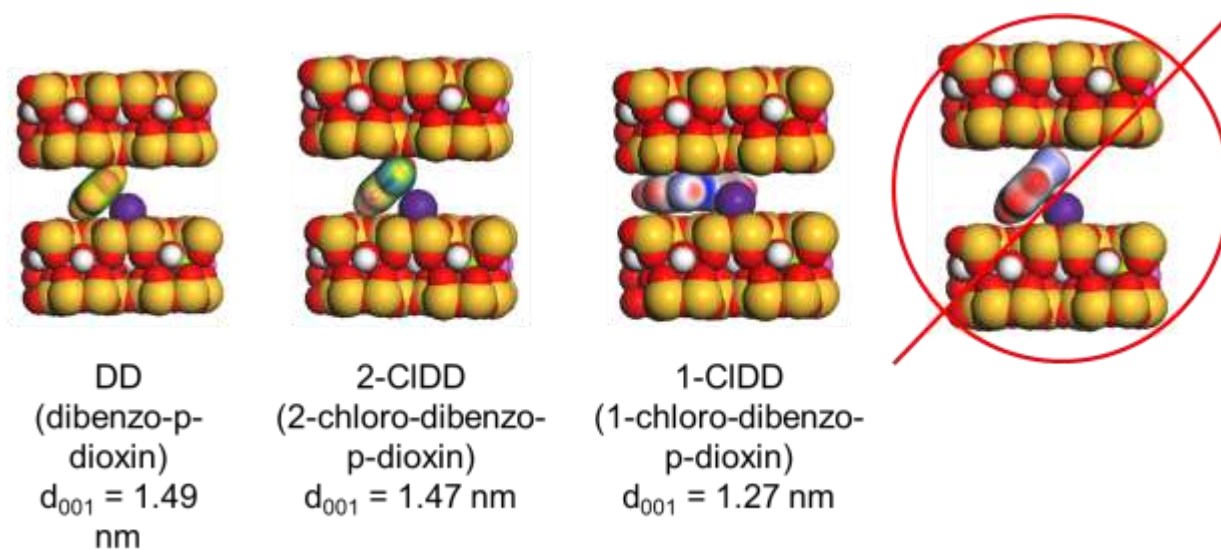
Figure 3.11 Proposed molecular model of DD -, 2-ClDD -, and 1-ClDD -smectite complex showing the arrangement of DD, 2-ClDD, and 1-ClDD in the interlayer space of the smectite clay.

The d_{001} spacing of 1-ClDD-Cs-saponite does not exceed 12.7 Å even at the highest surface loading of 1-ClDD of 4000 mg/kg. Additionally, sorption of 1-ClDD is accompanied by a decrease in water content, presumably due to displacement of interlayer water molecules by "incoming" 1-ClDD molecules. In the case of 2-ClDD, the molecule is apparently not sterically hindered by the Cl substituent in the 2 position. In this case, the d_{001} spacing increases from 12.3 to 14.65 Å which is slightly greater than the 14.49 Å reported for DD-Cs-saponite consistent with the larger size of 1-ClDD than DD (Rana et al., 2009).

These results are novel in that spectroscopic, sorption and structural data are presented for chlorinated congeners of dioxin interacting with smectite surfaces. The positions of the Cl-substituents govern the specific type of interlayer interactions that can occur.

3.6 Acknowledgement

CHAPTER 4.   SORPTION OF PLANAR AND NON-PLANAR COMPOUNDS TO Cs-EXCHANGED SMECTITE

4.1   Abstract

The sorption of chlorinated dibenzo-p-dioxins (dioxins) and polychlorinated biphenyls (PCBs) to soils and sediments is a key process in determining the transport, bioavailability and environmental fate of these compounds in soil- and sediment- water systems. Sorption studies of non-ionic organic compounds (NOC) have shown that certain NOCs, including dioxins and biphenyl, have a higher than expected affinity for expandable clay minerals particularly those saturated with weakly hydrated exchangeable cations. Sorption of NOCs on clay minerals is influenced by the molecular properties of the solute including structure (planar versus non-planar) and type, position and degree of substitution (e.g.-NO_2, Cl). In this work, sorption of six nonpolar dioxin and PCB compounds with similar octanol-partitioning coefficients (log K_{ow}) values but varying molecular planarity and degree of chlorination was evaluated. Batch sorption and XRD measurements of dibenzo-p-dioxin (DD), 1-chloro-dibenzo-p-dioxin (1-ClDD), 2-Cl-dibenzo-pdioxin (2-ClDD), PCB-1, PCB-4 and PCB-47 on a reference smectite (Cs-saponite) was compared. Overall, dioxins showed higher sorption affinities for Cs-smectite compared to all of the PCBs studied including both coplanar (PCB-1) and non-planar PCBs (PCB-4 and PCB-47). Among the PCBs, coplanar PCB-1 had higher sorption than the non-planar PCBs (PCB-4 and PCB-47). Sorption trends were correlated with differences in polarizability and dipole-moment Correlation trends suggested that high sorption affinity of planar dioxins could be due to a combination of *Van der Waals* interactions with the siloxane surface and site-specific interactions between dioxin and exchangeable cations. In contrast, the sorption of PCBs was highly influenced

by their molecular orientation and polarizability. These results further elucidate the sorption mechanism of dioxin and PCB compounds from bulk water to clay minerals.

4.2   Introduction

Polychlorinated dibenzo-p-dioxins (PCDDs or dioxins) along with polychlorinated biphenyls (PCBs) are classified as persistent organic pollutants (POPs) that are known for their acute toxicity and persistence in the environment (Broman et al., 1992; Fiedler et al., 2013; Halsall et al., 1995; Hoffman et al., 2006; Kjeller et al., 1991; Rappe, 1994). Toxicity of these POPs is attributed to their ability to activate the aryl hydrocarbon receptors (AhR) and induction of the adaptive xenobiotic metabolic pathway (Borlak, 2001; Denison and Nagy, 2003; Goldstein, 1989; Mandal, 2005; Safe, 1990; Swanson and Bradfield, 1993). Quantity structure activity relationship (QSAR) models to define the toxicity of dioxins, PCBs and other AhR ligands have shown that the ligand binding pocket of the AhR is a 'hydrophobic slot' measuring 1.4 nm x 1.2 nm x 0.5 nm. AhR binding and toxicity of AhR ligands such as dioxins and PCBs are significantly affected by molecular planarity and degree of substitution (e.g. –Cl and –Br) of ligands (Denison and Nagy, 2003; Mckinney, 1985; Petkov et al., 2010; Shiu, 1988; Waller and McKinney, 1992, 1995).

Dioxins and PCBs are characterized by low aqueous solubility, high lipophilicity and an overall high degree of physical and chemical stability under ambient conditions (Beyer and Biziuk, 2009; Halsall et al., 1995; Holmes and Harrison, 1993; P.J. Edgar, 2003; Shiu, 1988). The environmental fate of these pollutants is mainly influenced by sorption processes in surface soil-, subsurface soil- and sediment-water systems (Boyd et al., 2011; Karickhoff et al., 1979; Voice and W.J.Weber, 1983). Soil organic matter (SOM) has traditionally been considered as the dominant sorptive domain for sparingly soluble, nonionic organic compounds (NOCs) and partitioning is

viewed as the primary sorption mechanism (Boyd et al., 2011; Chiou, 1985; Choi, 2009; Frankki et al., 2006; Jonker and Smedes, 2000). Prior studies revealed that ceratin NOCs including dioxin, dibenzofurans, PCBs, nitroaromatics, triaizine and trichloroethene (TCE) have higher than expected affinity for the group of expandable 2:1 phyllosilicates (clay minerals) known as smectites (Aggarwal et al., 2006; Aggarwal et al., 2005; Johnston et al., 2004b; Rana et al., 2009). In some cases, sorption of NOCs on smectites can greatly exceeded that of other sorbents such as SOM. These data suggested that the role of clay minerals in the sorption of non-polar organic compounds should be incorporated along with traditional K_{OM} based model to predict the environmental fate of these compounds (Boyd et al., 2011; Liu et al., 2009).

Sorption studies of NOCs on smectite have shown that the uptake of these compounds is influenced by the properties of both the smectite (exchangeable interlayer cations, smectite clay type, charge density, surface area) and the NOCs (planarity, molecular dimesions, type and degree of substitution and functional groups (e.g. $-NO_2$, -Cl) (Johnston et al., 2004a; Teppen and Aggarwal, 2007). Sorption of DD, nitroaromatics and TCE from bulk water to homoionic smectites have shown that nature of the exchangeable cation is the strongest deteriminant of the sorption where weakly hydareted exchangeable cations (e.g., Cs^+ and K^+) clay manifest ~10 to 100 times greater soprtion than those exchanged with strongly hydrated cations such as Na^+. The smaller hydrated radii of cations like Cs^+ provide i) more 'charge-neutral siloxane surface' for hydrophobic interactions; ii) less competition between interlayer water molecules and sorbed organic molecule for favorable direct interactions with exchangeable cations; and iii) optimal interlayer spacing for organic molecule intercalation and thereby minimizing interaction of sorbed molecule with bulk water (Aggarwal et al., 2006; Aggarwal et al., 2005; Johnston et al., 2004b; Rana et al., 2009; Teppen and Aggarwal, 2007).

Additionally, 2:1 phyllosilicates (e.g. saponite) with isomorphic substitution exclusively in the tetrahedral layer of the clay lattice exhibit greater sorption (Aggarwal et al., 2006; Rana et al., 2009). For these clays, the charge from isomorphous substitution is distributed over a smaller number of siloxane oxygen atoms on the siloxane surface closest to the substitution, creating more charge neutral siloxane surface. In the case of smectites with isomorphous substitution dominantly in the octahedral layer, the charge is more delocalized over both siloxane surfaces (Aggarwal et al., 2006; Rana et al., 2009). Sorption of nitroaromatics and DD by smectites exchanged with weakly hydrated cations (e.g., K^+ and Cs^+) has shown that the dimensions of hydrophobic siloxane domains in clay interlayers are similar to the dimensions of the AhR binding slot (Jaynes and Boyd, 1991; Rana et al., 2009). Understanding the interaction of dioxins and PCBs to smectite exchange with weakly hydrated cations will aid to understand the binding mechanisms and environmental fate of these compounds

In this study, Cs-saturated saponite was used as a model sorbent. The objective of this study was to evaluate the role of molecular properties such as planarity, position and degree of chlorination of dioxin and PCBs on the magnitude of sorption from water by smectites. Sorption from aqueous suspension to smectite was evaluated for three dioxin molecules (DD, 1-Cl-DD and 2-Cl-DD) with varying planarity, hydrophobicity and solubility and three PCB molecules (PCB-1, PCB-4 and PCB-47) with varying planarity using macroscopic sorption and structural XRD techniques.

4.3   Materials and Methods

4.3.1   Reference Clay

The reference smectite clay used in this study was SapCa-2 saponite (saponite). The saponite was obtained from the Source Clays Repository of the Clay Minerals Society at Purdue

University, West Lafayette, IN and has a cation exchange capacity of 94 $cmol_c$ kg^{-1} and a surface area of 750 m^2 g^{-1} (Aggarwal et al., 2006). Prior to size fractionation, each clay was exchanged with Na^+ by placing 40 g of the raw clay in 1 L of 0.5 M NaCl for 24 h. Resulting Na-smectite suspension was washed to remove excess salts by repeated centrifugation with Millipore® water. The < 2µm size fractions was collected by centrifugation. Homoionic Cs- smectites were prepared by shaking Na-exchanged clay with 0.1M solution of the CsCl for 24 h. Fresh 0.1 M CsCl solution was used to replace the original solutions after centrifugation. This process was repeated four times to ensure complete cation exchange. Excess salt was removed by repeatedly washing with Millipore® water, using Spectra/Por® dialysis tubing, until a negative for Cl^- test using $AgNO_3$ was obtained. The resulting clay suspension was subsequently quick-frozen, freeze-dried and stored in a closed container for later use.

4.3.2   Solute

2-chloro-biphenyl (PCB-1, 99.4% pure), 2,2' dichloro-biphenyl (PCB-4, 99.5% pure), 2,2',4,4'tetrachloro-biphenyl (PCB-47, 98.1% pure), 1-chloro-dibenzo-p-dioxin (1-ClDD, 99% pure), 2-chloro-dibenzo-p-dioxin (2-ClDD, 99% pure), and dibenzo-p-dioxin (DD, 99% pure) were obtained from Chem Service, West Chester, PA.

Stock solutions of DD, 1-ClDD, PCB-1, PCB-4 and PCB-47 (100 mg L^{-1}), 1-ClDD, (250 mg L^{-1}) and 2-ClDD (400 mg L^{-1}) were prepared in anhydrous methanol (Mallinckrodt Chemicals, Chrom ARR) and were used to make aqueous solutions of respective solutes. The amount of methanol in the aqueous solutions was kept < 0.1 volume % to minimize cosolvent effects. Diluted aqueous solutions of solutes were sonicated for 60 min at room temperature in a water bath sonicator.

4.3.3 Batch sorption

All sorption isotherms were determined using the batch equilibrium method. Freeze-dried clay (1-100 mg) was placed in 30-mL centrifuge tubes (Kimble HS-5600-30) with polytetrafluoroethylene (PTFE)-lined screw caps. Aqueous solution of solutes (20 mL of DD, 1-ClDD, 2-ClDD and 15 mL of PCB 1, PCB-4, or PCB-47) over a range of initial solutes concentrations in a methanol carrier (< 0.1 volume %) were added to each tube. Control samples containing 0.8 mg L^{-1} DD, 0.4 mg L^{-1} 1-ClDD, 0.4 mg L^{-1} 2-ClDD, 5 mg L^{-1} PCB-1, 1.5 mg L^{-1} PCB-4 and 0.52 mg L^{-1} of PCB-47 without clay were prepared for calibration to quantify solute loss due to other processes. All experiments were conducted with two replicates. Cs-saponite and solute suspensions were vortexed for 30 sec and shaken at 80 strokes min^{-1} in a horizontal shaker at room temperature for 24 h to achieve apparent sorption equilibrium (as indicated from preliminary experiments). The smectite-solute suspensions were centrifuged at 5920 g for 20 min to separate the liquid and solid phases.

Table 4.1 Selected physicochemical properties of planar and non-planar solutes used in this study

	planar				Non planar	
	Dibenzo-p-dioxin	1-Chloro-dibenzo-p-dioxin [¶]	2-Chloro-dibenzo-p-dioxin [¶]	2-Chloro-biphenyl	2,2'-di-chlorobiphenyl	2,2',4,4'-tetra-chlorobiphenyl
Abbreviation	DD	1-ClDD	2-ClDD	PCB-1	PCB-4	PCB-47
Chemical formula	$C_{12}H_8O_2$	$C_{12}H_7O_2Cl$	$C_{12}H_7O_2Cl$	$C_{12}H_9Cl$	$C_{12}H_8Cl_2$	$C_{12}H_6Cl_4$
Molecular wt	184.2	218.6	218.6	188.6	223.1	292
Aq. Solubility (mg L^{-1})	0.901 [a]	0.422 [a]	0.278 [a]	6.05 [c]	1.69 [c]	0.103 [c]
Subcooled liquid state solubility (mg L^{-1}) **	8.429	2.648	1.197	12.366	2.272	0.079
M.P.($^{\circ}$C)	123 [b]	105.5 [b]	88 [b]	61 [d]	34 [d]	41.5 [d]
Log $K_{i,ow}$	4.30 [b]	4.90 [b]	5.45 [b]	4.30 [d]	4.90 [d]	5.90 [d]
Vapor pressure (@ 25°C) in Pa	5.4×10^{-2} [b]	1.2×10^{-2} [b]	1.7×10^{-2} [b]	0.26 [d]	0.50 [d]	0.02 [d]
Average polarizability (AU)	126.2 [f]	137.9 [f]	120.30 [f]	24.55 [g]	25.92 [g]	30.48 [g]
Dipole moment =μ (D)	0.64 [#]	1.35 [¥]	1.37 [¥]	1.6592 [¶]	2.3729 [¶]	1.9572 [¶]
Torsion angle [h]				55.8	82.1	82.1
Internal Rotation Barriers [h] (kJ-mole^{-1}): DE				28.6 (DE_o)	120 (DE_o),	120 (DE_o),

[a] Shiu (1988) ; [b] Åberg (2008) ; [c] Holmes and Harrison (1993); [d] (Mackay, 2006);; [f] Mhin et al. (2001); [g] Mckinney McKinney et al. (1983) et al., 1983; [h] Dorofeeva et al. (2005); # Fraschini et al. (1996); ¥ calculated using polarizability data from Mhin et al., 2001 and μx, μy from Urbaszek et al. (2017); ¶ Chana et al. (2002); **Subcooled liquid solubility (in water at 25°C) was estimated using published values of heat of fusion (ΔH), melting point (T$_m$), and aqueous solubility of solid and following Carmo et al. (2000).

4.3.4 Dioxin (DD, 1-ClDD and 2-ClDD) analysis

For DD, 1-ClDD, and 2-ClDD, one mL aliquots of the supernatant were transferred to high-performance liquid chromatography (HPLC) vials. In order to prevent the sorption of DD, 1-ClDD and 2-ClDD on HPLC vials, 0.5 mL of methanol (99.9% pure) was added to each vial prior to the addition of the supernatant. HPLC vials containing supernatant and methanol were vortexed for 30 sec and analyzed for DD, 1-ClDD and 2-ClDD concentrations by direct injection of 50 μl on a Shimadzu SLC-10 HPLC system equipped with a UV detector and a Supelcosil column (15 cm x 4.6 mm x 5 μm). Isocratic elution was performed using a mobile phase of 80% acetonitrile for 1-ClDD and 2-ClDD (80% methanol for DD): 20% water (v/v) with a flow rate 1.0 mL min^{-1}. Concentrations were quantitation using wavelengths of 223 nm for DD, 227 nm for 1-ClDD and 228 nm for 2-ClDD for detection. The amount of DD 1-ClDD, and 2-ClDD sorbed was calculated by difference assuming conservation of mass (difference between the initial chemical mass and what was remaining in the aqueous solution after equilibration was attributed to sorption). HPLC analysis of adsorption systems without the clay (DD1-ClDD and 2-ClDD solutions only) showed ~99.5% recovery of dioxins (DD, 1-ClDD, and 2-ClDD) from solution indicating minimal sorption on glass tubes, degradation or any other losses.

4.3.5 PCBs (PCB-1, PCB-4 and PCB-47) extraction

For PCB analysis, five mL aliquots of supernatant were transferred to 30-mL centrifuge tubes (Kimble HS-5600-30) with polytetrafluoroethylene (PTFE)-lined screw caps. Five mL of hexane (chromatography grade) was added to the centrifuge tubes and the solution was vortexed for a minute and horizontally shaken at the speed of 80 strokes min^{-1} in a horizontal shaker at room temperature for 15 min. The mixture was centrifuged at 5920 g for 20 min and 1.5 mL of the hexane layer was removed for GC-MS analysis of PCBs. To confirm sorption of PCBs on the clay

surface, 15 mL of methanol was added on the residual clay (from batch sorption experiment) and the suspension was then vortexed for 30 sec and horizontally shaken at the speed of 80 strokes min^{-1} in a horizontal shaker at room temperature for 24 h. The smectite (with PCB)-methanol suspension was centrifuged at 5920 g for 20 min to separate the liquid and solid phases and 5 mL aliquots of supernatant were transferred to 30 mL centrifuge tubes. PCBs were then extracted from methanol by hexane for analysis by gas chromatography/mass spectrometry (GC/MS) analysis.

4.3.6   GC/MS analysis of PCBs (PCB-1, PCB-4 and PCB-47)

Chlorinated biphenyls (PCB-1, PCB-4 and PCB-47) were analyzed by a GC/MS (Shimadzu GCMS-QP2010) equipped with AOC-20i/s sampler, in electron impact mode (EI+, 70 eV). The GC oven was equipped with DB-5ms (30 m x 0.25 mm i.d. x 0.25 mm d.f.) fused silica column. Samples (2 μM into the capillary inlet operated in splitless mode at 280°C) were introduced. Under a constant pressure (67.4 KPa) with column flow rate of 0.94 mL min-1, the following column temperature program was used for PCBs analysis: initial column temperature 100°C (0.5 min hold) $\rightarrow$ increase rate with 20°C min-1 $\rightarrow$ 280°C (10 min hold). The MS was operated in selected ion monitoring (SIM) mode with scanning at m/z values of 188, 152, 126 for PCB-1, 22, 187, 152 for PCB-4, and 292, 255 and 220 for PCB-47, with a 0,2-sec dwell time. The carrier gas was helium and the transfer line was maintained at 280°C.

4.3.7   X-ray diffraction (XRD)

X-ray diffraction patterns of Cs-saponite-dioxin or Cs-saponite-PCB complexes were collected using a PANalytical B.V. (Model X'Pert PRO diffractometer; Almelo, Netherlands) using Co radiation. One replicate sample of dilute clay-dioxin and clay-PCB suspensions from batch sorption experiment were passed through membrane filters (47 mm, 0.45 mm pore size, Millipore Co., Bedford, MA). The clay particles were then transferred into a vial and mixed with

200 mL of supernatant. The slurry was deposited on a glass slide and dried overnight at ambient conditions to obtain an oriented clay film. Data were collected from 2° to 60° 2θ, counting for 1s every 0.02° 2θ step. A 1° exit Soller slit was used between 2° to 12° 2θ. Data analysis was done using X'Pert HighScore Plus software Version 2.2 (PANalytical B.V.).

4.4   Results and Discussion

Sorption isotherms of PCBs and dioxins from water by Cs-montmorillonite (Cs-Sap-2) are compared in Figure 4.1a. To compare differences in sorption of chlorinated PCBs and dioxins to Cs-saponite from water that account for differences in solubility, subcooled liquid solubilizes (S_{scL}) needed to be calculated for normalizing aqueous concentration given their varying melting points (Carmo et al., 2000; le Site, 2001). Calculated SscL data for all six solutes are listed in Table 4.1.

The subcooled liquid solubility normalized sorption data (Figure 4-1B) were fitted to the Freundlich model expressed as:

$$C_s = K_f'(C_w/S_{scL})^{1/n} \quad \ldots\ldots (1)$$

where C_s is the amount of solute sorbed per g of smectite (mg kg^{-1}), C_w is equilibrium solute concentration (mg L^{-1}) in the bulk water, S_{scL} is the supercooled liquid aqueous solubility (mg L^{-1}), K_f' is the aqueous solubility normalized Freundlich isotherm coefficient (mg kg^{-1}), and 1/n (slope) is an indicator of nonlinearity of sorption isotherm. The S_{SCL} values (in water at 25°C) used for normalization were estimated using published values of heat of fusion (ΔH), melting point (T_m), and aqueous crystal solubility (S_w) and are listed in Table 4.1 (Mackay, 2006; Schwarzenbach, 2002).
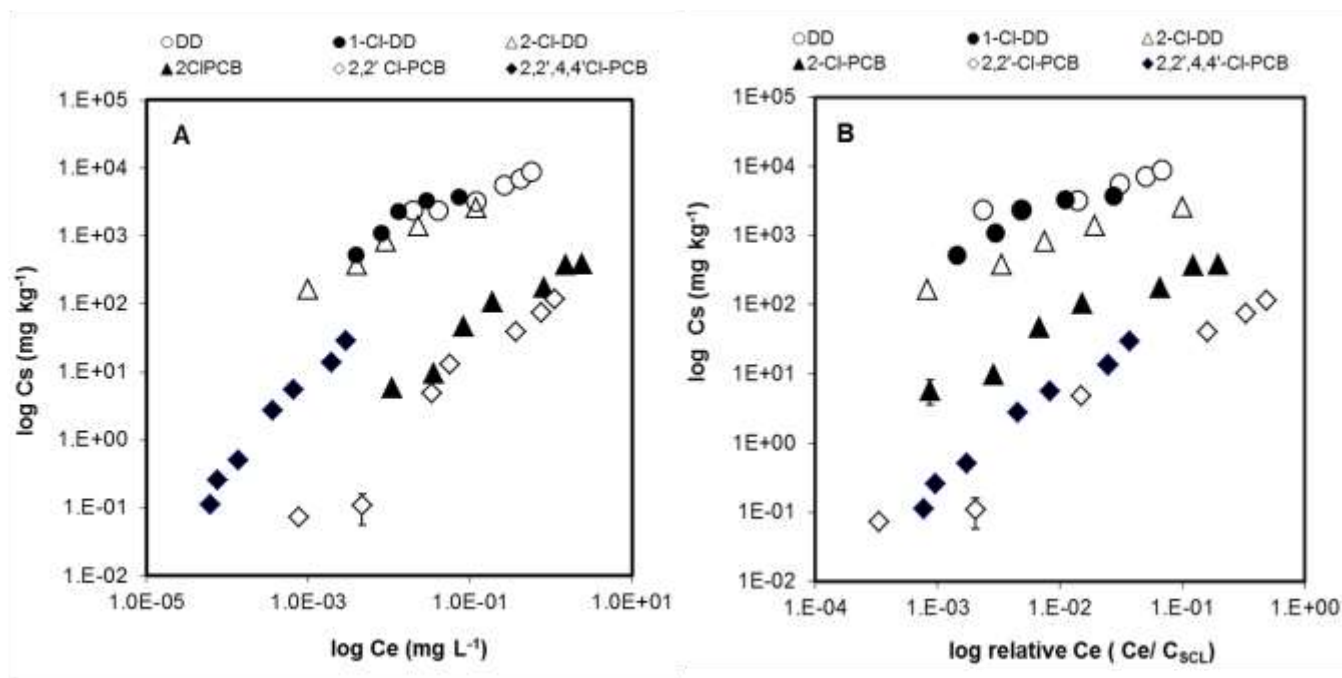
Figure 4.1 Sorption isotherm (a) and solubility normalized sorption isotherm (b) of planar dibenzo-p-dioxin (DD), 1-chloro-dibenzo-p-dioxin (1-ClDD) 2-chloro-dibenzo-p-dioxin (2-ClDD), 2-Chloro-bipehenyl(2-Cl-PCB) and non-planar 2,2'di-chloro-biphenyl(2,2'-PCB) and 2,2',4,4' tetra chloro-biphenyl (2,2',4,4'-Cl-PCB) on Cs-saponite

The Freundlich sorption coefficient (K_f') are listed in Table 4.2. The overall sorption affinity of dioxins from bulk water to Cs-saponite is 2 to 2.5 log units greater than that of PCBs and decreased in the following order: 1-Cl-DD > DD > 2Cl-DD >>>> PCB-1 >> PCB-47 ≥ PCB 4.

Dioxins have a planar molecular structure (DD has D_{2h} symmetry) comprised of two phenyl rings in the same plane bridged by a pair of oxygen atoms (Gastilovich et al., 2002; Klimenko et al., 2000). In case of PCBs, the two phenyl groups are connected through a single carbon-carbon (C-C) bond. The phenyl rings tend to rotate around the C-C bond with a preferred angle of ~38 degrees between the two phenyl rings (Dorofeeva et al., 1999). For 97 PCB congeners (including PCB-4 and PCB-47 that were used in the current study) out of a total of 209 PCBs, the two phenyl

rings are oriented in two different planes with torsion angle values close to 90° (Dorofeeva et al., 1999). The non-planar symmetry of these congeners is attributed to the presence of chlorine substitution at two or more ortho (2, 2', 6, 6') positions that inhibit free rotation of the phenyl rings. However, The remaining 112 PCB congeners (including PCB-1 used in this study), which do not have chlorine substitutions in two or more ortho (2, 2', 6, 6') positions can achieve close to flat structure that is similar to dioxin molecules and are commonly known as dioxin-like PCBs or co-planar PCBs (Chana et al., 2002; Nyffeler et al., 2018).

Table 4.2 Solubility normalized Freundlich sorption isotherm parameters for the Planar DD, 1-ClDD and, 2-ClDD, co-planar PCB-1 and non-planar PCB-4 and PCB-47 sorption to the Cs-saponite and their comparison to calculated log K_{oc}.

Solute	Log (K_f', mg kg^{-1})	1/n	Log K_{oc}
DD	3.9872	0.408	3.11[§]
1-ClDD	4.7508	0.6737	3.65[§]
2-ClDD	4.0844	0.5908	4.15[§]
PCB-1	3.2751	0.8125	3.55[‡]
PCB-4	2.4851	1.0877	3.72[‡]
PCB47	3.4471	1.2751	4.81[‡]

Log K_{oc} estimated using: [§] log K_{oc}= 0:904 log K_{ow} − 0.779 (Chiou et al., 1983)) [‡] log K_{oc}= 0:904 log K_{ow} − 0.479,

Sorption of PCB-1 and PCB-4 by Cs-saponite is much lower compared with DD and 1-ClDD despite the fact that both PCB-1 & DD and PCB-4 & 1-ClDD have same log K_{ow} values (or hydrophobicity) 4.30 and 4.90, respectively (Table 4.2). This sharp difference (2-2.5 log units) in sorption affinities of dioxins and PCBs, despite having similar dispersive interaction potential, is likely due to the steric effect or distinct sorption mechanisms for dioxins and PCBS.

Generally, sorption of hydrophobic sorbate on smectite clay is affected by i) hydrophobic (*Van der Waals*) interaction of sorbate with nonpolar siloxane domains between the exchangeable cations in the clay interlayer (dispersive effect); ii) site-specific interaction between the sorbate and the exchangeable cation in the clay interlayer; and iii) interlayer distance between the opposing clay sheets and thickness of sorbate (steric effect) (Aggarwal et al., 2006; Johnston et al., 2004b; Sheng et al., 1996). The K_{ow} of PCB-1 is lower than that of non-planar PCBs (PCB-4 and PCB-47); therefore, PCB-1 has lower dispersive interaction with planar siloxane surfaces of Cs-saponite. The higher sorption of co-planar (PCB-1) relative to non-planar PCBs (PCB-4 and PCB-47) suggested that hydrophobicity K_{ow} is not the only physicochemical parameter that can predict the sorption of hydrophobic compounds. The difference in the sorption of PCB-1 and non-planar PCBs (PCB-4, and PCB-47) can be explained by molecular planarity or steric effect. The torsional angle between two phenyl rings and internal rotation barrier of PCB-1 is smaller than those of di-ortho substituted PCB-4 and PCB-47 (Table 1) As a result; PCB-1 can easily adapt a planar molecular configuration. In contrast, for di-ortho-substituted PCBs (PCB-4 and PCB-47) it is energetically not favorable to adapt planar configuration and have a rigid and bulky (~8 Å thick) non-planar structure.

Rigid non-planar PCBs will be more sterically restricted to interact the with planar siloxane surface. These results are consistent with a previous study by Liu et al. (2015),which showed that the molecular planarity significantly influenced the sorption behavior. In this study tetra-chlorinated non-planar PCB-47 showed relatively higher affinity over di-chlorinated PCB-4 suggested that hydrophobic (*Van der Waals*) interaction is the major driving force for the sorption of non-planar PCBs.

Additionally, sorption affinity of dioxins is a log unit higher than estimated K_{oc} values (Table 4.2). A pronounced difference in the sorption affinity of planar dioxins and co-planar and non-planar PCBs to Cs-saponite can be attributed to combined effect of *Van der Waals* interaction, steric effect, site-specific interaction or combination of all three mechanisms.

XRD patterns of oriented deposits of Cs-saponite with different loadings of dioxins and PCBs are shown in Fig. 4-2. The d_{001} spacing of air-dried Cs-saponite without dioxin or PCB loading is 12.3 Å and corresponds to about one molecular layer of water in the interlayer (Liu et al., 2009).
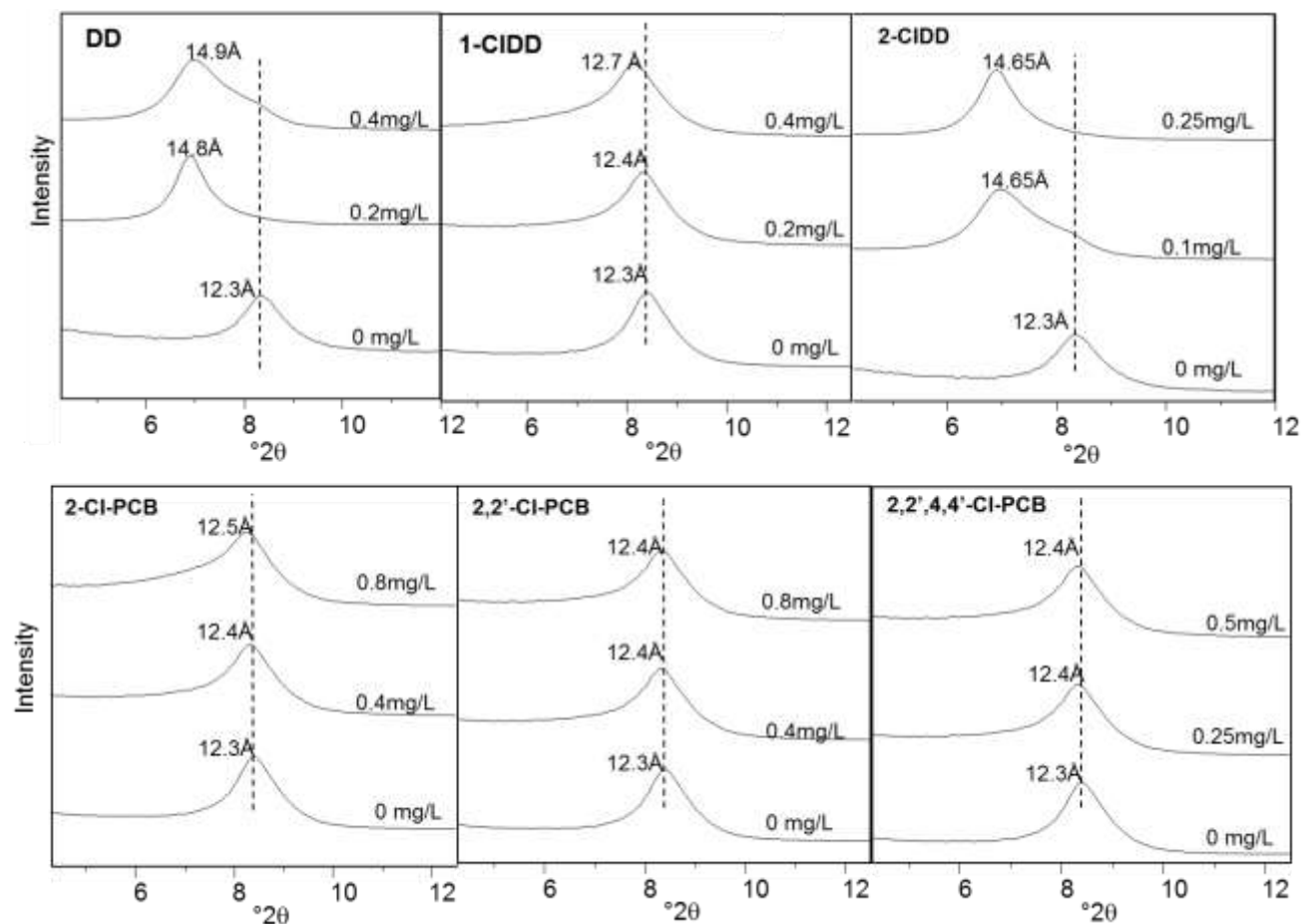
Figure 4.2 X-ray diffraction patterns of Cs-Saponite clay films equilibrated with increasing concentrations of dibenzo-p-dioxin (DD), 1-chloro-dibenzo-p-dioxin (1-ClDD) 2-chloro-dibenzo-p-dioxin (2-ClDD), 2-Chlorol-bipehnyl(2-Cl-PCB),2,2'di-chloro-biphenyl(2,2'-PCB) and 2,2',4,4' tetra chloro-biphenyl(2,2',4,4'-Cl-PCB) solution.

A gradual increase in the d_{001} spacing from 12.3 to 14.9 Å, 14.7 Å, 12.7 Å and 12.5 Å for DD, 2-ClDD, 1-ClDD and PCB-1, respectively. Gradual increase in d_{001} spacing with increasing loading of DD,1-ClDD, 2-ClDD and PC-1confirms the intercalation of these molecules in the Cs-saponite interlayer. The thickness of a clay layer alone is ~ 9.6 Å, which means the distance between the opposing clay sheets is ~3 Å. This interlayer distance is similar to the thickness (~ 3 Å), of the planar dioxins (DD, 1-ClDD and 2-ClDD) and co-planar PCB-1 molecules thus dioxins and coplanar PCB could fit between the clay interlayer and can interact directly with neutral siloxane domain between two charge sites and with exchangeable cation (Aggarwal et al., 2006).

Modest increase in d_{001} spacing after 1-ClDD and PCB-1 indicates that 1-ClDD and PCB-1 molecules are oriented with its molecular plane parallel to the basal surface of the clay (Chapter 3- Kiran Rana Bangari; Bushra Khan; Sheng et al., 2002). In contrast, a significant increase in the d_{001} spacing for DD, 2-ClDD suggest that DD and 2-ClDDhave adopted a tilted orientation in the clay interlayer (Liu et al., 2009; Rana et al., 2009). For PCB-4 and PCB-47 no significant increase d_{001} basal spacing and therefor no evidence of intercalation was observed. No increase in d_{001} spacing of PCB-4 and PCB-47 and comparatively lower sorption of these nonplanar molecules suggested that sorption is likely only occurring on external surface and the structural bulkiness (~ 8 Å thickness) which inhibits intercalation; due to steric effect, in the Cs-saponite interlayer.

Multivariate analysis of sorption isotherm coefficients (K_f') with physicochemical properties and molecular attributes of dioxins and PCBs (Figure Appendix B-3 and Figure 4.3.) suggested that sorption of these compounds is linearly influenced by dipole moment and polarizability. Molecular dipole moment is expressed as a sum of discrete charges (multiplied by distance from origin to the charge) which arises from differences in the electronegativity. Polarizability is the relative tendency of the electron cloud distortion by an external electric field

resulting in dipoles, thus a nonpolar molecule can have a molecular charge distribution (Chang, 2005; Council, 2014). These molecular attributes are important in determining the intermolecular forces and geometry of molecules.

Categorical analysis (dioxin vs. PCBs) of these linear relationships revealed that adsorption of dioxins to smectite clay is highly influenced by molecular dipole moment (Figure 4.4), while PCB adsorption is influenced for net molecular polarizability. Dipole moment (Table 4.1) of aromatic molecules is influenced by presence of electronegative hetero-atom(s) or functional group and degree and position of chlorine substitution (Chana et al., 2002). The dioxin molecule has two oxygen hetero-atoms and the correlation between the dipole moment and log K_f' suggests that sorption of dioxins is facilitated by the electrostatic cation-dipole interactions between heterocyclic oxygen atoms of dioxins and Cs^+ in combination with *Van der Waals* interactions. Saponite is a trioctahedral clay with surface area cation exchange capacity of 94 cmol kg^{-1}, a total surface area of 750 m^2 g^{-1} and 100% of the charge is originating from trioctahedral sheet of clay. In this configuration, 71m^2 surface of saponite clay is influenced by exchangeable cation while 679 m^2 of its area is neutral (siloxane surface) in nature which can stabilize the sorption of semi-polar and neutral organic compounds on smectites (Jaynes and Boyd, 1991). Our previous studies showed that site-specific interactions occur between dioxin central ring and exchangeable cations (Chapter 2 and Chapter 3)
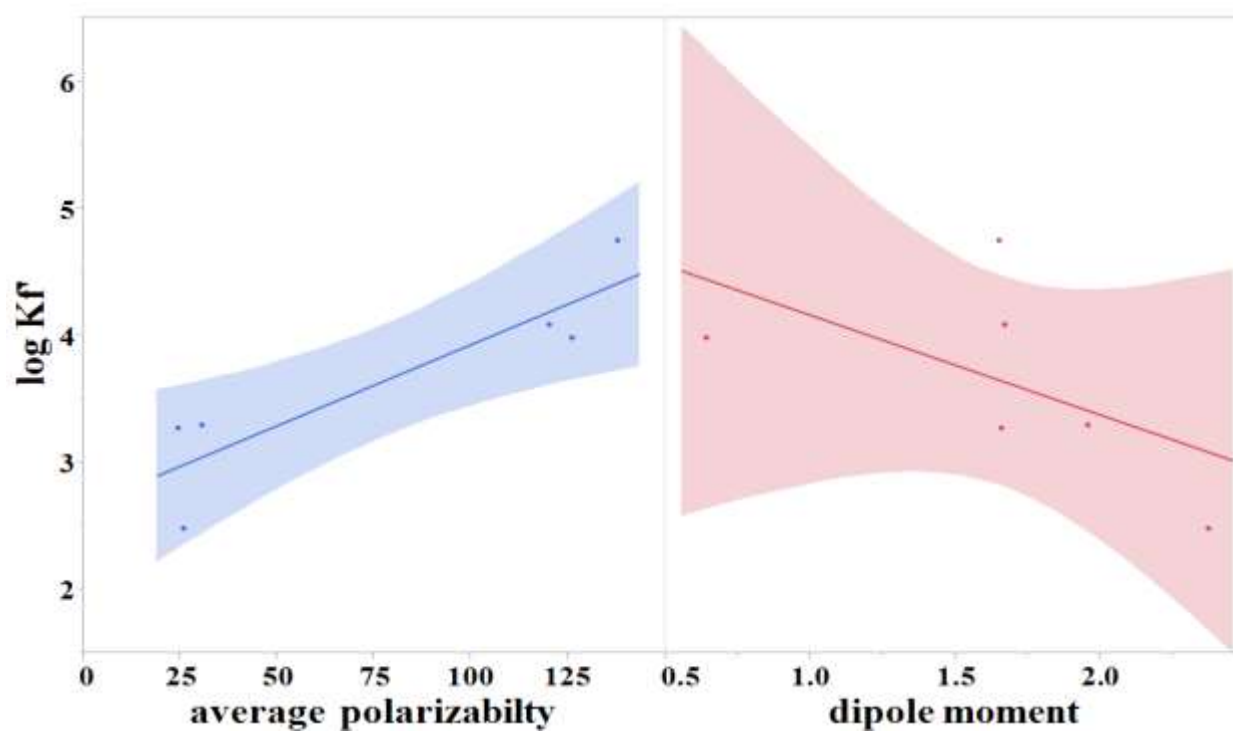
Figure 4.3 Expanded multivariate analysis scatter plot matrix of sorption isotherm coefficients and physicochemical properties of dioxins (DD, 1-ClDD, 2-ClDD) and PCBs (2Cl-PCB, 2, 2'-Cl-PCB, and 2,2',4,4'-Cl-PCB). Shaded area is showing confidence of fit.
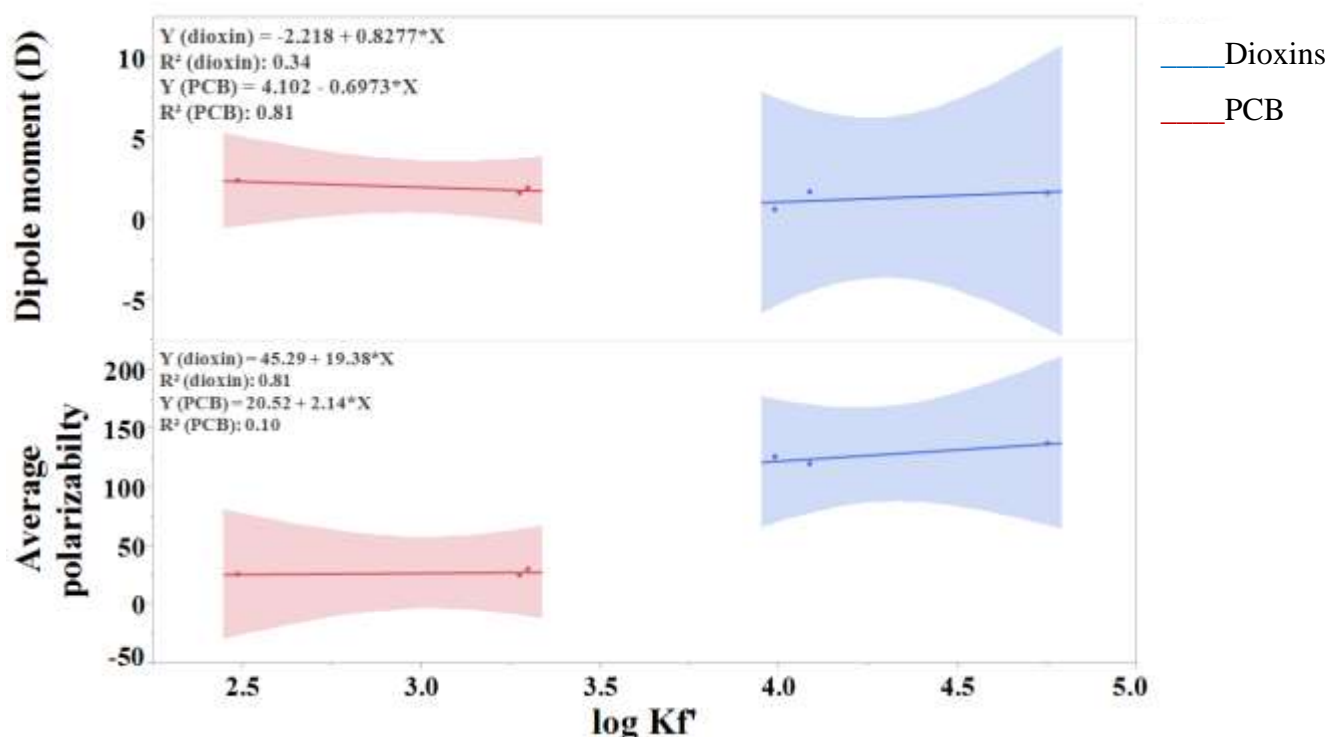
Figure 4.4 Relation between the solubility normalized Freundlich sorption isotherm coefficients (log $K_f^{'}$) and polarizability and dipole moment dioxins (DD, 1-ClDD, 2-ClDD) and PCBs (2Cl-PCB, 2,2' -Cl-PCB, and 2,2',4,4' -Cl-PCB). Shaded area is showing confidence of fit.

Linear relation between K_f' and polarizability of PCBs (Figure 4.4) suggests that orientation of the PCB molecule and dispersive interactions are the major drivers for the adsorption of PCBs to the smectite clays. Molecular orientation and degree of chlorination affects the net polarizability of the molecule and dispersive attractions between nonpolar molecule and charged surface is directly proportional the net polarizability of molecule (Chang, 2005; Mckinney and Singh, 1981).

In summary, the strong variation in the sorption of planar and non-planar compounds (with similar K_{ow} values) from bulk water to Cs-saponite suggests that K_{ow} (hydrophobicity) is not the only physicochemical parameter to be considered in the prediction of sorption of dioxins and PCBs to the clay surfaces. Polarizability and dipole moment of sorbate appear to be the important factors

in determining the sorption affinity of dioxins and PCBs for clay minerals. Dispersive attractions; which is directly influenced by polarizability and molecular orientation with respect to charged ions or surface, are major drivers for PCB adsorption and due to steric effect nonplanarity and bulkiness of non-planar PCB prevents the intercalation of these molecules to the clay interlayer. High sorption affinity of dioxins is attributed to combination of direct interactions between dioxins and exchangeable cations, *Van der Waals* interactions and the competition between the dioxin and interlayer water molecules. Results of our study contributed toward a better understanding of how the smectites saturated with weakly hydrated exchangeable cations contribute to the sorption of nonpolar compounds.

CHAPTER 5.   CONCLUSIONS AND FUTURE WORK

5.1   Conclusion

The research presented in this thesis focused on interaction of dioxin and chlorinated biphenyl (PCB) congeners with expandable clay mineral (smectite) water systems. Influence of clay mineral properties such as nature of exchangeable cations and type of isomorphic substitution in clay lattice on dioxin sorption was investigated using dibenzo-p-dioxins as a model solute. Integrated batch sorption and *in-situ* microscopic (infrared spectroscopy (IR), Raman spectroscopy and X-ray diffraction (XRD) and computational methods were used to characterize the extent and mechanism of sorption of dioxins. Furthermore, influence of solutes properties, especially solutes structure and degree of chlorination, on sorption was investigated. The major findings of this study are:

1. Both dioxin congeners (DD and 1-Cl-DD) shows high affinity for smectites, especially for clay minerals exchanged with weakly hydrated monovalent cations (e.g., Cs^+). The sorption of both dioxin congeners on Cs-saturated smectites were equal or greatly exceeded that by other naturally occurring sorbents such as soil organic matter. These results indicate that the clay is dominant sorptive domain for dioxin and clay interlayer is an important sorption site for dioxin.

2. Regarding clay specificity, highest sorption was observed on saponite, a trioctahedral smectite with isomorphous substitution in the tetrahedral sheet. Of the cation-smectite variables explored in this study, the nature of the exchangeable cation was the most significant determinant followed by the type of clay. Adsorption was promoted by clay interlayer exchangeable cations with low hydration energies, and negative charge in the smectite arising from the tetrahedral siloxane sheets.

3. Polarized FTIR and Raman spectra of sorbed DD and 1-ClDD on the clay minerals revealed information about the orientation of the sorbed species and, in the case of DD on saponite, specific information about the interaction of the sorbed DD species with the interlayer cation. Specifically, Raman spectra of dioxin associated with Cs-saponite showed that the molecular symmetry of the interlayer species was reduced. Integrated batch sorption, spectroscopic and XRD data suggested DD and 2-ClDD molecules adopted a tilted orientation while 1-ClDD molecules were oriented nearly parallel to the siloxane surface of the clay.

4. Sorption of dibenzo-p-dioxin (DD), 1-chloro-dibenzo-p-dioxin (1-ClDD) and 2-ClDD. For all the smectites studied, sorption of 1-ClDD was greater than that of DD and 2-ClDD In-situ- ATR-FTIR data of 1-Cl-DD sorption on Cs-saponite revealed that the sorption of 1-Cl-DD is accompanied by dehydration of the clay interlayer

5. The location of the chlorine constituent in 1-ClDD prevents the molecule from its apparent energetically more favorable orientation. In addition, to the XRD results, *in-situ* ATR-FTIR spectra revealed that sorption of 1-ClDD to Cs-saponite resulted in the loss of interfacial H_2O and suggest the sorption 1-ClDD displaces interlayer H_2O. 2-ClDD is less sterically restricted in the clay interlayer. The sorption free energies calculated for 1-ClDD and DD molecules by adaptive biasing force (ABF) method with an extended interlayer–micropore two-phase model consisting of cleaved clay hydrates and "bulk water" manifesting higher sorption of 1-ClDD was attributed to the hydrophobic interactions and partial dehydrations.

6. Sorption isotherms results of six nonpolar compounds (DD, 1-Cl-DD, 2-ClDD, PCB-1, PCB-4, PCB47), with similar K_{ow} and varying molecular planarity on reference Cs-

saponite shows that planar (DD, 1-Cl-DD, 2-ClDD, PCB-1) solutes have higher sorptive affinity for smectites than those of non-planar (PCB-4, PCB-47). XRD data supports the intercalation of planar and coplanar molecules in the clay interlayer was inhibited by steric effects and suggested that sorption of non-planar PCBs (PCB-4 and PCB47) is likely only occurring on external surface due to their structure bulkiness.

7. The structure activity relationships (SARs) between the sorption coefficients, molecular attributes and physiological properties of dioxin and PCBs demonstrate that sorption trends were correlated with differences in polarizability, dipole-moment and Henry's constant. SARs also suggested that high sorption affinity of planar dioxins could be due to a combination of *Van der Waals* interactions with the siloxane surface, and site-specific interactions between dioxin and exchangeable cations. In contrast, the sorption of PCBs was highly influenced by their molecular orientation and polarizability.

5.2   Future Work

The current study has provided a better understanding of the mechanisms controlling the sorption of dioxins in smectites and potential contribution of clay minerals in the sorption of dioxins and chlorinated PCBs in the environment. From this work, the need for additional research becomes apparent as itemized below.

1. In this study, we have measured the individual contribution of smectite clay in the sorption of dioxins and PCBs. The Freundlich sorption coefficient (log K_f) of DD and 1-Cl-DD sorbed on Cs-saponite were approximately one order of magnitude higher their respective K_{oc} value. However, in the soil environment, clay minerals tends to bind to SOM and most SOM exists as SOM-Clay complexes. The sorption studies on humic substance-clay

complexes and other soil components, e.g., activated carbon, will improve the predictions on the uptake of dioxins and dioxin-like toxic pollutants by soils.

2. Integrated sorption and spectroscopic results presented in this dissertation clearly shows that smectite with poorly hydrated cations on the exchange sites have a high capacity to adsorb dioxins and that site-specific interaction between the exchangeable cation of smectite and dioxin drives the sorption. Sorption tends to separate the direct contact between microorganisms and contaminants, which is necessary for biodegradation to occur. Additionally, dioxin forms inner-sphere complexes with poorly hydrated exchangeable cations of smectite and cation exchange with more highly hydrated cations may facilitate the desorption of the smectite-sorbed dioxins. Understanding the desorption kinetics of sorbed dioxin is an important step towards understanding the transport, bioavailability, degradation and toxicity of dioxins in soil.

3. Dioxin profiles detected in prehistoric clay deposits were enriched in octa-chloro-dibenzo-p-dioxin (OCDD) and the concentration of other dioxin congeners were inversely related to the degree of chlorination. Many hypotheses, including clay mediated dioxin formation from precursor chlorophenol and sequestration of prehistoric dioxins during sedimentation, have been proposed. In this research, we have evaluated sorption of non-chlorinated dibenzo-p-dioxin (DD) and mono-chlorinated-DD. However, sequestration and high affinity OCDD to clay minerals and the mechanisms behind sequestration still to need to be investigated.

REFERENCES

Abad, E., Llerena, J. J., Saulo, J., Caixach, J., and Rivera, J. (2002). Comprehensive study on dioxin contents in binder and anti-caking agent feed additives. *Chemosphere* **46**, 1417-1421.

Åberg, A. W., K. ; MacLeod, M. (2008). Physical-Chemical Property Data for Dibenzo-p-dioxin (DD), Dibenzofuran (DF), and Chlorinated DD/Fs: A Critical Review and Recommended Values. *Journal of Physical and Chemical Reference Data* **37**.

Aggarwal, V., Li, H., Boyd, S. A., and Teppen, B. J. (2006). Enhanced sorption of trichloroethene by smectite clay exchanged with Cs+. *Environmental Science & Technology* **40**, 894-899.

Aggarwal, V., Li, H., and Teppen, B. J. (2005). Triazine Adsorption by Saponite and Beidellite Clay Minerals. *Environmental Toxicology & Chemistry*.

Ahn, D. J., and Franses, E. I. (1992). Orientations of chain axes and transition moments in Langmuir-Blodgett monolayers deterimined by polarized FTIR-ATR spectroscopy. *Journal of Physical Chemistry* **96**, 9952-9959.

Beyer, A., and Biziuk, M. (2009). Environmental Fate and Global Distribution of Polychlorinated Biphenyls. *In* "Reviews of Environmental Contamination and Toxicology, Vol 201" (D. M. Whitacre, ed.), Vol. 201, pp. 137-158.

Borlak, J. T. T. (2001). Induction of nuclear transcription factors, cytochrome P450 monooxygenases, and glutathione S-transferase alpha gene expression in Aroclor 1254-treated rat hepatocyte cultures. *Biochemical Pharmacology* **61**, 8.

Boyd, S. A., G.Y.Sheng, B.J.Teppen, and C.J.Johnston (2001a). Mechanisms for the adsorption of substituted nitrobenzenes by smectite clays. *Environ. Sci. Technol. 35* (**2001**) 4227-4234. *Environmental Science & Technology* **35**, 4227-4234.

Boyd, S. A., Johnston, C. T., Laird, D. A., Teppen, B. J., and Li, H. (2011). Comprehensive Study of Organic Contaminant Adsorption by Clays: Methodologies, Mechanisms, and Environmental Implications. *In* "In *Biophysico-Chemical Processes of Anthropogenic Organic Compounds in Environmental Systems.*", pp. 51-71. John Wiley & Sons, Inc.,.

Boyd, S. A., Sheng, G., Teppen, B. J., and Johnston, C. T. (2001b). Mechanisms for the adsorption of substituted nitrobenzenes by smectite clays. *Environ. Sci. Technol* **35**, 4227-4234.

Broman, D., Naf, C., and Zebuhr, Y. (1992). Occurrence and Dynamics of Polychlorinated Dibenzo-Para-Dioxins and Dibenzofurans and Other Combustion Related Organic Pollutants in the Aquatic Environment of the Baltic. *Chemosphere* **25**, 125-128.

Brzuzy, L. P., and Hites, R. A. (1996). Global mass balance for polychlorinated dibenzo-p-dioxins and dibenzofurans - Response. *Environmental Science & Technology* **30**, 3647-3648.

C.T., J., S.A, B., B.J., T., and G.Y., S. (2004). Sorption of nitroaromatic compounds on clay surfaces. *In* "Handbook of layered materials" (A. S.M., C. K.A. and D. P.K., eds.), pp. 155-189. Marcel Dekker, Inc., New York.

Carmo, A. M., Hundal, L. S., and Thompson, M. L. (2000). Sorption of hydrophobic organic compounds by soil materials: Application of unit equivalent Freundlich coefficients. *Environmental Science & Technology* **34**, 4363-4369.

Chana, A., Concejero, M. A., de Frutos, M., Gonzalez, M. J., and Herradon, B. (2002). Computational studies on biphenyl derivatives. Analysis of the conformational mobility, molecular electrostatic potential, and dipole moment of chlorinated biphenyl: searching for the rationalization of the selective toxicity of polychlorinated biphenyls (PCBs). *Chem Res Toxicol* **15**, 1514-26.

Chang, R. (2005). Intermolecular Forces/ Ion-Induced Dipole and Dipole-Induced Dipole Interactions/ Dispersion, or London, Interactions. *In* " Physical Chemistry for the Biosciences. ", pp. 495-98. Sansalito, CA: University Science,.

Chappell, M. A., Laird, D. A., Thompson, M. L., Li, H., Teppen, B. J., Aggarwal, V., Johnston, C. T., and Boyd, S. A. (2005). Influence of smectite hydration and swelling on atrazine sorption behavior. *Environmental Science & Technology* **39**, 3150-3156.

Chapter 3- Kiran Rana Bangari; Bushra Khan, C. L., Stephen A. Boyd, Brian J. Teppen, Hui Li and Cliff. T. Johnston Molecular Mechanisms of chlorinated dibenzo-p-dioxins interactions with smectites

Charles, S., Teppen, B. J., Li, H., Laird, D. A., and Boyd, S. A. (2006). Exchangeable cation hydration properties strongly influence soil sorption of nitroaromatic compounds. *Soil Science Society of America Journal* **70**, 1470-1479.

Chiou, C. (1985). Partition Coefficients of Organic Compounds in Lipid-Water Systems and Correlations with Fish Bioconcentration Factors. *Environmental Science and Technology* **19**, 57-62.

Chiou, C. T. (1990). Roles of organic matter, minerals, and moisture in sorption of nonionic compounds and pesticides by soil. *In* "Humic substances in soil and crop sciences: selected readings" (P. MacCarthy, C. E. Clapp, R. L. Malcom and P. R. Bloom, eds.), pp. 111-160. SSSA, Madison, Wisconsin.

Chiou, C. T., Porter, P. E., and Schmedding, D. W. (1983). Partition equilibria of nonionic organic compounds between soil organic matter and water. *Environmental Science and Technology* **17**, 227-231.

Choi, H., and S.R.Al-Abed (2009). PCB congener sorption to carbonaceous sediment components: Macroscopic comparison and characterization of sorption kinetics and mechanism. . *Journal of Hazardous Materials* **165**, 6.

Cordes, A. W., and Fair, C. K. (1974). Dibenzo Para Dioxin. *Acta Crystallographica Section B-Structural Science* **B 30**, 1621-1623.

Council, N. R. (2014). Physicochemical Properties and Environmental Fate. *In* "A Framework to Guide Selection of Chemical Alternatives". Washington (DC): National Academies Press (US).

De Oliveira, M. F., Johnston, C. T., Premachandra, G. S., Teppen, B. J., Li, H., Laird, D. A., Zhu, D. Q., and Boyd, S. A. (2005). Spectroscopic study of carbaryl sorption on smectite from aqueous suspension. *Environmental Science & Technology* **39**, 9123-9129.

Denison, M. S., and Nagy, S. R. (2003). Activation of the aryl hydrocarbon receptor by structurally diverse exogenous and endogenous chemicals. *Annual Review of Pharmacology and Toxicology* **43**, 309-334.

Dorofeeva, O. V., Iorish, V. S., and Moiseeva, N. F. (1999). Thermodynamic properties of dibenzo-p-dioxin, dibenzofuran, and their polychlorinated derivatives in the gaseous and condensed phases. 1. Thermodynamic properties of gaseous compounds. *Journal of Chemical and Engineering Data* **44**, 516-523.

Dorofeeva, O. V., Novikov, V. P., Moiseeva, N. F., and Yungman, V. S. (2005). Density functional calculation of conformations and potentials of internal rotation in polychlorinated biphenyls. *Journal of Structural Chemistry* **46**, 237-242.

EPA (2000). "Information Sheet 1: Dioxin: Summary of the Dioxin Reassessment Science." U.S. Environmental Protection Agency. Office of Research and Development. .

Eriksen, T. K., Hansen, B. K. V., and Spanget-Larsen, J. (2008). The vibrational structure of dibenzo-p-dioxin. IR linear dichroism, Raman spectroscopy and quantum chemical calculations. *Polish Journal of Chemistry* **82**, 921-934.

Ferrario, J., and Byrne, C. (2000). The concentration and distribution of 2,3,7,8-dibenzo-p-dioxins/-furans in chickens. *Chemosphere* **40**, 221-224.

Ferrario, J., and Byrne, C. (2002). Dibenzo-p-dioxins in the environment from ceramics and pottery produced from ball clay mined in the United States. *Chemosphere* **46**, 1297-1301.

Ferrario, J., Byrne, C., and Schaum, J. (2007). Concentrations of polychlorinated dibenzo-p-dioxins in processed ball clay from the United States. *Chemosphere* **67**, 1816-1821.

Ferrario, J. B., Byrne, C. J., and Cleverly, D. H. (2000). 2,3,7,8-dibenzo-p-dioxins in mined clay products from the United States: Evidence for possible natural origin. *Environmental Science & Technology* **34**, 4524-4532.

Fiedler, H., Abad, E., van Bavel, B., de Boer, J., Bogdal, C., and Malisch, R. (2013). The need for capacity building and first results for the Stockholm Convention Global Monitoring Plan. *Trac-Trends in Analytical Chemistry* **46**, 72-84.

Frankki, S., Persson, Y., Tysklind, M., and Skyllberg, U. (2006). Partitioning of CPs, PCDEs, and PCDD/Fs between particulate and experimentally enhanced dissolved natural organic matter in a contaminated soil. *Environ Sci Technol* **40**, 6668-73.

Franzblau, A., Hedgeman, E., Chen, Q., Lee, S. Y., Adriaens, P., Demond, A., Garabrant, D., Gillespie, B., Hong, B., Jolliet, O., Lepkowski, J., Luksemburg, W., Maier, M., and Wenger, Y. (2008). Case report: human exposure to dioxins from clay. *Environ Health Perspect* **116**, 238-42.

Fraschini, E., Bonati, L., and Pitea, D. (1996). Molecular Polarizability as a Tool for Understanding the Binding Properties of Polychlorinated Dibenzo-p-Dioxins: Definition of a Reliable Computational Procedure. *The Journal of Physical Chemistry* **100**, 10564-10569.

Friedman, H. L., and Krishnan, C. V. (1973). Thermodynamics of Ionic Hydration. *In* "Water: A comprehensive treatise. Volume 3 Aqueous solutions of simple electrolytes" (F. Franks, ed.), pp. 1-118. Plenum, New York.

Gadomski, D., Tysklind, M., Irvine, R. L., Burns, P. C., and Andersson, R. (2004). Investigations into vertical distribution of PCDDs and mineralogy in three ball clay cores from the United States exhibitinh the natural formation pattern. *Environmental Science & Technology* **38**, 4956-4963.

Gastilovich, E. A., Klimenko, V. G., Korol'kova, N. V., and Nurmukhametov, R. N. (2000). Optical spectra and photophysical properties of polychlorinated dibenzo-p-dioxins. *Uspekhi Khimii* **69**, 1128-1148.

Gastilovich, E. A., Klimenko, V. G., Korol'kova, N. V., and Nurmukhametov, R. N. (2002). Spectroscopic data on nuclear configuration of dibenzo-p-dioxin in S-0, S-1, and T-1 electronic states. *Chemical Physics* **282**, 265-275.

Gaus, C., Brunskill, G. J., Connell, W., Prange, J., Muller, J. F., Papke, O., and Weber, R. (2002). Transformation processes, pathways, and possible sources of distinctive polychlorinated dibenzo-p-dioxin signatures in sink environments. *Environ Sci Technol* **36**, 3542-9.

Gaus, C., Brunskill, G. J., Weber, R., Papke, O., and Muller, J. F. (2001). Historical PCDD inputs and their source implications from dated sediment cores in Queensland (Australia). *Environmental Science & Technology* **35**, 4597-4603.

Goldstein, J. A. a. S., S., (1989). Mechanism of action and structure-activity relationships for the chlorinated dibenzo-p-dioxins and related compounds. . *In* "Halogenated Biphenyls, Terphenyls, Naphthalenes, Dibenzodioxins and Related Products" (R. D. a. J. Kimbrough, A. A. , ed.), pp. 239-293. Elsevier Science, Eds.,Elsevier, Amsterdam, The Netherlands.

Grahn, M., Lobanova, A., Holmgren, A., and Hedlund, J. (2008). Orientational Analysis of Adsorbates in Molecular Sieves by FTIR/ATR Spectroscopy. *Chemistry of Materials* **20**, 6270-6276.

Grainger, J., Reddy, V. V., and Patterson, D. G. (1988). Molecular-Geometry Approximations for Chlorinated Dibenzodioxins by Fourier-Transform Infrared-Spectroscopy. *Applied Spectroscopy* **42**, 643-655.

Grainger, J., Reddy, V. V., and Patterson, D. G. (1989). Molecular Geometry-Toxicity Correlations for Laterally Tetrachlorinated Dibenzo-Para-Dioxins by Fourier-Transform Infrared-Spectroscopy. *Chemosphere* **18**, 981-988.

Green, N. J. L., Hassanin, A., Johnston, A. E., and Jones, K. C. (2004). Observations on historical, contemporary, and natural PCDD/Fs. *Environmental Science & Technology* **38**, 715-723.

Gu, C., Liu, C., Ding, Y., Li, H., Teppen, B. J., Johnston, C. T., and Boyd, S. A. (2011). Clay mediated route to natural formation of Polychlorodibenzo-p-dioxins. *Environ Sci Technol* **45**, 3445-51.

Halsall, C. J., Lee, R. G. M., Coleman, P. J., Burnett, V., Harding-Jones, P., and Jones, K. C. (1995). PCBs in U.K. Urban Air. *Environmental Science & Technology* **29**, 2368-2376.

Hayward, D. G., and Bolger, P. M. (2005). Tetrachlorodibenzo-p-dioxin in baby food made from chicken produced before and after the termination of ball clay use in chicken feed in the United States. *Environmental Research* **99**, 307-313.

Hayward, D. G., Nortrup, D., Gardner, A., and Clower, M. (1999). Elevated TCDD in chicken eggs and farm-raised catfish fed a diet with ball clay from a southern United States mine. *Environmental Research* **81**, 248-256.

Hoekstra, E. J., De Weerd, H., De Leer, E. W. B., and Brinkman, U. A. T. (1999). Natural formation of chlorinated phenols, dibenzo-p-dioxins, and dibenzofurans in soil of a Douglas fir forest. *Environmental Science & Technology* **33**, 2543-2549.

Hoffman, M. K., Huwe, J., Deyrup, C. L., Lorentzsen, M., Zaylskie, R., Clinch, N. R., Saunders, P., and Sutton, W. R. (2006). Statistically designed survey of polychlorinated dibenzo-p-dioxins, polychlorinated dibenzofurans, and co-planar polychlorinated biphenyls in US meat and poultry, 2002-2003: Results, trends, and implications. *Environmental Science & Technology* **40**, 5340-5346.

Holmes, D. A., and Harrison, B. K. (1993). Estimation of Gibbs free energies of formation for polychlorinated biphenyls. *Environmental Science and Technology* **27**, 725-731.

Holmstrand, H., Gadomski, D., Mandalakis, M., Tysklind, M., Irvine, R., Andersson, P., and Gustafsson, O. (2006). Origin of PCDDs in ball clay assessed with compound-specific chlorine isotope analysis and radiocarbon dating. *Environmental Science & Technology* **40**, 3730-3735.

Holt, E., Von Der Recke, R., Vetter, W., Hawker, D., Alberts, V., Kuch, B., Weber, R., and Gaus, C. (2008). Assessing dioxin precursors in pesticide formulations and environmental samples as a source of octachlorodibenzo-p-dioxin in soil and sediment. *Environmental Science & Technology* **42**, 1472-1478.

Horii, Y., Ok, G., Ohura, T., and Kannan, K. (2008a). Occurrence and profiles of chlorinated and brominated polycyclic aromatic hydrocarbons in waste incinerators. *Environmental Science & Technology* **42**, 1904-1909.

Horii, Y., van, B. B., Kannan, K., Petrick, G., Nachtigall, K., and Yamashita, N. (2008b). Novel evidence for natural formation of dioxins in ball clay. *Chemosphere* **70**, 1280-1289.

IARC. (1997.). "Polychlorinated dibenzo-para-dioxins and polychlorinated dibenzofurans.

Vol. 69, IARC monographs on the evaluation of carcinogenic risks to humans. International

Agency for Research on Cancer (IARC), World Health Organization (WHO), Lyon, France.."

Jaynes, W. F., and Boyd, S. A. (1990). Trimethylphenylammonium-smectite as an effective adsorbent of water soluble aromatic-hydrocarbonds. *Journal of the Air & Waste Management Association* **40**, 1649-1653.

Jaynes, W. F., and Boyd, S. A. (1991). Hydrophobicity of siloxane surfaces in smectites as revealed by aromatic hydrocarbon adsorption from water. *Clays and Clay Minerals* **39**, 428-436.

Jaynes, W. F., Boyd, S.A. (1991). Hydrophobicity of Siloxane Surfaces in Smectites as Revealed by Aromatic Hydrocarbon Adsorption from Water. *The Clay Minerals Society* **39**, 428-436.

Johnston, C. T., Boyd, S. A., Teppen, B. J., and Sheng, G. (2004a). Sorption of nitroaromatic compounds on clay surfaces. *In* "Handbook of layered materials" (S. M. Auerbach, K. A. Carrado and P. K. Dutta, eds.), pp. 155-189. Marcell Dekker Inc., New York, NY.

Johnston, C. T., Helsen, J., Schoonheydt, R. A., Bish, D. L., and Agnew, S. F. (1998). Single crystal Raman spectroscopic study of dickite. *American Mineralogist* **83**, 75-84.

Johnston, C. T., M.F., D. O., B.J., T., G.Y., S., and S.A, B. (2001a). Spectroscopic study of nitroaromatic-smectite sorption mechanisms. *Environmental Science & Technology* **35**, 4767-4772.

Johnston, C. T., Oliveira, M. F. D., Sheng, G., and Boyd, S. A. (2001b). Spectroscopic Study of Nitroaromatic-Smectite Sorption Mechanisms. *Environ. Sci. Technol* **35**, 4767-4772.

Johnston, C. T., Oliveira, M. F. D., Sheng, G., and Boyd, S. A. (2001c). Spectroscopic study of nitroaromatic-smectite sorption mechanisms. *Environmental Science & Technology* **35**, 4767-4772.

Johnston, C. T., and Premachandra, G. S. (2001). Polarized ATR-FTIR Study of Smectite in Aqueous Suspension. *Langmuir* **17**, 3712-3718.

Johnston, C. T., S.A., B., Teppen, B. J., and Sheng, G. (2004b). Sorption of Nitroaromatic Compounds on Clay Surfaces. *In* "Handbook of Layered Materials", pp. 155-189.

Johnston, C. T., Sheng, G., Teppen, B. J., Boyd, S. A., and De Oliveira, M. F. (2002a). Spectroscopic study of dinitrophenol herbicide sorption on smectite. *Environ. Sci. Technol* **36**, 5067-5074.

Johnston, C. T., Sheng, G., Teppen, B. J., Boyd, S. A., and De Oliveira, M. F. (2002b). Spectroscopic study of dinitrophenol herbicide sorption on smectite. *Environmental Science & Technology* **36**, 5067-5074.

Johnston, C. T., and Tombacz, E. (2002). Surface chemistry of soil minerals. *In* "Soil mineralogy with environmental applications" (J. B. Dixon and D. G. Schulze, eds.), pp. 37-67. Soil Science Society of America, Madison.

Jonker, M. T. O., and Smedes, F. (2000). Preferential sorption of planar contaminants in sediments from Lake Ketelmeer, The Netherlands. *Environmental Science & Technology* **34**, 1620-1626.

Karickhoff, S., Brown, D., and Scott, T. (1979). Sorption of Hydrophobic Pollutants on Natural Sediments. *Water Research* **13**, 241-248.

Kim, E. J., Oh, J. E., and Chang, Y. S. (2003). Effects of forest fire on the level and distribution of PCDD/Fs and PAHs in soil. *Science of the Total Environment* **311**, 177-189.

Kjeller, L. O., Jones, K. C., Johnston, A. E., and Rappe, C. (1991). Increases in the Polychlorinated Dibenzo-P-Dioxin and Dibenzo-P-Furan Content of Soils and Vegetation Since the 1840S. *Environmental Science & Technology* **25**, 1619-1627.

Klimenko, V. G., Nurmukhametov, R. N., and Gastilovich, E. A. (1999). Fine-structure phosphorescence and vibrations of 2,3,7,8-tetrachlorodibenzo-n-dioxine. *Optics and Spectroscopy* **86**, 198-204.

Klimenko, V. G., Nurmukhametov, R. N., Gastilovich, E. A., and Lebedev, S. A. (2000). Intramolecular vibrational modes of polychlorodibenzo-p-dioxines of the D-2h symmetry. *Optics and Spectroscopy* **88**, 339-345.

Koppaka, V., and Axelsen, P. H. (2001). Evanescent electric field amplitudes in thin lipid films for internal reflection infrared spectroscopy. *Langmuir* **17**, 6309-6316.

Krauss, M., and Wilcke, W. (2002). Sorption strength of persistent organic pollutants in particle-size fractions of urban soils. *Soil Science Society of America Journal* **66**, 430-437.

Labouriau, A., Johnston, C. T., and Earl, W. L. (2003). Cation and Water Interaction in the Interlamellae of a Smectite Clay. *In* "**Nuclear Magnetic Resonance Spectroscopy in Environmental Chemistry**" (M. A. Nanny, R. A. Minear and J. A. Leenheer, eds.), pp. 181-197. Oxford University Press, New York.

Laird, D. A., Barriuso, E., Dowdy, R. H., and Koskinen, W. C. (1992). Adsorption of atrazine on smectites. *Soil Science Society of America Journal* **56**, 62-67.

Laird, D. A., Yen, P. Y., Koskinen, W. C., Steinheimer, T. R., and Dowdy, R. H. (1994). Sorption of Atrazine on Soil Clay Components. *Environmental Science and Technology* **26**, 1054-1061.

Larsen, G., Fan, Z., Casey, F., and Hakk, H. (2004). Sorption, mobility, and fate of 1, 4, 7, 8-tetrachlorodibenzo-p-dioxin in soil. *Organohalogen compounds* **66**, 2317-2321.

Lawrence, M. A. M. R. K. K. a. S. A. B. (1998). Adsorption of phenol and chlorinated phenols from aqueous solution by tetramethylammonium- and tetramethylphosphonium-exchanged montmorillonite. *Appl. Clay Sci.* **13**, 7.

le Site, A. (2001). Factors affecting sorption of organic compounds in natural sorbent/water systems and sorption coefficients for selected pollutants. A review. *Journal of Physical and Chemical Reference Data* **30**, 187-439.

Lee, J. E., Choi, W., Odde, S., Mhin, B. J., and Balasubramanian, K. (2005). Electron affinity and inversion distortion of dibenzo-p-dioxin. *Chemical Physics Letters* **410**, 142-146.

Lee, J. F., Mortland, M. M., Chiou, C. T., Kile, D. E., and Boyd, S. A. (1990). Adsorption of benzene, toluene, and xylene by two tetramethylammonium-smectites having different charge densities. *Clays and Clay Minerals* **38**, 113-120.

Li, H., Sheng, G., Teppen, B. J., Johnston, C. T., and Boyd, S. A. (2003). Sorption and desorption of pesticides by clay minerals and humic acid-clay complexes. *Soil Sci. Soc. Am. J* **67**, 122-131.

Li, H., Teppen, B. J., Johnston, C. T., and Boyd, S. A. (2004a). Thermodynamics of nitroaromatic compound adsorption from water by smectite clay. *Environmental Science & Technology* **38**, 5433-5442.

Li, H., Teppen, B. J., Laird, D. A., Johnston, C. T., and Boyd, S. A. (2004b). Geochemical modulation of pesticide sorption on smectite clay. *Environmental Science & Technology* **38**, 5393-5399.

Liu, C., Gu, C., Yu, K., Li, H., Teppen, B. J., Johnston, C. T., Boyd, S. A., and Zhou, D. (2015). Integrating structural and thermodynamic mechanisms for sorption of PCBs by montmorillonite. *Environ Sci Technol* **49**, 2796-805.

Liu, C., H., B.J., T., C.T., J., and S.A, B. (2008). Mechanisms Associated with the High Adsorption of Dibenzo-p-dioxin from Water by Smectite Clays. *Environ. Sci. Technol*.

Liu, C., Li, H., Johnston, C. T., Boyd, S. A., and Teppen, B. J. (2012). Relating Clay Structural factors to dioxin Adsorption by smectites: Molecular Dynamics Simulations. *SSSAJ* **76**, 110-120.

Liu, C., Li, H., Teppen, B. J., Johnston, C. T., and Boyd, S. A. (2009). Mechanisms associated with the high adsorption of dibenzo-p-dioxin from water by smectite clays. *Environ Sci Technol* **43**, 2777-83.

Ljubic, I., and Sabljic, A. (2005). Dibenzo-p-dioxin. An ab initio CASSCF/CASPT2 study of the pi-pi* and pi-pi* valence excited states. *Journal of Physical Chemistry A* **109**, 8209-8217.

Ljubic, I., and Sabljic, A. (2006). Theoretical study of structure, vibrational frequencies, and electronic spectra of polychlorinated dibenzo-p-dioxins. *Journal of Physical Chemistry A* **110**, 4524-4534.

Lu, M., Wang, G., Zhang, Z., and Su, Y. (2012). Characterization and Inventory of PCDD/F Emissions from the Ceramic Industry in China. *Environmental Science & Technology* **46**, 4159-4165.

Mackay, D. W. Y., Shiu; Kuo-Ching, Ma; Sum Chi, Lee (2006). "Handbook of Physical-Chemical Properties and Environmental Fate for Organic Chemicals " Second Edition/Ed. CRC Press Taylor & Francis Group, LLC

6000 Broken Sound Parkway NW, Suite 300, Boca Raton, FL 33487-2742

Mandal, P. K. (2005). Dioxin: a review of its environmental effects and its aryl hydrocarbon receptor biology. *Journal of Comparative Physiology B-Biochemical Systemic and Environmental Physiology* **175**, 221-230.

Mckinney, J. D. (1985). The Molecular-Basis of Chemical Toxicity. *Environmental Health Perspectives* **61**, 5-10.

McKinney, J. D., Gottschalk, K. E., and Pedersen, L. (1983). The polarizability of planar aromatic systems. An application to polychlorinated biphenyls (PCB's), dioxins and polyaromatic hydrocarbons. *Journal of Molecular Structure: THEOCHEM* **105**, 427-438.

Mckinney, J. D., and Singh, P. (1981). Structure-Activity-Relationships in Halogenated Biphenyls - Unifying Hypothesis for Structural Specificity. *Chemico-Biological Interactions* **33**, 271-283.

Mhin, B. J., Choi, J., and Choi, W. (2001). A simple rule for classification of polychlorinated dibenzo-p-dioxin congeners on the basis of IR frequency patterns. *Journal of the American Chemical Society* **123**, 3584-3587.

Michot, L. J., Villieras, F., Francois, M., Yvon, J., LeDred, R., and Cases, J. M. (1994). The structural microscopic hydrophilitcy of talc. *Langmuir* **10**, 3765-3773.

Mortland, M. M., and Halloran, L. J. (1976). Polymerization of aromatic molecules on smectite. *Soil Science Society of America Journal* **40**, 367-370.

Nolan, T., K.R.Srinivasan, and H.S.Fogler (1989). Dioxon (sic) Sorption By Hydroxy-Aluminum-Treated Clays. *Clays and Clay Minerals* **37**, 487-492.

Nyffeler, J., Chovancova, P., Dolde, X., Holzer, A.-K., Purvanov, V., Kindinger, I., Kerins, A., Higton, D., Silvester, S., van Vugt-Lussenburg, B. M. A., Glaab, E., van der Burg, B., Maclennan, R., Legler, D. F., and Leist, M. (2018). A structure–activity relationship linking non-planar PCBs to functional deficits of neural crest cells: new roles for connexins. *Archives of Toxicology* **92**, 1225-1247.

P.J. Edgar, A. S. H., J.E. Matthews, I.M. Davies (2003). An investigation of geochemical factors controlling the distribution of PCBs in intertidal sediments at a contamination hot spot, the Clyde Estuary, UK. *Appl. Geochem* **18**, 11.

Pereira, T. R., Laird, D. A., Thompson, M. L., Johnston, C. T., Teppen, B. J., Li, H., and Boyd, S. A. (2008). Role of smectite quasicrystal dynamics in adsorption of dinitrophenol. *Soil Science Society of America Journal* **72**, 347-354.

Petkov, P. I., Rowlands, J. C., Budinsky, R., Zhao, B., Denison, M. S., and Mekenyan, O. (2010). Mechanism-based common reactivity pattern (COREPA) modelling of aryl hydrocarbon receptor binding affinity. *SAR QSAR Environ Res* **21**, 187-214.

Phillips, B. L., and Kirkpatrick, R. J. (1994). Short-range Si-Al order in leucite and analcime: determination of the configurational entropy from 27Al and variable-temperature 29Si NMR spectroscopy of leucite, its Cs- and Rb-exchanged derivatives, and analcime. *American Mineralogist* **79**, 1025-1031.

Pius, C., Sichilongo, K., Koosaletse Mswela, P., and Dikinya, O. (2019). Monitoring polychlorinated dibenzo-p-dioxins/dibenzofurans and dioxin-like polychlorinated biphenyls in Africa since the implementation of the Stockholm Convention-an overview. *Environ Sci Pollut Res Int* **26**, 101-113.

Prange, J. A., Gaus, C., Papke, O., and Muller, J. F. (2002). Investigations into the PCDD contamination of topsoil, river sediments and kaolinite clay in Queensland, Australia. *Chemosphere* **46**, 1335-1342.

Rana, K., Boyd, S. A., Teppen, B. J., Li, H., Liu, C., and Johnston, C. T. (2009). Probing the microscopic hydrophobicity of smectite surfaces. A vibrational spectroscopic study of dibenzo-p-dioxin sorption to smectite. *Phys Chem Chem Phys* **11**, 2976-85.

Rappe, C. (1994). Dioxin, Patterns and Source Identification. *Fresenius Journal of Analytical Chemistry* **348**, 63-75.

Rappe, C. (1996). Sources and environmental concentrations of dioxins and related compounds. *Pure and Applied Chemistry* **68**, 1781-1789.

Rappe, C. (2000). Polychlorinated dioxins and dibenzofurans in different environmental matrices: Atmosphere, soil, sediment and water. *Annali di Chimica* **90**, 1-8.

Rappe, C., Bergek, S., Fiedler, H., and Cooper, K. R. (1998). PCDD and PCDF contamination in catfish feed from Arkansas, USA. *Chemosphere* **36**, 2705-2720.

Ras, R. H. A., Johnston, C. T., Franses, E. I., Ramaekers, R., Maes, G., Foubert, P., De Schryver, F. C., and Schoonheydt, R. A. (2003). Polarized infrared study of hybrid Langmuir-Blodgett monolayers containing clay mineral nanoparticles. *Langmuir* **19**, 4295-4302.

Ras, R. H. A., Schoonheydt, R. A., and Johnston, C. T. (2007). Relation between s-polarized and p-polarized internal reflection spectra: Application for the spectral resolution of perpendicular vibrational modes. *Journal of Physical Chemistry A* **111**, 8787-8791.

Roberts, M. G., H. Li, B.J. Teppen, and S.A.Boyd. (2006). Sorption of nitroaromatics by ammonium- and organic ammonium-exchanged smectite: Shifts from adsorption/complexation to a partition-dominated process. *Clays Clay Min.* **54** 8.

Ruan, X. Z., L. ; and Chen, B. (2008). Adsorptive Characteristics of the Siloxane Surfaces of Reduced-Charge Bentonites Saturated with Tetramethylammonium Cation *Environmental Science and Technolgy* **42**, 6.

Safe, S. (1990). Polychlorinated biphenyls (PCBs), dibenzo-p-dioxins (PCDDs), dibenzofurans (PCDFs) and related compounds: environmental and mechanistic considerations which support the development of toxic equivalency factors (TEFs). *Crit. Rev. Toxicol., , .* **21**, 37.

Schecter, A. (1994). "Dioxins and health," Plenum Press, New York, NY.

Schecter, A., Birnbaum, L., Ryan, J. J., and Constable, J. D. (2006). Dioxins: An overview. *Environmental Research* **101**, 419-428.

Schmitz, M., Scheeder, G., Bernau, S., Dohrmann, R., and Germann, K. (2011). Dioxins in primary kaolin and secondary kaolinitic clays. *Environ Sci Technol* **45**, 461-7.

Scholtzova, E., Tunega, D., and Nagy, L. T. (2003). Theoretical study of cation substitution in trioctahedral sheet of phyllosilicates. An effect on inner OH group. *Journal of Molecular Structure-Theochem* **620**, 1-8.

Schoonheydt, R. A., and Johnston, C. T. (2007). Surface and interface chemistry of clay minerals. *In* "Handbook of Clay Science I" (F. Bergaya and B. K. G. Theng, eds.), pp. 87-112. Elsevier Science LTD, Amsterdam.

Schwarzenbach, R. A. G., P.M.; Imboden, D.M. (2002). "Environmental Organic Chemistry " 2ND/Ed. John Wiley & Sons, Inc.

Sheng, G., Johnston, C. T., Teppen, B. J., and Boyd, S. A. (2002). Adsorption of dinitrophenol herbicides from water by montmorillonite. *Clays and Clay Minerals* **50**, 25-34.

Sheng, G. Y., C.T.Johnston, B.J.Teppen, and S.A.Boyd (2001a). Potential contributions of smectite clays and organic matter to pesticide retention in soils. *Journal of Agriculture Food Chemistry* **49**, 2899-2907.

Sheng, G. Y., Johnston, C. T., Teppen, B. J., and Boyd, S. A. (2001b). Potential contributions of smectite clays and organic matter to pesticide retention in soils. *J. Agric. Food Chem* **49**, 2899-2907.

Sheng, G. Y., Xu, S. H., and Boyd, S. A. (1996). Mechanism(s) controlling sorption of neutral organic contaminants by surfactant-derived and natural organic matter. *Environ. Sci. Technol* **30**, 1553-1557.

Shiu, W. Y. D., W.;Gobas, Fapc; Andren, A.; Mackay, D. (1988). Physical-Chemical Properties of Chlorinated Dibenzo-p-dioxins *Environmental Science & Technology* **22**, 651-658.

Steenland, K., Bertazzi, P., Baccarelli, A., and Kogevinas, M. (2004). Dioxin revisited: Developments since the 1997 IARC classification of dioxin as a human carcinogen. *Environmental Health Perspectives* **112**, 1265-1268.

Sutton, R., and Sposito, G. (2001). Molecular simulation of interlayer structure and dynamics in 12.4 angstrom Cs-smectite hydrates. *Journal of Colloid and Interface Science* **237**, 174-184.

Swanson, B. I. (1973). General notation for polarized Raman scattering from gases, liquids, and single crystals. *Appl. Spectrosc* **27**, 382-385.

Swanson, H. I., and Bradfield, C. A. (1993). The Ah-Receptor - Genetics, Structure and Function. *Pharmacogenetics* **3**, 213-230.

Teppen, B. J., and Aggarwal, V. (2007). Thermodynamics of organic cation exchange selectivity in smectites. *Clays and Clay Minerals* **55**, 119-130.

Urbaszek, P., Gajewicz, A., Sikorska, C., Haranczyk, M., and Puzyn, T. (2017). Modeling adsorption of brominated, chlorinated and mixed bromo/chloro-dibenzo-p-dioxins on C(60) fullerene using Nano-QSPR. *Beilstein journal of nanotechnology* **8**, 752-761.

van den Berg, M., Kypke, K., Kotz, A., Tritscher, A., Lee, S. Y., Magulova, K., Fiedler, H., and Malisch, R. (2017). WHO/UNEP global surveys of PCDDs, PCDFs, PCBs and DDTs in human milk and benefit-risk evaluation of breastfeeding. *Archives of toxicology* **91**, 83-96.

Van Olphen, H., and Fripiat, J. J. (1979). "Data handbook for clay materials and other non-metallic minerals," 1/Ed. Pergamon Press, Oxford.

Voice, T. C., and W.J.Weber (1983). Sorption of Hydrophobic Compounds By Sediments, Soils and Suspended-Solids .1. Theory and Background. . *Water Research 17* **1433-1441.**, 1441.

Waller, C. L., and McKinney, J. D. (1992). Comparative molecular field analysis of polyhalogenated dibenzo-p-dioxins, dibenzofurans, and biphenyls. *J Med Chem* **35**, 3660-6.

Waller, C. L., and McKinney, J. D. (1995). Three-dimensional quantitative structure-activity relationships of dioxins and dioxin-like compounds: model validation and Ah receptor characterization. *Chem Res Toxicol* **8**, 847-58.

Walters, R. W., Ostazeski, S. A., and Guiseppielie, A. (1989). Sorption of 2,3,7,8-Tetrachlorodibenzo-P-Dioxin from Water by Surface Soils. *Environmental Science & Technology* **23**, 480-484.

Weissmahr, K. W., Haderlein, S. B., and Schwarzenbach, R. P. (1998). Complex formation of soil minerals with nitroaromatic explosives and other pi-acceptors. *Soil Sci. Soc. Am. J* **62**, 369-378.

Wong, T. W., Wong, A. H., Nelson, E. A., Qiu, H., and Ku, S. Y. (2013). Levels of PCDDs, PCDFs, and dioxin-like PCBs in human milk among Hong Kong mothers. *Sci Total Environ* **463-464**, 1230-8.

APPENDIX A. CALCULATED RAMAN AND IR VIBRATIONAL FREQUENCIES OF DIBENZO-P-DIOXIN (DD)

Table A. 1 Observed and calculated Raman and IR vibrational frequencies (cm^{-1}) of dibenzo-p-dioxin in crystalline and a polar solvents

Experimental				N	Theoretical[‡]	Band Assignment
Raman frequency (cm^{-1})		IR frequency (cm^{-1})			predicted by	
Crystalline DD	DD solution (in CCl_4)	Crystalline DD (in KBr Pellet)	DDsolution (in $CHCl_3$)		BLYP/631G[++]	
242	233			ν_{20}	239	C-O-C oop def
267	271			ν_{15}	286	δCH oop , skel def oop
399	395			ν_{11}	390	skel def
441	438			ν_{30}	433	δC-O-C,skel def
450	459	450		ν_{14},ν_{58}	450	skel def oop
534	531			ν_{29}	534	skel def
552				ν_{49}	551	δCH oop
565				ν_{10}	564	δC-O-C,skel def
		609		ν_{55}	610	skel def
		668		ν_{44}	667	δC-O-C,skel def
725	731			ν_{9}	713	benzene ring breth
749	747	746		$\nu_{18,}$ ν_{57}	738	δCH oop
762				ν_{43}	753	δCH oop
		831	830	ν_{54}	837	ring breath
		851		ν_{43}	851	δC-O-C,skel def
		858				
897	895			ν_{19}	906	skel def
		908				
927	928	925	928	$\nu_{42,}$ ν_{56}	928	δCH oop
980				ν_{16}	1013	δCH oop
		966				
1030	1030	1030	1030	$\nu_{8,}$ ν_{53}	1032	δCH ,skel def , benzene ring breath
1095				ν_{27}	1077	δCH , skel def
		1116	1113	ν_{28}	1112	δCH ,skel def , benzene ring breath
1153	1151	1150		$\nu_{7,}$ ν_{52}	1157	δCH
1191	1186	1195		$\nu_{26,}$ ν_{41}	11671203	δCH, $^{\nu}$ C-O-C, skel def
1225	1227	1225		ν_{6}	1241, 1203	$^{\nu}$C-C, $^{\nu}$ C-O-C
1278				ν_{25}	1246	δCH
		1287	1288	ν_{40}	1267	$^{\nu}$C-C, $^{\nu}$ C-O-C
		1295	1296	ν_{51}	1285	$^{\nu}$C-C, $^{\delta}$ CH
		1303		ν_{50}	1296	$^{\nu}$ C-O-C, skel def
1317	1315			ν_{5}	1311	$^{\nu}$ C-O-C, skel def
		1339				
		1396				
1416		1412				
1464		1465		$\nu_{24,}$ ν_{39}	1441, 1463	$^{\nu}$C-C
		1489	1489	ν_{35}	1481	δCH,skel def
1502		1498		ν_{4}	1497	$^{\nu}$C-C, $^{\nu}$ C-O-C, $^{\delta}$ CH
		1512				
		1553				
		1567				
1587	1588	1591	1591	$\nu_{23,}$ ν_{48}	15641596	δCH,skel def
1622	1623	1626		$\nu_{3,}$ $\nu_{38,}$	1608	δCH,skel def
	3022		3075	$\nu_{32,}$	3075	$^{\nu}$CH
	3041		3086	ν_{12}	3086	$^{\nu}$CH
	3059		3094	ν_{33}	3094	$^{\nu}$CH
	3088		3100	ν_{13}	3100	$^{\nu}$CH

‡ = normalized by factor 0.9628, ν = stretching, δ=bending, Skel= skeleton, oop= out of plane, def= deformation

Table A. 2 Observed Raman and IR vibrational modes of dibenzo-p-dioxin (DD) in a polar solvents and in DD-Cs-saponite complex

Ref DD solution‡	Cs-saponite-DD complex			Ref DD solution§	Band Assignment
IR	ATR-FTIR	FTIR-SSCF	Raman-SSCF	Raman§	
				233	C-O-C oop def
				271	δCH oop, skel def oop
			361	395	skel def
				438	skel def
				459	skel oop def
		493			Mg–OH or δSi–O of clay
		482			Mg–OH or δSi–O of clay
			566	531	skel def
		660			Mg–O of clay
	720		676	731	benzene ring breath
	746		729	747	skel def ·δCH oop
830	828				ring breath
928					δ CH oop
	974	942			ν Si-O of clay
	1016	1014			ν Si-O oop of clay
1030	1019	1067	1019	1030	δCH ,skel def, ring breath
1113	1128	1121	1130		δ CH , skel def
	1195	1181		1151	δCH
		1227		1186	δCH
				1227	νC-O-C, skel def
1288	1285	1285	1266		νC-O-C, νC-C
1296	1298	1297	1293		νC-C ,δ CH
			1363	1315	δCH, skel def
1489	1493	1491	1491		δCH, skel def
				1588	δCH, skel def
1591	1542		1586		δCH, skel def
			1616	1623	δCH, skel def
			1696		
	1639	1628			δH-O-H band of water
	2119				Sym νO-H of clay and water
	3504	3677			Asym νO-H of clay

‡ = CHCl₃, § =CCl₄, ν = stretching, ν = stretching, δ=bending, Skel= skeleton, def= deformation, Sym= symmetric Asym= asymmetric, oop= out of plane

APPENDIX B. CALCULATED RAMAN AND IR VIBRATIONAL FREQUENCIES OF 1-CHLORO-DIBENZO-P-DIOXIN

Table B. 1 Observed and calculated Raman and IR vibrational frequencies (cm^{-1}) of 1-chloro-dibenzo-p-dioxin in crystalline and a polar solvents

Experimental				Theoretical‡	Band Assignment
Raman frequency (cm⁻¹)		IR frequency (cm⁻¹)		predicted by	
Crystalline1-Cl- DD	1Cl-DD solution (in CCl₄)	Crystalline DD (in KBr Pellet)	1-Cl- DDsolution (in CCl₄)	BLYP/631G⁺⁺	
233	248			235	C-O-C oop def
287	275			266	δCH oop , skel def oop
307				295	δC-O-C,skel def
325				368	skel def
335					skel def
383	381				skel def
440				410	δC-O-C,skel def
457		455		442	δ CH oop
489				473	skel def
529				516	skel oop def
542	537			528	skel def
551				533	skel def
574				564	δC-O-C,skel def
649	648	648	648	655	skel def
676	672	673		655	C-O-C δCH oop def
707		706	709	669	νC-Cl
729				738	δCH oop
755		753	744	745	δCH oop
763		766		750	δCH oop , skel def
		772	808	826	νC=C skel aromatic ring
		843	844	856	δCH oop
889	886	886	888	901	νC=C skel aromatic ring
934	932	931	936	934	ν C-O-C (sym),
1033	1029	1029	1029	1018	ring breathing
1102		1103	1103	1084	δC-C-C tri. ring
1153	1150	1152	1151	1156	C-H in-plane def
1177	1175	1176	1175	1172	C-H in-plane def
1217	1220	1222	1216	1224	C-H in-plane def
1312	1244	1245	1245	1258	C-H in-plane def
		1295	1293	1287	νC-O-C, C=C skel vib in aromatic ring
1410		1399		1435	νC=C skel aromatic ring
		1465	1467	1453	νC=C skel aromatic ring
		1477	1475	1461	νC=C skel aromatic ring
1493		1498	1496	1486	νC=C skel aromatic ring
1576	1582	1581	1584	1598	νC=C skel aromatic ring
1615	1621	1618	1618	1618	νC=C skel aromatic ring
		3015	3021	3087	νCH
		3060	3062	3101	νCH
		3082	3086	3109	νCH

‡ = normalized by factor 0.9628, ν = stretching, δ=bending, Skel= skeleton, oop= out of plane, def= deformation

Table B. 2 Observed Raman and IR vibrational modes of 1-chloro-dibenzo-p-dioxin (1-ClDD) in a polar solvents and in 1-ClDD -Cs-saponite complex

Ref 1-Cl-DD solution§	Cs-saponite-1-Cl-DD complex			Ref 1-Cl DD solution§	Band Assignment
IR	ATR-FTIR	FTIR-SSCF	Raman-SSCF	Raman	
				247.6	C-O-C oop def
			281	275.2	δCH oop, skel def oop
			361	380.6	skel def
			425	420.9	skel def
			561	537.3	skel def
			675	672.3	C-O-C δCH oop def
708.7	704	660	712		νC-Cl
743.9					δCH oop
807.8	757	763			δCH oop
843.6					δCH oop
888				886.3	νC=C skel aromatic ring
935.5				931.7	νC-O-C (sym),
1029			1027	1029	ring breathing
1061	1071			1062	δCH oop
1103					δC-C-C tri. ring
1151				1150	C-H in-plane def
1175				1175	C-H in-plane def
1216				1220	C-H in-plane def
1245	1245	1244		1244	C-H in-plane def
1293	1295	1295		1312	νC-O-C, C=C skel vib in aromatic ring
1467	1470	1470			νC=C skel aromatic ring (semicircle)
1475	1480	1480			νC=C skel aromatic ring (semicircle)
1496	1498	1495			νC=C skel aromatic ring (semicircle)
1584				1582	νC=C skel aromatic ring (quadrant)
1618				1621	νC=C skel aromatic ring (quadrant)
	1636	1633			δH-O-H band of water
	1898				Sym νO-H of clay and water
	3641	3677			Asym νO-H of clay

§ =in CCl₄, ν = stretching, ν = stretching, δ=bending, Skel= skeleton, def= deformation, Sym= symmetric, Asym= asymmetric, oop= out of plane
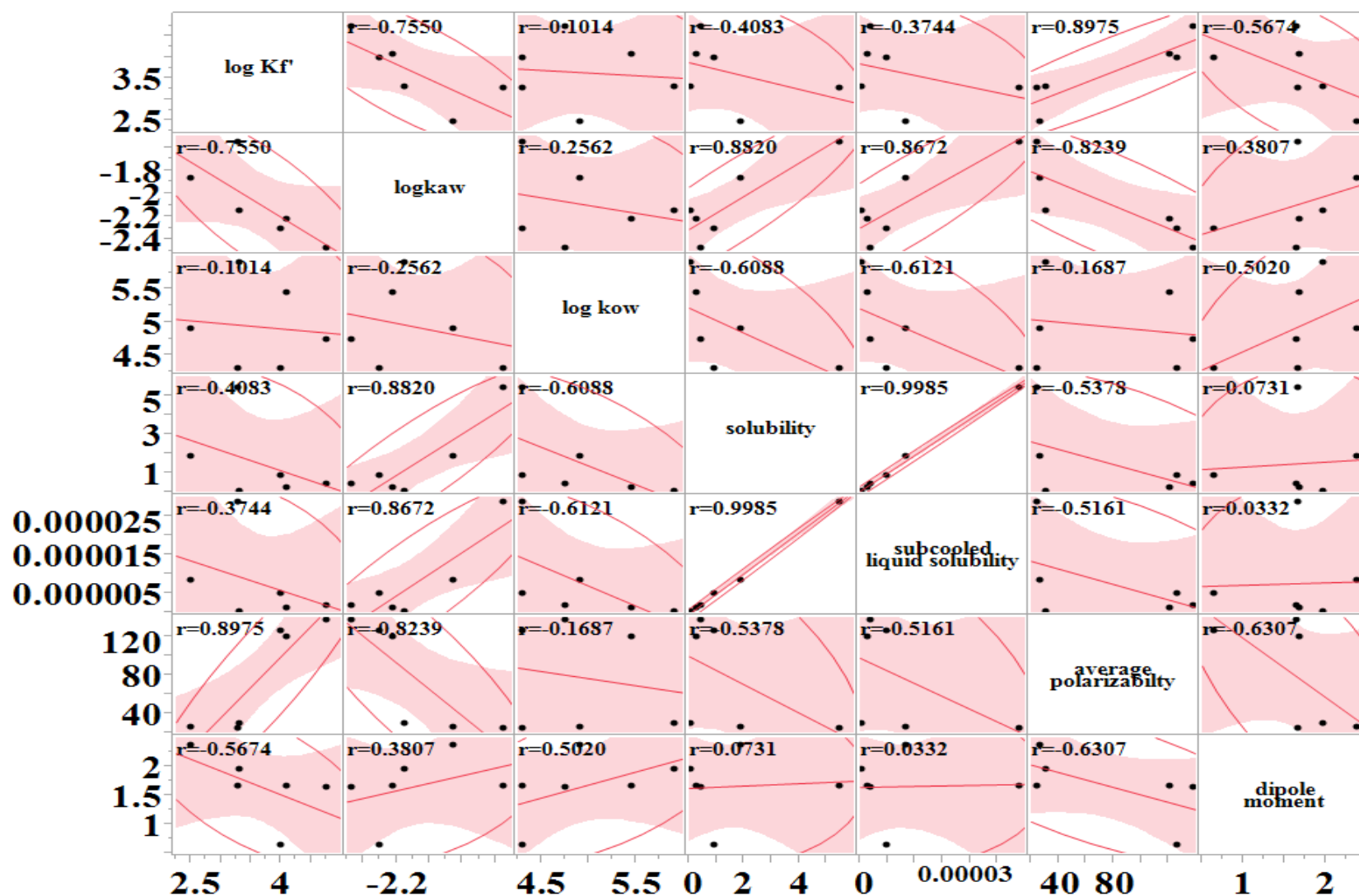
Figure B. 1. Multivariate analysis scatter plot matrix of sorption isotherm coefficients and physicochemical properties of dioxins (DD, 1-ClDD, 2-ClDD) and PCBs (2Cl-PCB, 2, 2' -Cl-PCB, and 2,2',4,4' -Cl-PCB).

APPENDIX C. POLIZED SINGLE CRYTAL RAMAN SPECTRA OF DIBENZO-P-DIOXIN

Abstract

The single crystal polarized Raman spectra facilitate the opportunity to correlate the observed vibrational spectra with the structural information regarding molecular orientation and molecular environment. The single crystal Raman spectra of dibenzo-p-dioxin (DD) from (100), (010) and (001) faces at known orientations have been investigated for this work and have been reported for the first time. While the observed Raman bands agree well with a previous Raman study, this work provides a consistent interpretation of the Raman spectra by assignment of fundamental modes, overtones, and combination bands. All six possible Raman polarizations from 001,010, 100 face, along with mid IR and theoretical B3LYP density functional theory (DFT) harmonic analysis were used to confirm vibrational band assignment for the molecular symmetry modes for D_{2h} configuration proposed previously by many researchers.

Introduction

Dioxins are class of persistent organic pollutants (POP) known for their high toxicity and physio-chemical stability and the persistence in the environment (Denison and Nagy, 2003; EPA, 2000; IARC., 1997. ; Pius et al., 2019; Schecter et al., 2006; van den Berg et al., 2017; Wong et al., 2013). There are 75 dioxin congeners varied in degree and position of chlorine substitutions and 2, 3, 7, 8-tetrachloro-dibenzo-*p*-dioxin (TCDD) is the most potent toxin while non-chlorinated dibenzo-p-dioxin (DD) is not considered toxic.

Quality structure activity relationship (QSAR) modeling and spectroscopic analysis tools has been extensively used to understand the nuclear configuration and it's link to the toxicity and

photo-stability of dioxin congeners (Grainger et al., 1988, 1989; Klimenko et al., 1999; Klimenko et al., 2000; Lee et al., 2005; Ljubic and Sabljic, 2005, 2006; Mhin et al., 2001).

Detailed *ab initio* computational calculations and vibrational spectroscopic studies of DD concluded that DD has a planar, D2h symmetrical geometry (shown in Figure C 1) (Eriksen et al., 2008; Gastilovich et al., 2002; Ljubic and Sabljic, 2006) There are 60 normal vibrational modes of DD and for D_{2h} point symmetry these vibrational modes corelate into 11 A_g + 4 B_{1g}+ 5 B_{2g} +10B_{3g} + 5A_u + 10 B_{1u}+10B_{2u} +5 B_{3u} symmetries. For D_{2h} point symmetry the thirty fundamentals of Ag, B1g, B2g and B3g symmetry are Raman active, 25 fundamentals of B1u, B2u, 10 B3u and Au symmetry fundamentals are neither IR active and or Raman active.

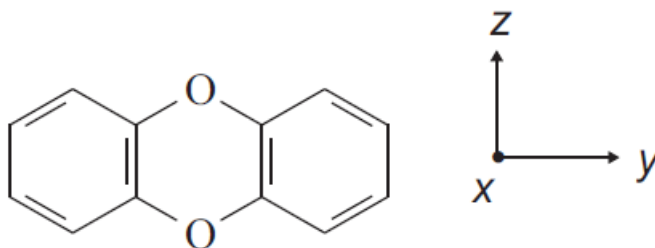
Figure C.1 Planar D2h Geometric configuration of dibenzo-p-dioxin (DD)

Although assignments to fundamental vibration peaks has been done by many researchers. (Eriksen et al., 2008; Gastilovich et al., 2002; Ljubic and Sabljic, 2006), discrepancy in band assignments, especially for weak intensity Raman active out of plane fundamentals, among different studies have been observed. This discrepancy in band assignment could be because most of the Raman spectra were obtained using powder dioxin. The polarized single crystal Raman data is helpful in determining the frequencies and symmetries of the high intensity as well as weak intensity molecular modes. The single crystal Raman data associated with IR spectra and

theoretical calculation presented in this work will improve our understanding of the different vibrational frequencies and symmetry of molecular modes. The goal of this work is to provide Raman tensor using polarized single crystal Raman data and integrate this with the IR and computational band assignment of dibenzo-p-dioxin

Materials and Methods

Solute

Dibenzo-p-dioxin (DD) (99% pure) used in this study was purchased from CHEM SERVICE, West Chester, PA. Crystalline DD (Lot # 319-145 D) was used for taking reference Raman and IR spectra.

Raman spectroscopy

Single crystal formation

Dibenzo-p-dioxin was recrystallized by dissolving 3.32 mg dibenzo-p-dioxin was in 1mL Diethyl ether (unstabilized 99.9%) and solution in a covered petri dish was left to evaporate slowly at room temperature.

Raman Spectra:

Polarized Raman spectra of dioxin crystal were obtained on an Acton Research Corporation SpectroPro500 spectrograph. A Melles-Griot helium–neon laser with 632.8 nm wavelength and power output of 40 mW measured at the laser head was used as the excitation source. Raman-scattered radiation was collected in a 1800 backscattering configuration. The entrance slits to the spectrograph were set to 50μm. The spectrograph used a holographic super notch filter. The detector was a Princeton Instruments liquid N_2 cooled CCD detector. The spectrograph was calibrated daily using a Ne-Ar calibration lamp based upon known spectral lines.

Raman spectra were collected through an Olympus BX-60 microscope using a 50X objective. Digital photographs of the specimens were recorded through camera (Olympus DP12) which was attached to the microscope. Grams /32 (Galactic software) program was used to analyze and plot spectra. Spectral manipulations such as baseline correction and normalization were done in the same software.

Raman spectroscopy of single crystal of dioxin:

A schematic of Raman instrument is shown in Figure C 2 and illustrates the laboratory coordinate system used for this study. The excitation laser beam is incident along the z axis. Raman-scattered radiation was collected in a 180° backscattering configuration and passed through a polarization analyzer that could be switched between two positions to pass the Raman scattered radiation with a polarization parallel to x or y axis. Single crystals of dioxin were mounted on a glass capillary tube and mounted on the translation stage of the microscope. The dioxin crystals were electrostatically attracted to the capillary surface and could be manipulated on a glass capillary surface without falling off. A glass capillary with dioxin crystals was mounted on a glass slide using molding clay on the edges of the glass slide so that capillary tube can be rotated. The glass capillary tube mounted on sample stage had x, y and z translation and x and y rotation. Initially dioxin crystal was placed with the (010) face parallel to the x-y plane of microscope stage. Using crossed polarizer and a 550 nm quartz retardation plate, the crystallographic a axis was aligned parallel to the x axis. The laser was incident on the (010) face, electric vector of laser was parallel to the x axis and the analyzer was set parallel to the x axis. In this configuration, the Raman scattering geometry for this spectrum is described by b (cc) b using the Porto notations (Swanson 1973). Raman spectrum of the crystal with laser incident on the (010) face, electric vector of laser was parallel to x axis and analyzer was set parallel to the y axis was also taken. In this configuration,

the Raman scattering geometry for this spectrum is described by *b(ca)b* using the Porto notations. (Swanson, 1973). Other Raman spectra were collected at *b(aa)b, b(ac)b, a(cc)a, a(cb)a, a(bb)a, a(bc), c(bb)c and c(ba)c* setups by rotating crystal at 90° angle from the face (010). Raman spectra of selected crystals at constant polarization of laser were obtained by positioning the crystal in the desired orientation. The Polarized Raman spectra were collected using 4 x 15s (60 s) of acquisition on the CCD array. A polarization analyzer was used to select the polarization of the Raman-scattered light along either the *x* or the *y* axis. A calcite-wedge polarization scrambler was placed next to the analyzer to minimize unwanted polarization effects in the spectrograph. The Raman spectra were normalized and integrated with the molecular simulation model of dioxin crystal at (001), (010), and (001) orientations. The molecular structure and crystal lattice structure of dioxin were generated using the material studio software are shown in Figure C 3-5. The parameters used for crystal lattice were from Cordes and Fair (1974). Dioxin crystal is a monoclinic with lattice dimension: a=11.69, b=5.09 and 15.11 Å and, β= 100.29.

FTIR study

Infrared spectra were obtained on a Perkin-Elmer GX2000 Furior transformed infrared (FTIR) spectrometer equipped with deuterated triglycine (DTGS) and Mercury-cadmium-telluride (MCT) detectors, an internal wire grid IR polarizer, a KBr beam splitter, and a sample compartment purged with dry air and nitrogen gas. Grams /32 (Galactic software) program was used to analyze and plot spectra.

KBr pellet preparation

One mg dioxin was mixed with 250 mg oven dried KBr and this mixture was pressed into pellet (13 mm in diameter) under 20,000 pounds of pressure under vacuum. The dioxin concentrations in KBr pellet containing 1 mg dioxin was 4.1 micromoles cm^{-2}. Infrared spectra of

KBr pellets were obtained using a DTGS detector. The unapodized resolution for the FTIR spectra was 2.0 cm^{-1}, and a total of 128 scans were collected for each spectrum.

Computational analysis:

The molecular structure and crystal lattice structure of dibenzo-p-dioxin were generated using the material studio software. The parameters used for crystal lattice were from Cordes and Fair (1974). The DFT method was utilized in geometry optimization, and subsequent IR and Raman harmonic vibration frequency calculations. The *ab initio* calculation at the level of hybrid Becke-3Lee_Yang_parr parameters (B3LYP) density functional theory with the 6-31 G** basis set using the Gaussian 03W version 6. The geometry optimization was done, and the optimized geometry was characterized as local minima by harmonic vibrations frequency analysis. Harmonic wavenumber obtained by B3LYP 6-31 G** have transformed into empirical scale by the factor 0.9628.
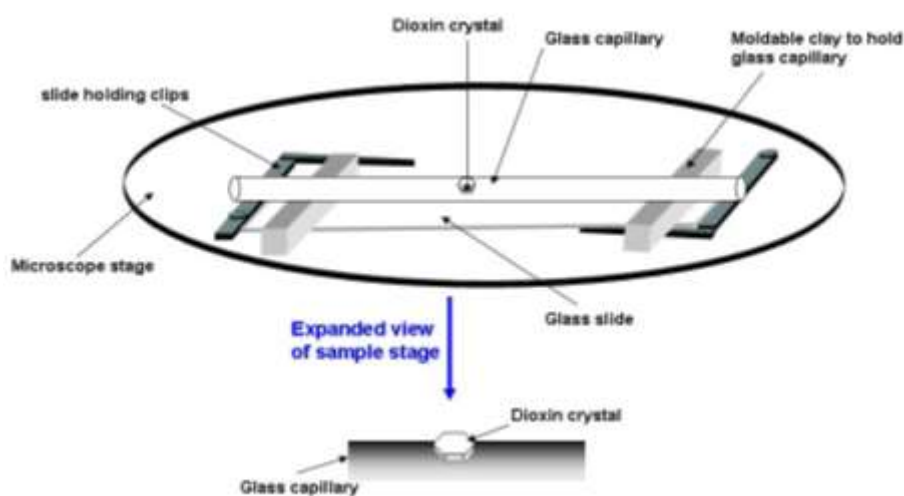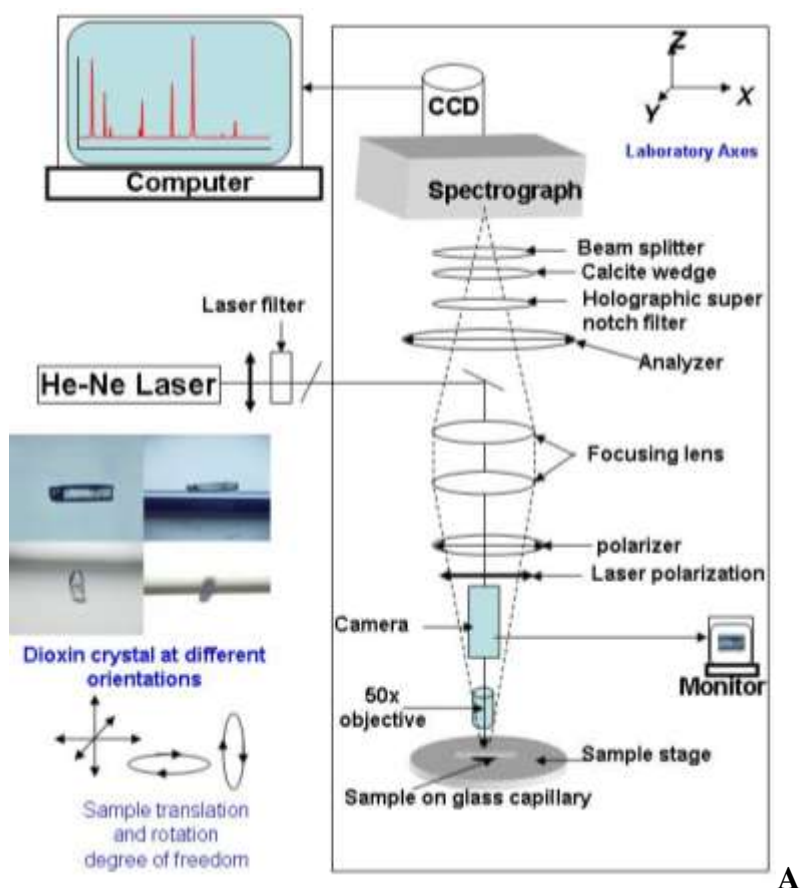
Figure C.2 Raman spectroscopy of single crystal of dioxin. A) Schematic diagram of the Raman spectrograph showing the laser, polarizer, optics, sample orientation, analyzer spectrograph and laboratory axis. The sample stage had xyz translation and x and z rotation. Pictures of dioxin crystal at different orientations are also shown. B) Sample stage and an expanded view of sample stage show the dioxin crystal attached to the glass capillary tube by electrostatic attraction.

Results and discussion

The molecular structures of a Brávais unit cell of dibenzo-p-dioxin at different orientations (001,010, and100) are shown in Figure C 3-5. Dioxin crystal is a monoclinic with lattice dimension: a=11.69, b=5.09 and 15.11 Å and, β= 100.29. The Brávais unit cell contains 4 dibenzo-p-dioxin molecules. Each molecule consists of 22 atoms and hence DD molecule has total 60 (22x3-6) normal vibrational modes. The calculated; using material studio, surface area of dioxin molecule, was ~11Å x 7Å. Directional cosine transformation matrices were calculated following (Johnston et al., 1998) are shown in Table C 1.

Raman spectra of dibenzo-p-dioxin single crystal at c(aa)c, c(bb)c, a(cc)a, b(ac)b, , c(ab)c, and a(bc)a orientations are in region 200 to 1800 cm^{-1} are shown in Figure C 6 . Twenty six Raman vibrational frequencies were observed in this regions. The geometries employed and the associated polarizability tensor components contributing to the Raman spectrum are listed in Table C 2. Computed harmonic frequencies for DD were calculated using Density functional calculations (B3LYP) with 6-31g**and calculated frequencies were scled by the factor 0.9628 to acount for anharmonicity and other systemic effects. Spectral overlay of observed and calculated Raman and IR observations are shown in Figure C 7-8 . Fundamental vibrational transitions of DD and their band assignments are listed in Table C 3-4.
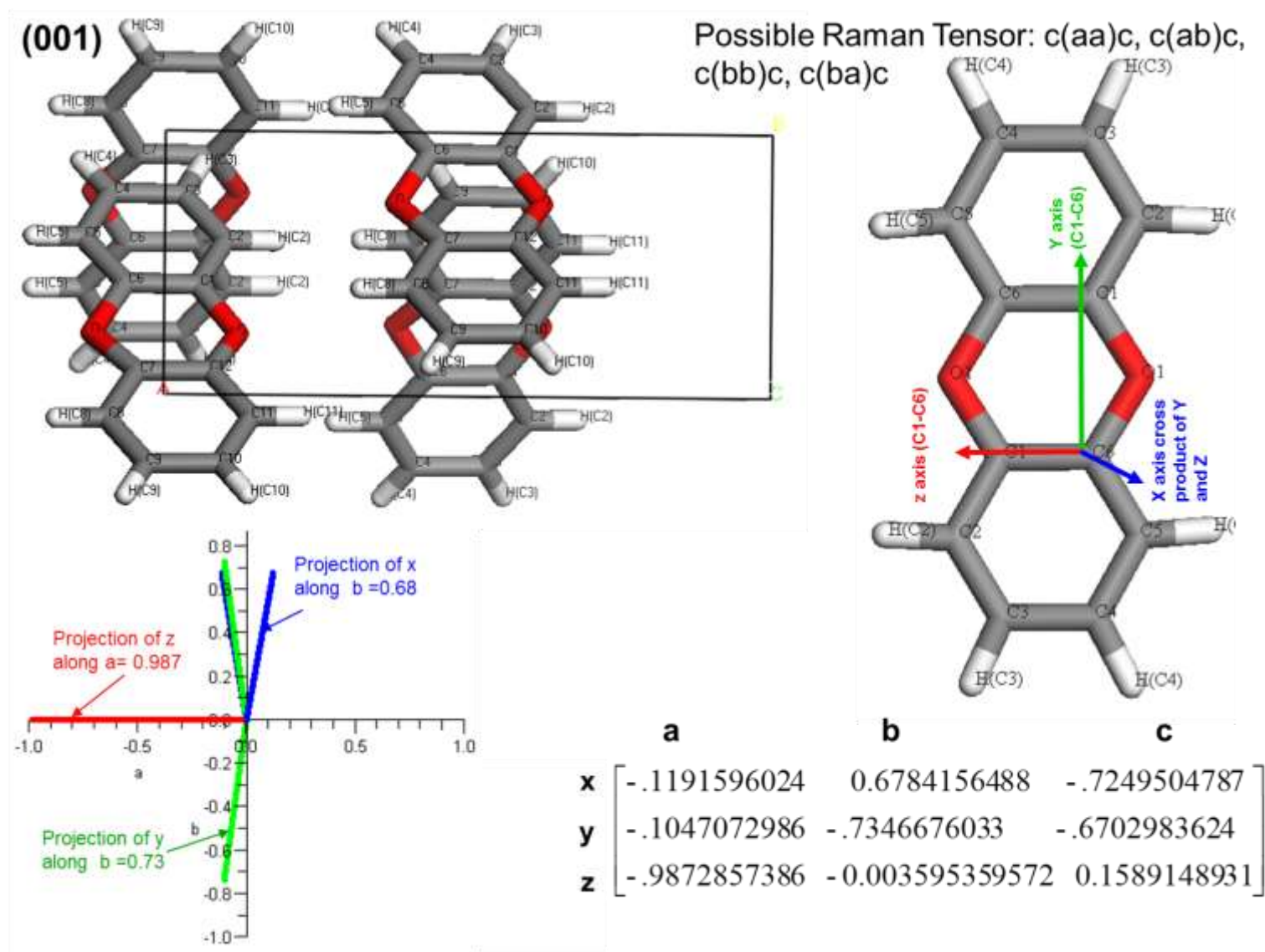
Figure C.3 Brávais unit cell of dibenzo-p-dioxin and principal (i.e. local) axis system (x, y, z) of the local Raman tensor for dioxin monomers projected onto the crystal axis system (a, b, c) of dioxin on the (001) face.

Figure C.4 Brávais unit cell of dibenzo-p-dioxin and principal (i.e. local) axis system (x, y, z) of the local Raman tensor for dioxin monomers projected onto the crystal axis system (a, b, c) of dioxin on the (001) face.

Figure C.5 Brávais unit cell of dibenzo-p-dioxin and principal (i.e. local) axis system (x, y, z) of the local Raman tensor for dioxin monomers projected onto the crystal axis system (a, b, c) of dioxin on the (010) face.
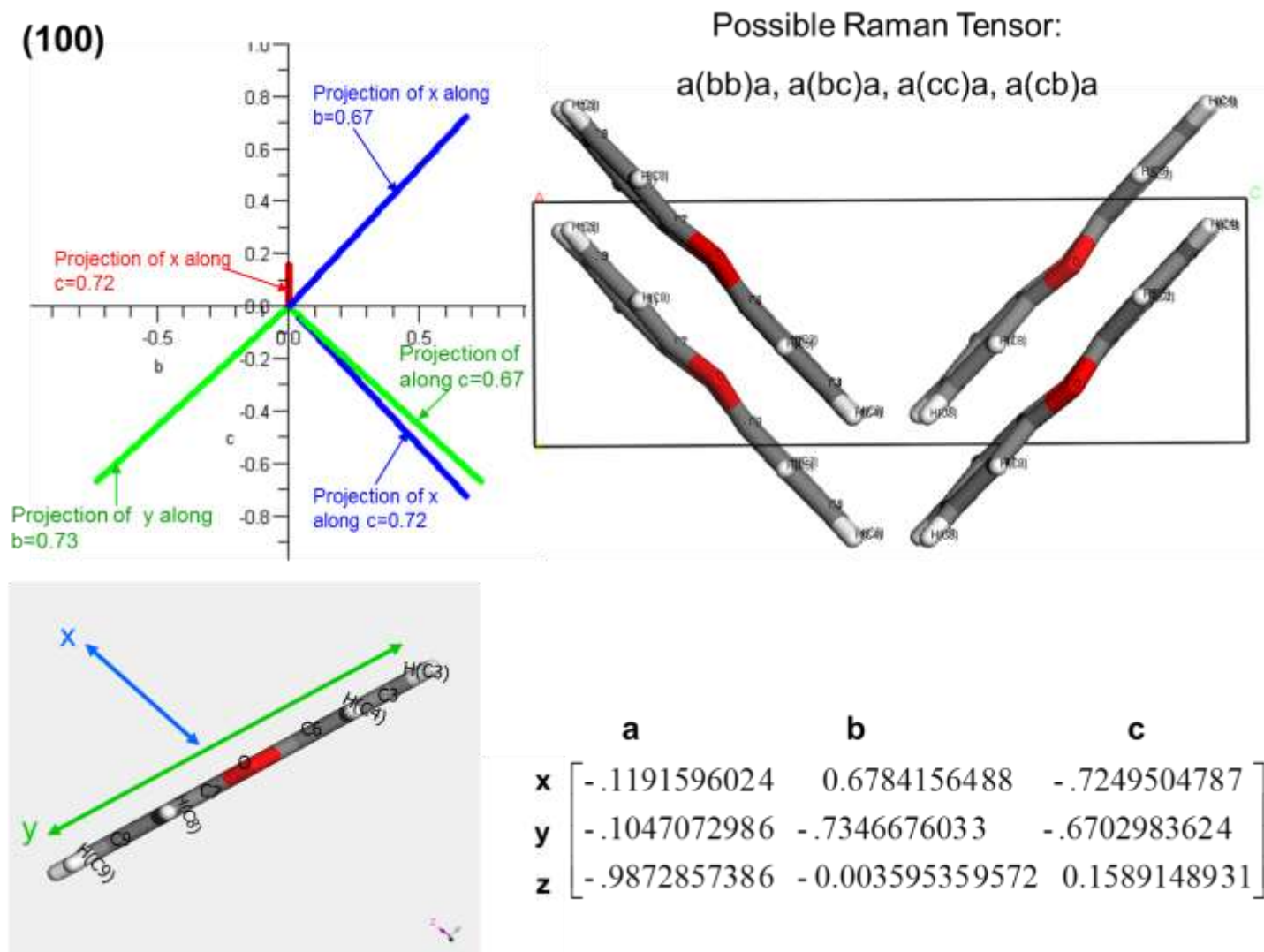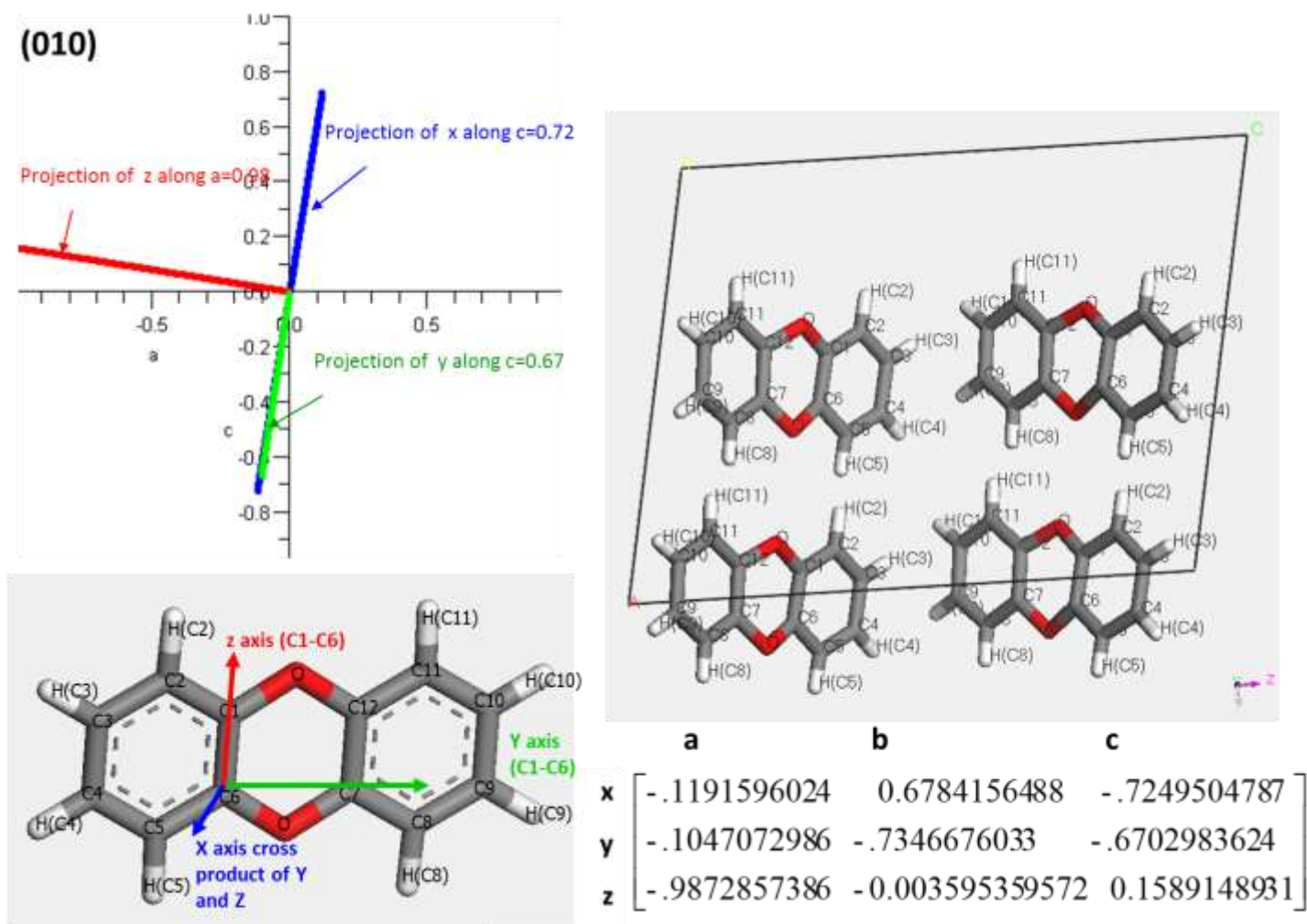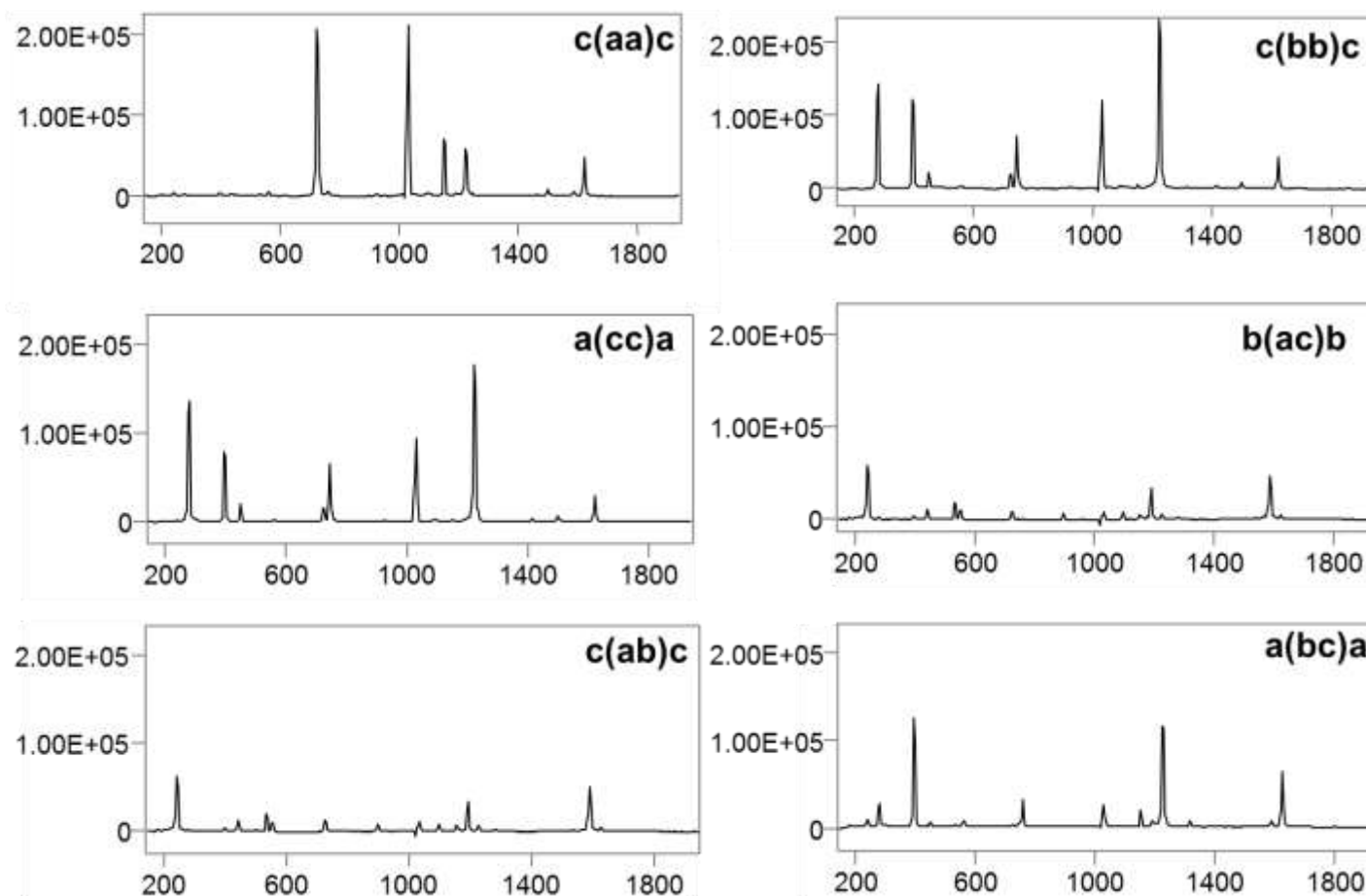
Figure C.6 Single-crystal, polarized, Raman spectra of DD in different geometries from 200 to 1800 cm−1. The modal symmetries are identified and the scattering geometries are given in modified Porto notation. c(aa)c , c(bb)c, and a(cc)a Ag symmetry, Ag symmetry; scattering geometry, B1g symmetry; scattering geometry: b_ab_a. _e_ B2g symmetry; scattering geometry: b_ac_a. _f_ B3g symmetry; scattering geometry: b_cb_a. Polarized single crystal Raman spectra of dibenzo-p-dioxin at different geometries in the region of 200-1800 cm^{-1}.

Table C.1 Directional cosine transformation matrices

	Monomer 1			Monomer 2			Monomer 3			Monomer 4		
	a	B	c	a	B	c	a	b	c	a	b	c
x	-0.1192	0.6784	-0.7250	-0.1192	0.6784	-0.7250	0.1192	0.6784	0.7250	0.1192	0.6784	0.7250
y	-0.1047	-0.7347	-0.6703	-0.1047	-0.7347	-0.6703	-0.1047	0.7347	-0.6703	0.1047	-0.7347	-0.6703
Z	-0.9873	0.0036	0.1589	-0.9873	0.0036	0.1589	-0.9873	0.0036	0.1589	0.9873	0.0036	0.1589

Eularian angles: $\theta=1.41$, $\phi=-0.004$ $\chi=-0.7463$

Table C.2 Various illumination-observation geometries and the associated polarizability tensor components contributing to the Raman spectrum

Axis along incident light	Axis along polarization of incident light	Axis along polarization of Scattered light	Axis along Scattered light	Contributing polarizability tensor	symmetry
c	a	a	c	α_{aa}	Ag
c	b	b	c	α_{bb}	Ag
a	c	c	a	α_{cc}	Ag
c	a	b	c	α_{ab}	B1g
a	b	c	a	α_{bc}	B2g
b	a	c	b	α_{ac}	B3g

Figure C.7 Comparison of predicted and observed Raman and IR frequencies of dibenzo-p-dioxin (DD) in the 200-1000 cm^{-1} region. The spectra labeled A and B correspond to predicted Raman and IR spectra using B3LYP/631G** and C to H are experimental polarized Raman spectra at c(aa)c, c(bb)b, a(cc)a, c(ba)c, a(bc)a and b(ac)b orientations and FTIR absorption spectrum of DD in KBr pellet.
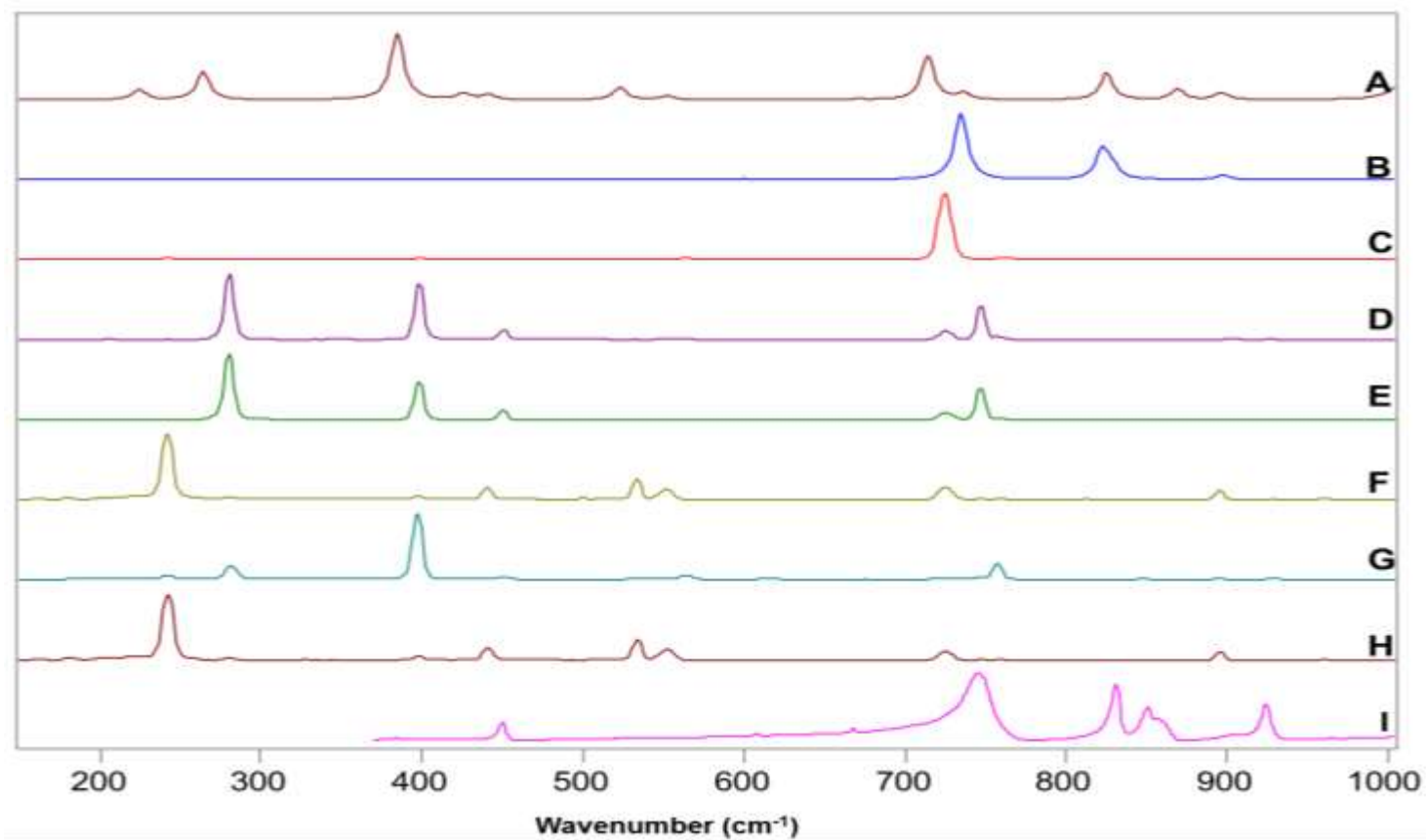
Figure C.8 Comparison of predicted and observed Raman and IR frequencies of dibenzo-p-dioxin (DD) in the 950-1800 cm^{-1} region. The spectra labeled A and B correspond to predicted Raman and IR spectra using B3LYP/631G** and C to H are experimental polarized Raman spectra at c(aa)c, c(bb)b, a(cc)a, c(ba)c, a(bc)a and b(ac)b orientations and FTIR absorption spectrum of DD in KBr pellet.
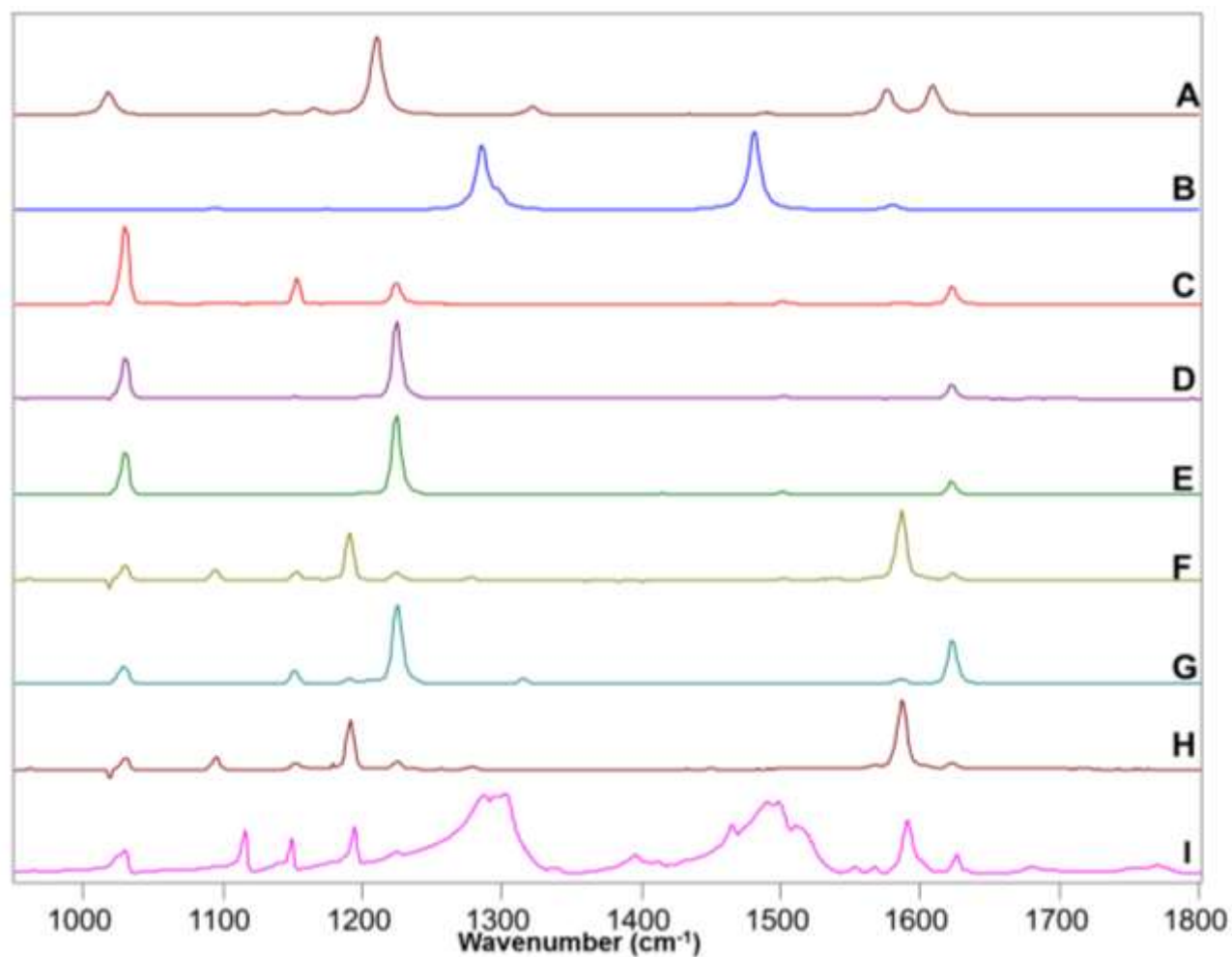
Table C.3 Observed Raman active vibrational modes of dibenzo-p-dioxin (DD) and their band assignments calculated fundamentals.

Vibration numbering (N)	V_{Ca}	V_{Ra}	Approx Band Assignment
A$_g$ (in plane)			
1	3101	NM	CH *s*
2	3087	NM	CH *s*
3	1609	1623	skel *def,* CH *b*
4	1490	1502	skel *def*, CH *b*
5	1317	1316	C-O-C *b*, skel *def*
6	1210	1226	C-O-C *b*, skel *def*
7	1136	1149	CH *b*
8	1018	1030**	CH *b*
9	714	726	ring breathing
10	553	564	C-O-C b, skel *def*
11	399	397	C-O-C b, skel *def*
B$_{1g}$ (out of plane)			
15	263	283	CH oop b, skel oop def
14	426	450**	skel oop def
13	825	763	CH oop *b*
12	916	927	CH oop *b*
B$_{2g}$ (out of plane)			
20	223	242	COC oop *def*
19	522	535	CH oop *b*
18	736	750	CH oop *b*, skel oop *def*
17	897	897	CH oop *b*
16	930*	929	CH oop *b*
B$_{3g}$ (in plane)			
21	3096	NM	CH *s*
22	3075	NM	CH *s*
23	1576	1587	CH *b*
24	1435	1416	CH *b*
25	1322*	1316	CH *b*
26	1165	1192	CH *b*
27	1076	1096	CH *b*
28	870	897	skel *def*
29	535	534	skel *def*
30	441	450	skel *def*

V_{ca} = Frequency calculated using B3LYP631G**, frequencies were scaled by the factor 0.9628,   VRa = Raman Frequency, skel= skeleton, def= deformation, *b*= bending, oop= out of plane

Table C.4: Observed IR active vibrational modes of dibenzo-p-dioxin (DD) and their band assignments calculated fundamentals.

Vibration numbering (N)	V_{Ca}	V_{IR}	Approx Band Assignment
Au[¶] (out of plane)			
31	930		
32	898	843	
33	655	706	
34	530	543	
35	121	155	
B₁ᵤ (in plane)			
36	3096	3060	CH *s*
37	3076	3022	CH *s*
38	1623	1626	CH b, skel def
39	1456	1465	CH b, skel def
40	1286	1287	CH *b*, C-O-C *s*
41	1174	1195	C-O-C *s*
42	1136	1116	CH b, skel def
43	829	851	C-O-C b, skel def
44	657	668	C-O-C b, skel def
45	232		skel *def*
B₂ᵤ (in plane)			
46	3101	3088	CH *s*
47	3087	3041	CH *s*
48	1581	1591	CH *b*
49	1481	1496	CH *b*
50	1297	1303	C-O-C *s*, skel *def*
51	1286	1295	C-O-C *b*, skel *def*
52	1095	1150	CH *b*
53	1018	1030	CH *b*, skel *def*
54	823	831	ring breathing
55	600	609	skel *def*
B₃ᵤ (out of plane)			
56	898	925	CH oop *b*
57	735	746	CH oop *b*
58	448	450	skel oop *def*
59	293	NM	skel oop *def*
60	35	NM	butterfly

V_{ca} = Frequency calculated using B3LYP631G**, frequencies were scaled by the factor 0.9628, VIR = IR Frequency, skel= skeleton, def= deformation, *b*= bending, oop= out of plane, s= stretching, [¶]experimental data from Gastilovich et al. (2002)